Patterns on the rocks II

Complex morphologies with continuous curvature

Juan Manuel García-Ruiz

Laboratorio de Estudios Cristalográficos
Instituto Andaluz de Ciencias de la Tierra (CSIC-UGR), Granada, España

2013 Santalo's School on the Mathematics of the Planet Earth
Santander, July 15 2013

- Oldest material Zircon ≈ 4.2 Gy
- Oldest rock, gneiss ≈ 4.0 Gy
- Oldest sedimentary rocks, Putative Isotopic marks Issua ≈ 3.8 Gy.
- Oldest putative microfossils, Warrawoona 3.5 Gy

- ✓ Isotopic signature of carbonaceous remnants
- ✓ Morphology of putative microfossils
- ✓ Chemical composition of carbonaceous compounds
- ✓ Stromatolitic structures

History of the Primitive Earth

Main Microbiota	My		Main Life Events
	4500	ARCHEAN	Formation of Earth
	4000		*Origin of Life as seen from microfossils*
Issua	3800		Oldest sedimentary rocks Oldest putative fossils and stromatolites
Warrawoona Onwerwacht Fig Tree Moodies	3500		
Insuzi Fortescue	2800		Cianobacteria and Stromatolites
Hamersley Ventersdorp Gowganda Transvaal	2500	Proterozoic	Change in the tectonic regime of the earth. Greenstones and komaitites becomes later rare Iron Banding Formations
Gunflint Belcher	2100		Latest detrital Uraninite and Pyrite
	1900		Atsmosferic oxygen
	1800		Nucleated cells (Phytoplankton)
Dismal Lakes			
Belt			
Bitter Springs Chuar Little Dal	1100		Complex (sexual) Phytoplankton
Chichkan	850		Seaweeds and protozoans
Ediacara	600	Phanerozoic	Animals without backbones

Mostly based on data from

J. W. Schopf. Major events in the History of Life (Jones and Bartlett, Boston, 1992)
E.C. Nisbet, The young Earth Allen & Unwin, Boston 1987

Morphological convergence of silica biomorphs with primitive life forms

Some structures found in Precambrian rocks (cherts) which are interpreted as fossils remnants of primitive life and its laboratory made silica/carbonate counterparts

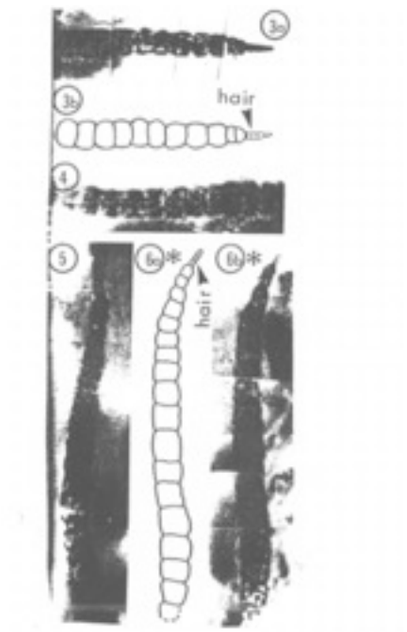

Cephalophyton rivularioides (Bitter Springs)
Schopf J. of Paleontology 42 (1968) 651

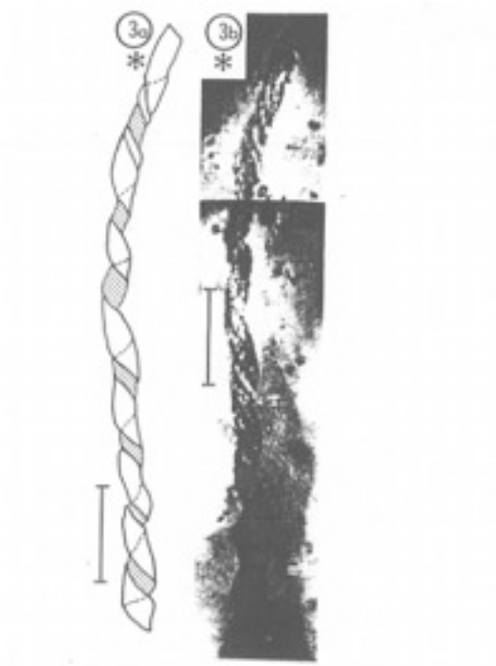

Heliconema Australiensis (Bitter Springs)
Schopf J. of Paleontology 42 (1968) 651

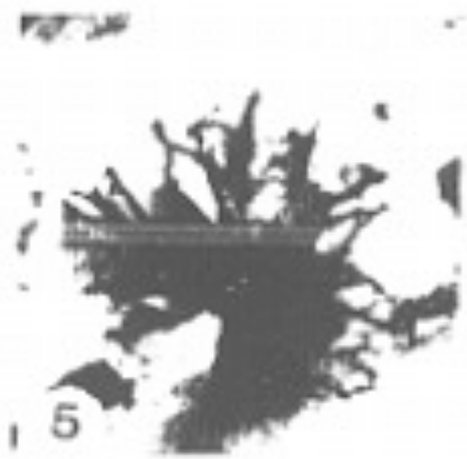

Eoastrion Barghoon (DUCK CREEK)

From: Knoll and Barghoorn Origins of Life 7 (1976) 417

Primitive life detection (On Earth, Mars and meteorites)

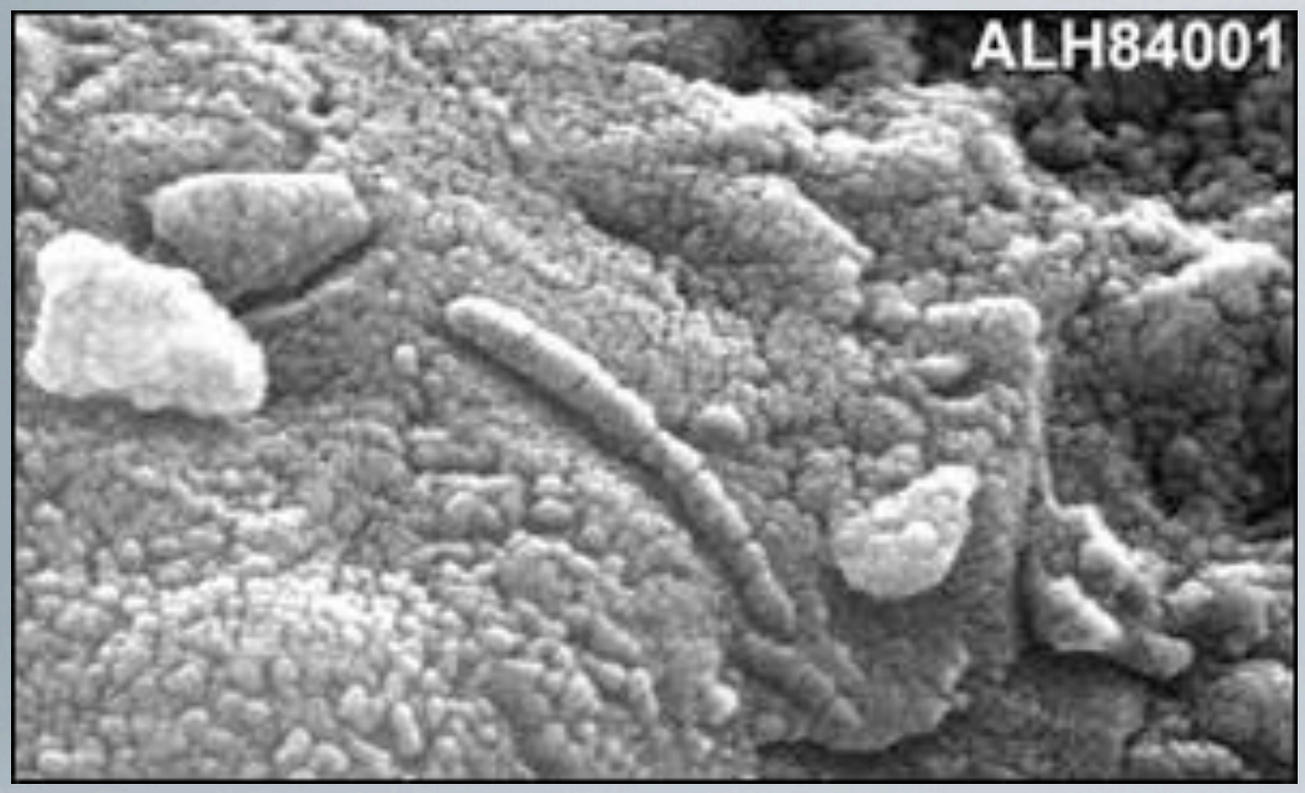

FESEM view of morphologies found in the Martian meteorite ALH84001 and proposed as evidence of primitive life on Mars.

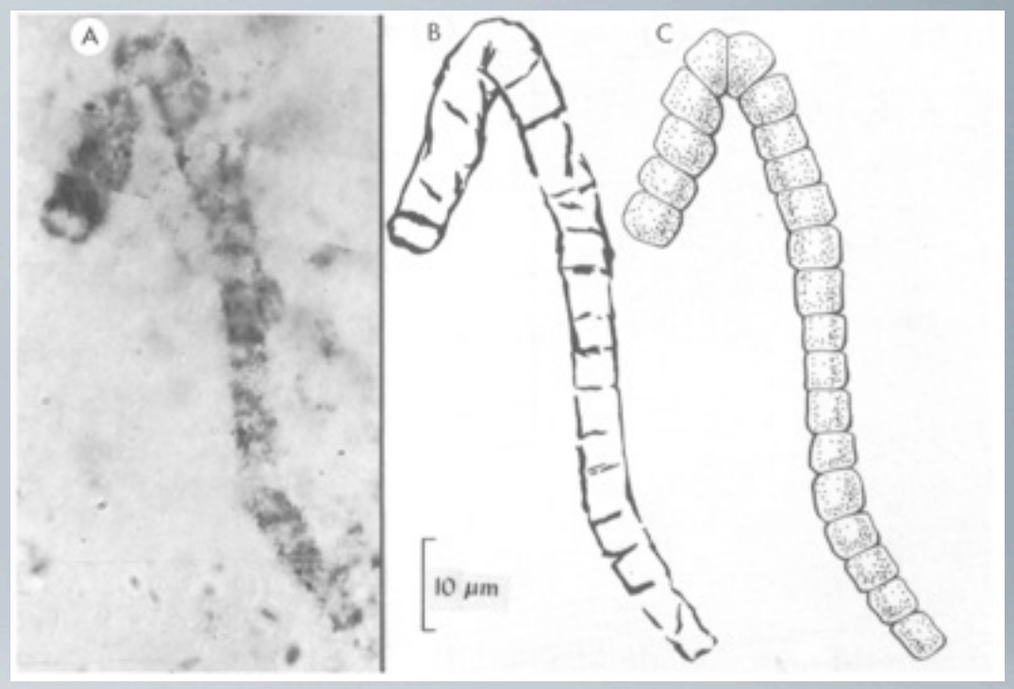

Microstructures found in Achaean rocks and interpreted as one of the oldest remnants of life on planet Earth.

"Some of the features in ALH84001 (e.g. filaments) are common biogenic markers on Earth. We conclude that the evidence for fossilized microbes and their products ……***cannot be readily explained by non-biologic processes ..***"

LPI Workshop, "*Martian meteorites: Where do we stand and where are we going?*"

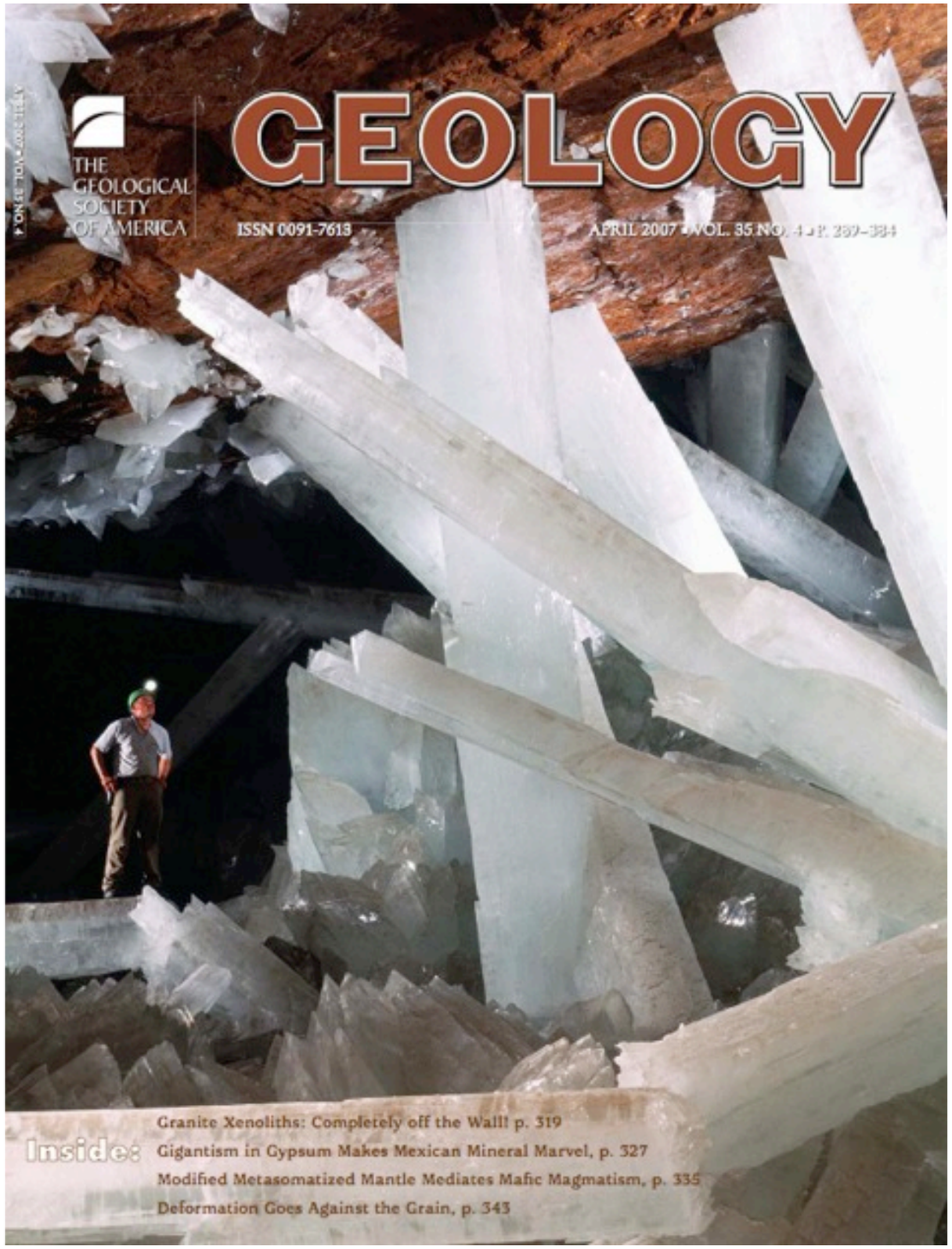

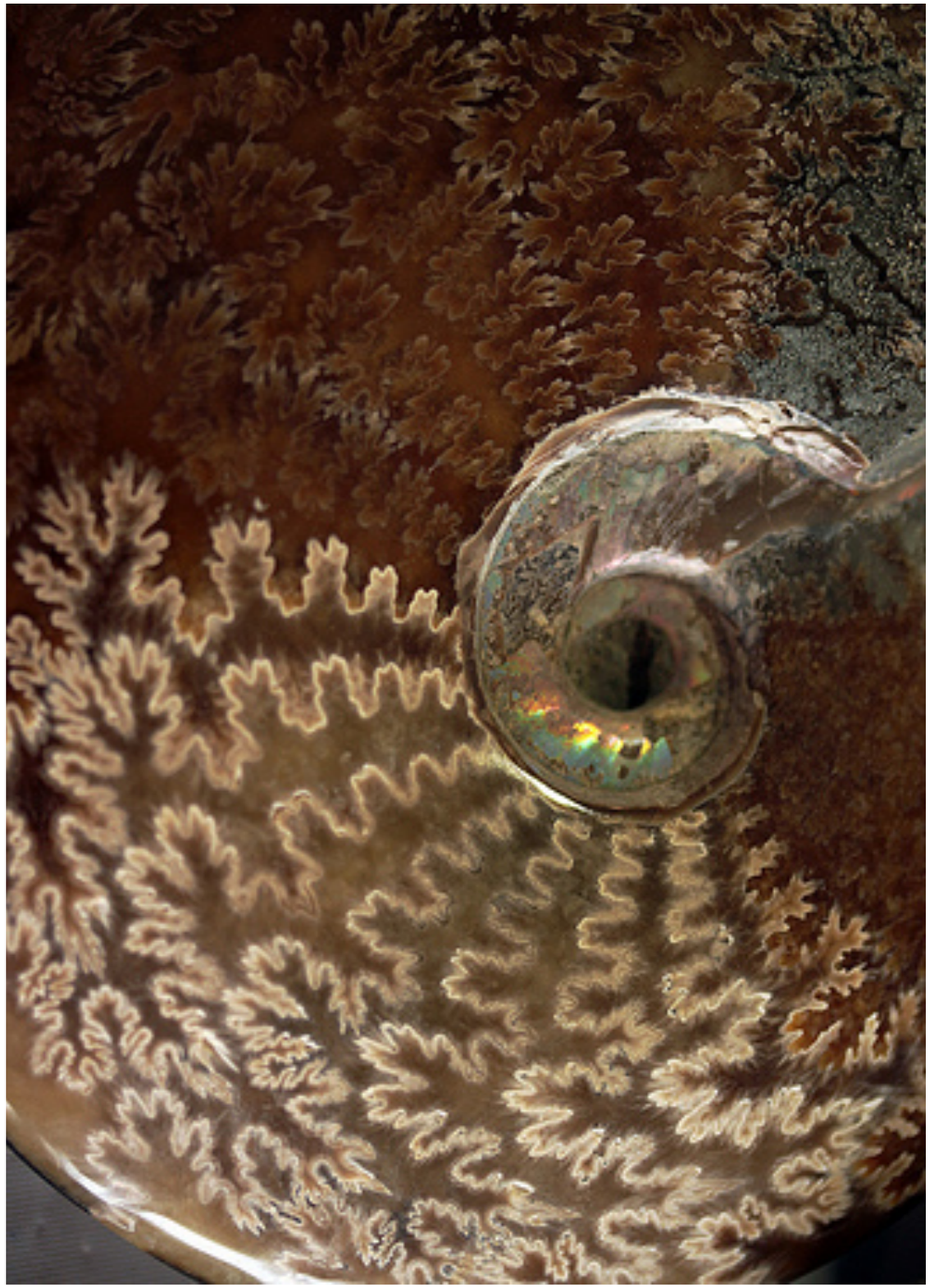

The existence of a sharp boundary dividing the realm of biology and sensuality and the realm of minerals and cold rationality has pervaded the landscape of arts and philosophy for centuries. Crystals and crystallographic theories have played an important role in the intellectual construction of that proposed boundary.

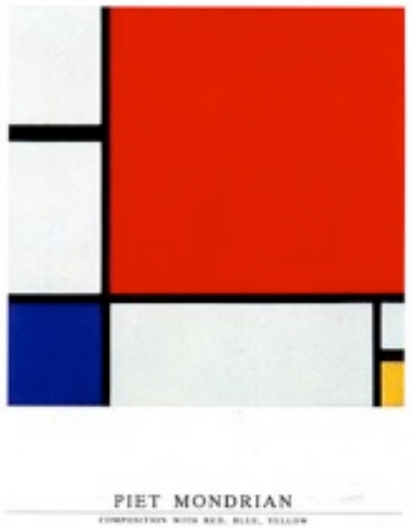

The cold shapes of crystals, volumes delimited by sharp volumes of fixed angles

The sensual shapes of life displaying continuous curvature

Dali Naked In Ecstasy Before Five Regular Bodies

A debate on aesthetic

From García Lorca
Ode to Dali

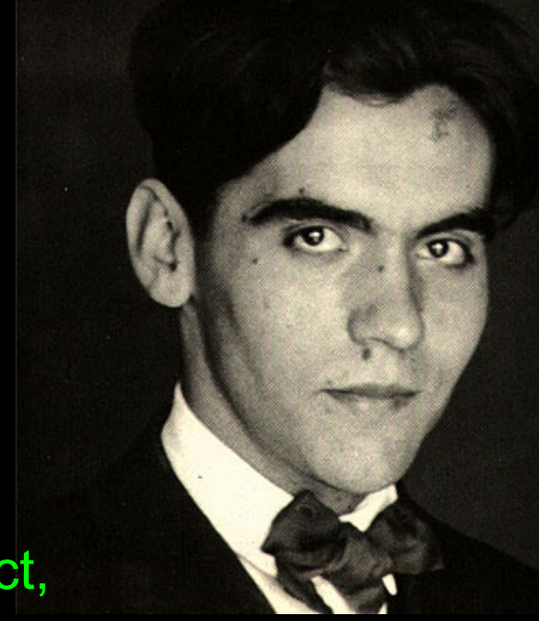

You love a matter definite and exact,
where the toadstool cannot pitch its camp.
You love the architecture that builds on the absent
and admit the flag simply as a joke.

The steel compass tells its short, elastic verse.
Unknown clouds rise to deny the sphere exists.
The straight line tells of its upward struggle
and the learned crystals sing their geometries.

But also the rose of the garden where you live.
Always the rose, always, our north and south!
Calm and ingathered like an eyeless statue,
not knowing the buried struggle it provokes.

Pure rose, clean of artifice and rough sketches,
opening for us the slender wings of the smile.
(Pinned butterfly that ponders its flight.)
Rose of balance, with no self-inflicted pains.
Always the rose!

A debate on aesthetic

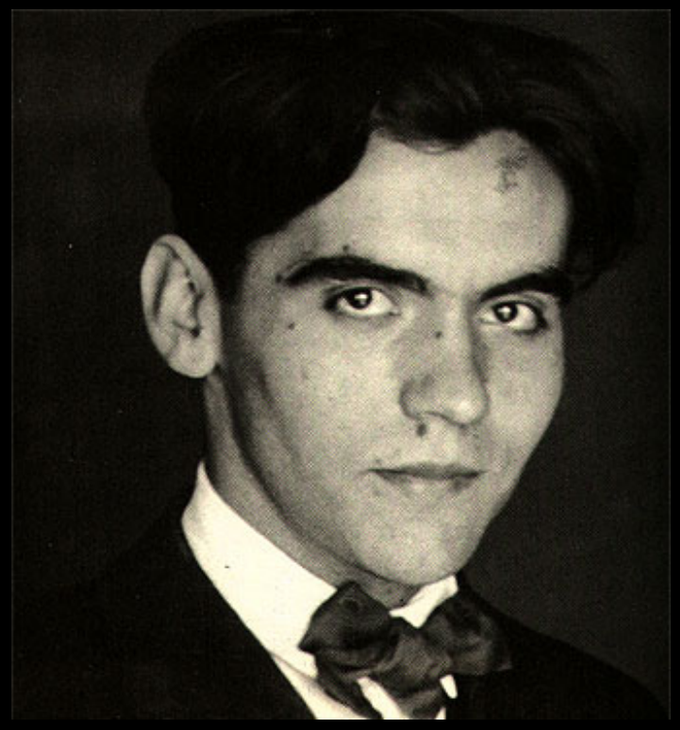

Federico Garcia Lorca
Poet in Nueva York

Assassinated by the sky,
between forms moving towards the serpent
and forms that seek the **crystal**,
I will let my hair grow.

Crystalline Shapes controlled by crystal structure

$32\ G^3_0 \subset K$

$A_i \gamma_i$ = minimum

Faceted crystals, sharp angles, crystallographic dendrites, twining, fluid inclusions, hopper crystals

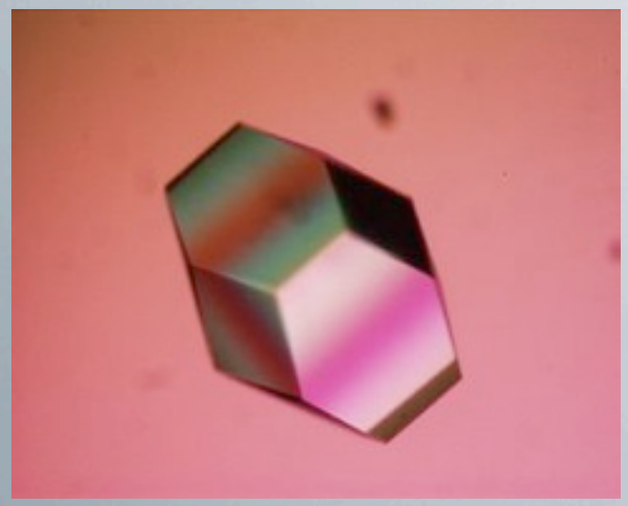

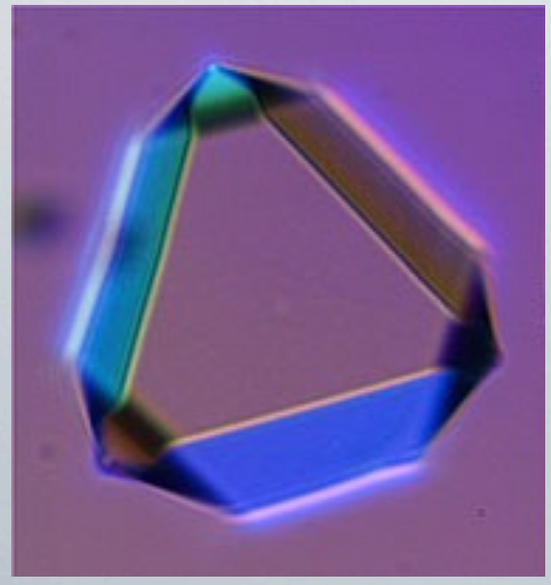

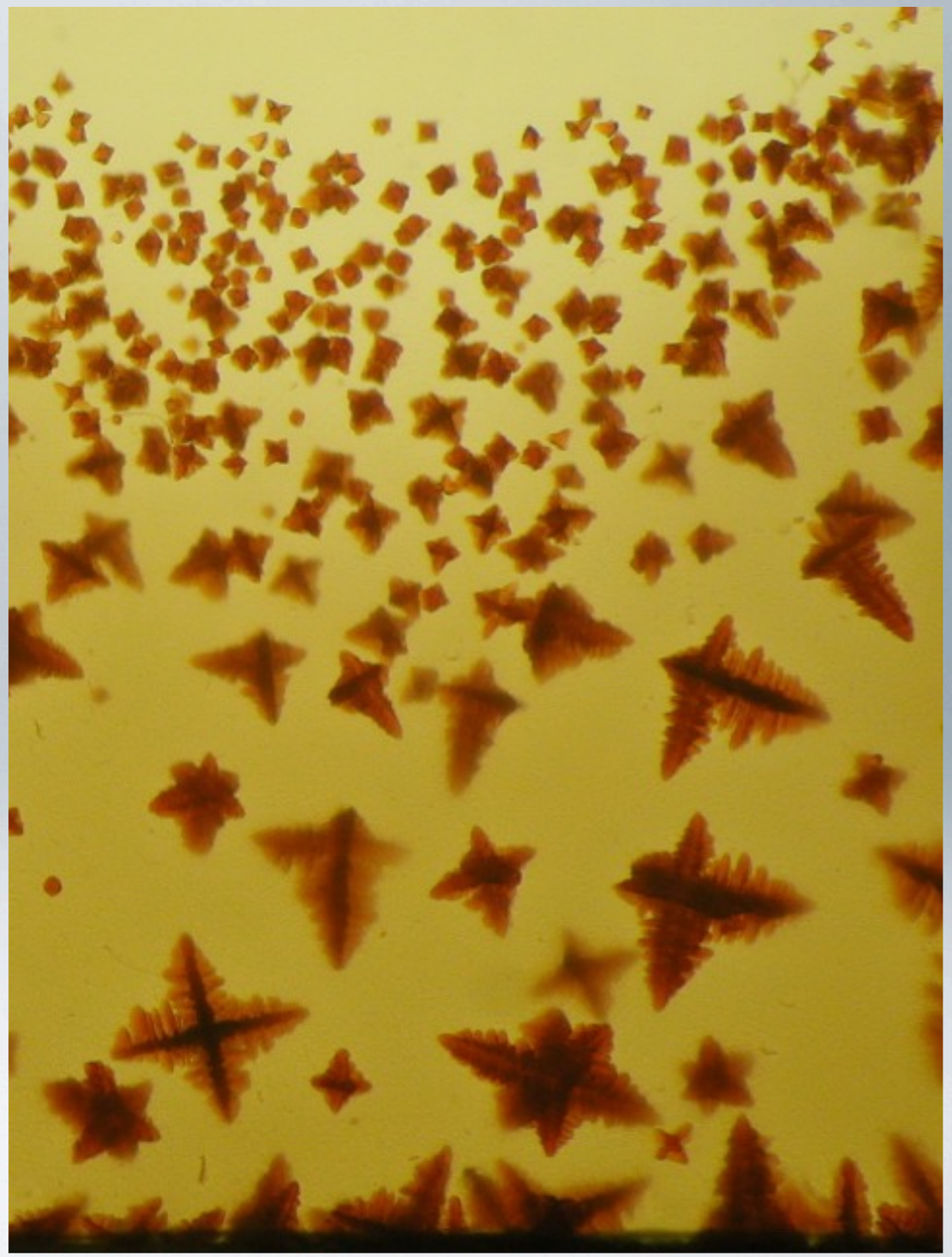

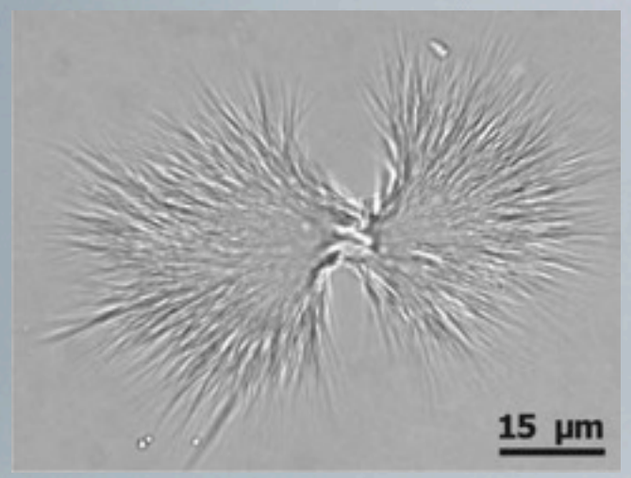
15 µm

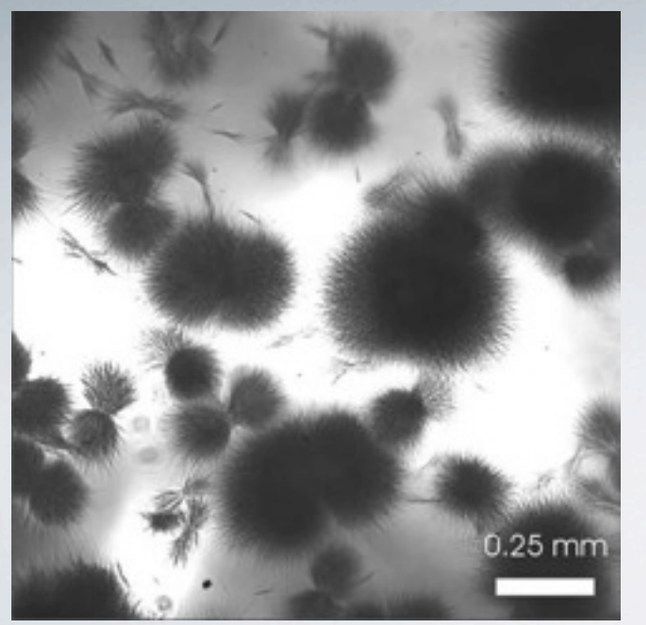
0.25 mm

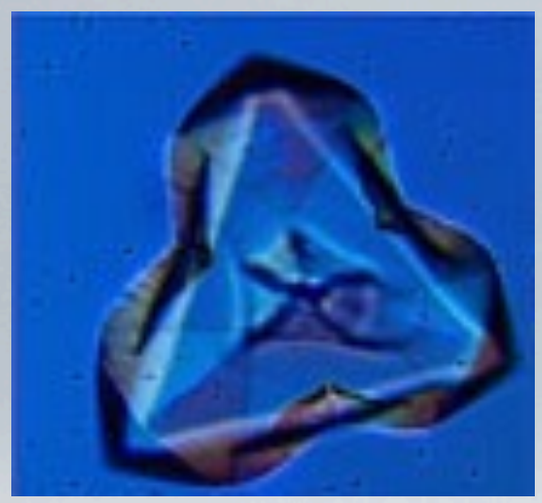

Crystalline Patterns not controlled by crystal structure

$\infty\ G^3_0 \not\subset K$

$A_i\gamma_i >$ minimum

The symmetry of natural shapes

(classical thought)

The realm of the crystal

Inorganic symmetry

Polyhedral, faceted shapes
Deterministic angles
Forbidden symmetry operators

$32\ G^3_0 \subset K$

$A_i\gamma_i$ = minimum

The realm of life

Organic symmetry

Sinuous shapes
Continuous curvature
Unrestricted symmetry

$\infty\ G^3_0 \not\subset K$

$A_i\gamma_i$ > minimum

Are there abiotic precipitation mechanisms producing materials with morphologies reminiscent of primitive life or biomineral textures?

Yes, there are many. But to be relevant for the problem of primitive life detection they have to fulfill three conditions:

1. They must be the result of self-assembled processes

Mineral patterns uncontrolled by crystal structure

There are two ways to break the symmetry restriction imposed by the single crystal structure

Top-down approach: THE TEMPLATE's WAY

Induced morphologies by using templates such a treated surfaces with continuous curvature

- Langmuir-Schäferfilms (Berman, et al., Science, 1995, 269, 515-518)
- Stearic acid monolayers, Pouget et al., Science 323 (2009) 1455
- Functionalized self-assembled monolayers, Aizenberg, JACS 121 (1999) 4500
- Micelles, by-layers and colloidal structured surfaces

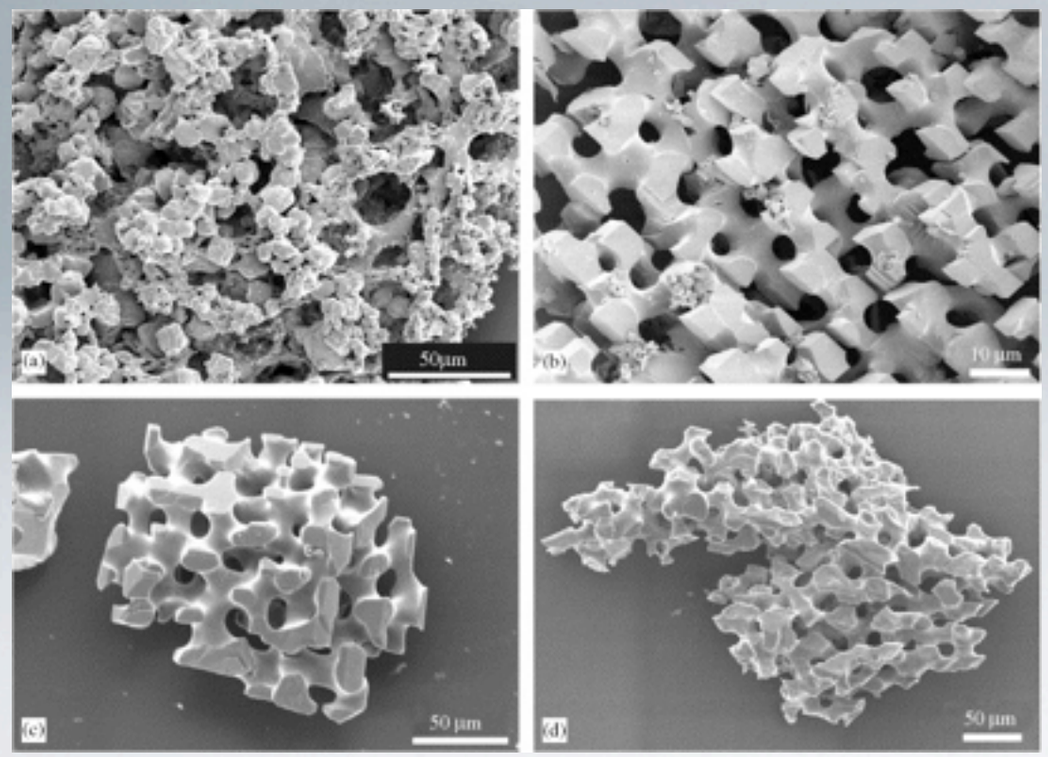

Yue et al., J. Crystal Growth 294 (2006) 69

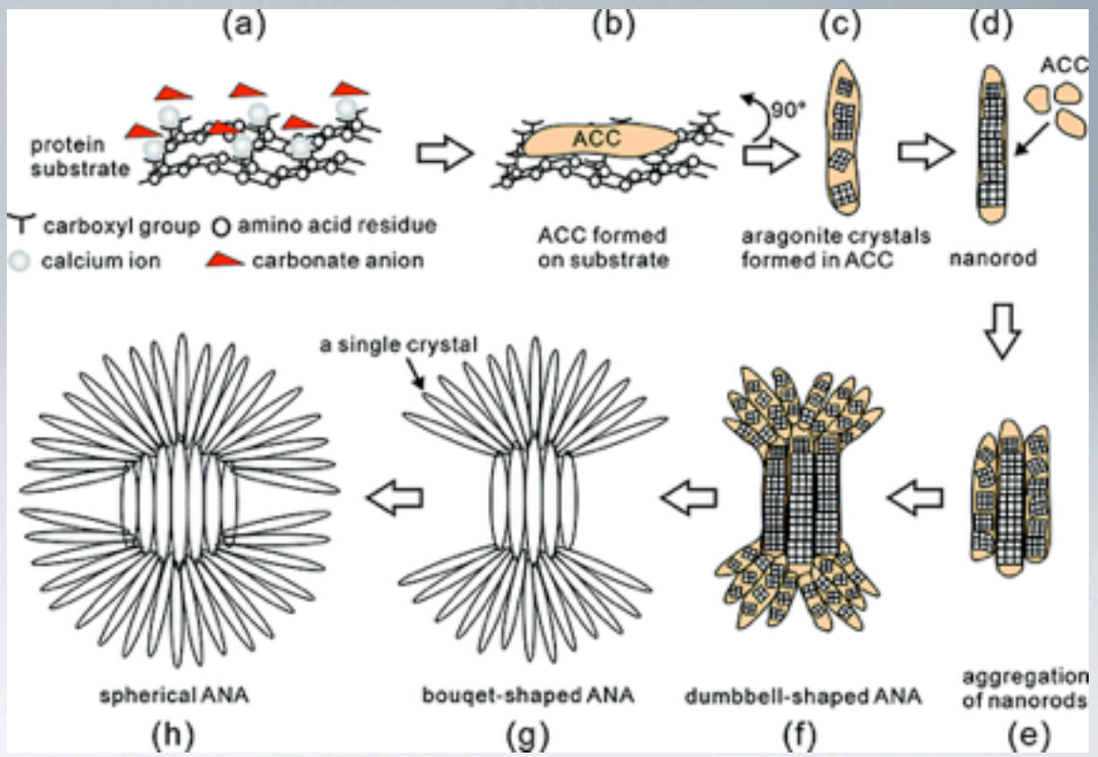

Z. Huang and G. Zhang , Crystal Growth & Design 12 (2012)1816

Are there abiotic precipitation mechanisms producing materials with morphologies reminiscent of primitive life or biomineral textures?

Yes, there are many. But to be relevant for the problem of primitive life detection, they have to fulfill three conditions:

1. They must be the result of self-assembled processes
2. They must be fully inorganic

Biomineralization:

Key role of the organic compounds in controlling the nucleation, size and orientation of carbonate crystals, thus breaking symmetry restriction of single crystals

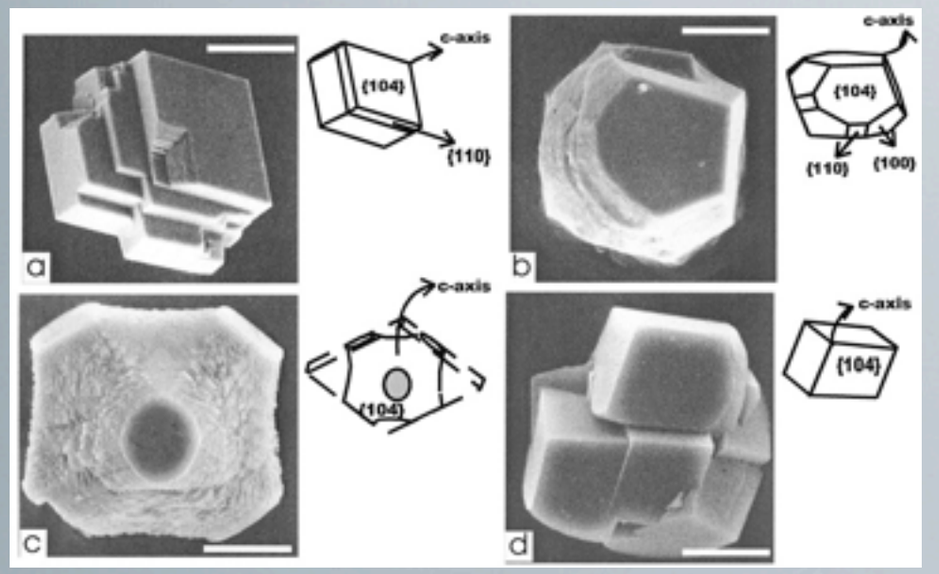

C. Jimenez-Lopez et al., Geoch. Cosmoch. Acta 67 (2003) 1667

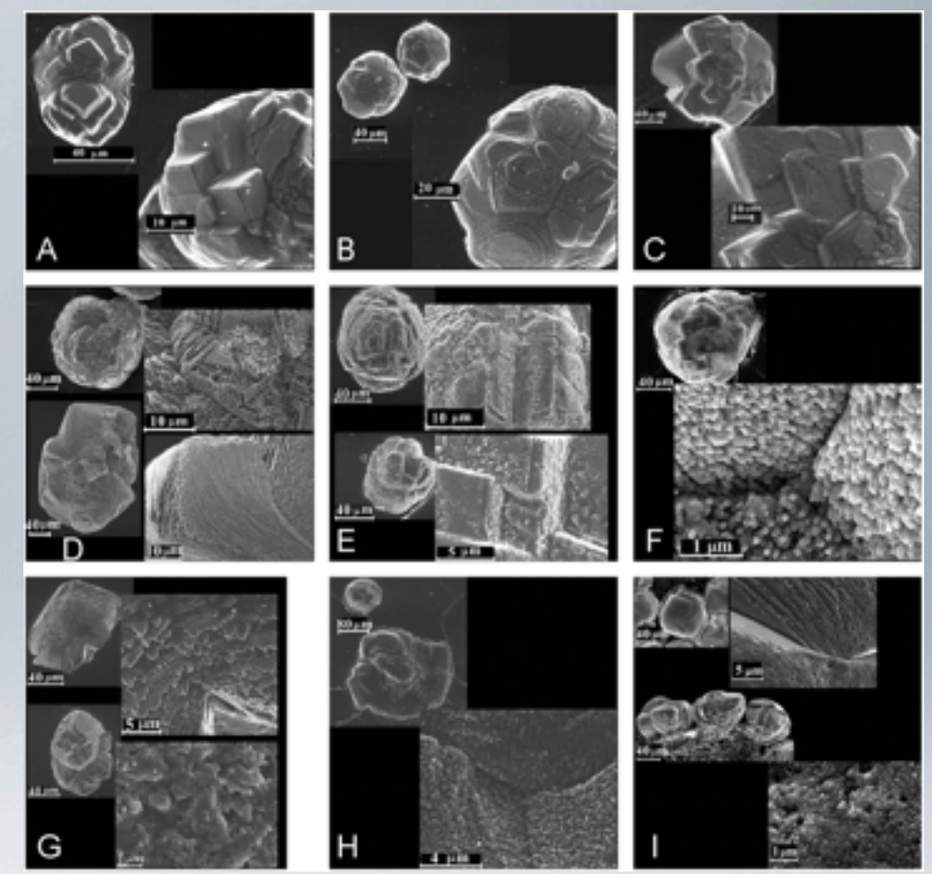

A. Hernandez-Hernandez et al. , Journal of Crystal Growth 310 (2008) 1754–1759

Are there abiotic precipitation mechanisms producing materials with morphologies reminiscent of primitive life or biomineral textures?

Yes, there are many. But to be relevant for the problem of primitive life detection, they have to fulfill three conditions:

1. They must be the result of self-assembled processes
2. They must be fully inorganic
3. They must be geochemically plausible

Mineral patterns uncontrolled by crystal structure

Bottom-up approach: THE SELF-ORGANIZED WAY

- Additives adhering preferentially on crystalline faces
- Patterns controlled by fluid structures
- Mesoscopic phases, liquid crystals,
- Diffusion-reaction systems, such as Liesegang's precipitation,
- Dissipative structures,
- Chaotic mixing of fluids,
- Fractal viscous fingering and DLA
- Competitive crystallization,
- **Silica biomorphs**
- **Chemical gardens**

Why silica ?

Silica is ubiquitous in Earth

In addition silica played a main role in Earth's chemistry before any complex organic compound appeared

Mineral patterns uncontrolled by crystal structure

Bottom-up approach: THE SELF-ORGANIZED WAY

- Additives adhering preferentially on crystalline faces
- Patterns controlled by fluid structures
- Mesoscopic phases, liquid crystals,
- Diffusion-reaction systems, such as Liesegang's precipi
- Dissipative structures,
- Chaotic mixing of fluids,
- Fractal viscous fingering and DLA
- Competitive crystallization,
- **Silica biomorphs**
- **Chemical gardens**

Why silica ?

Silica is ubiquitous in Earth

In addition silica played a main role in Earth's chemistry before any complex organic compound appeared

A: Silica Biomorphs B: Silica gardens

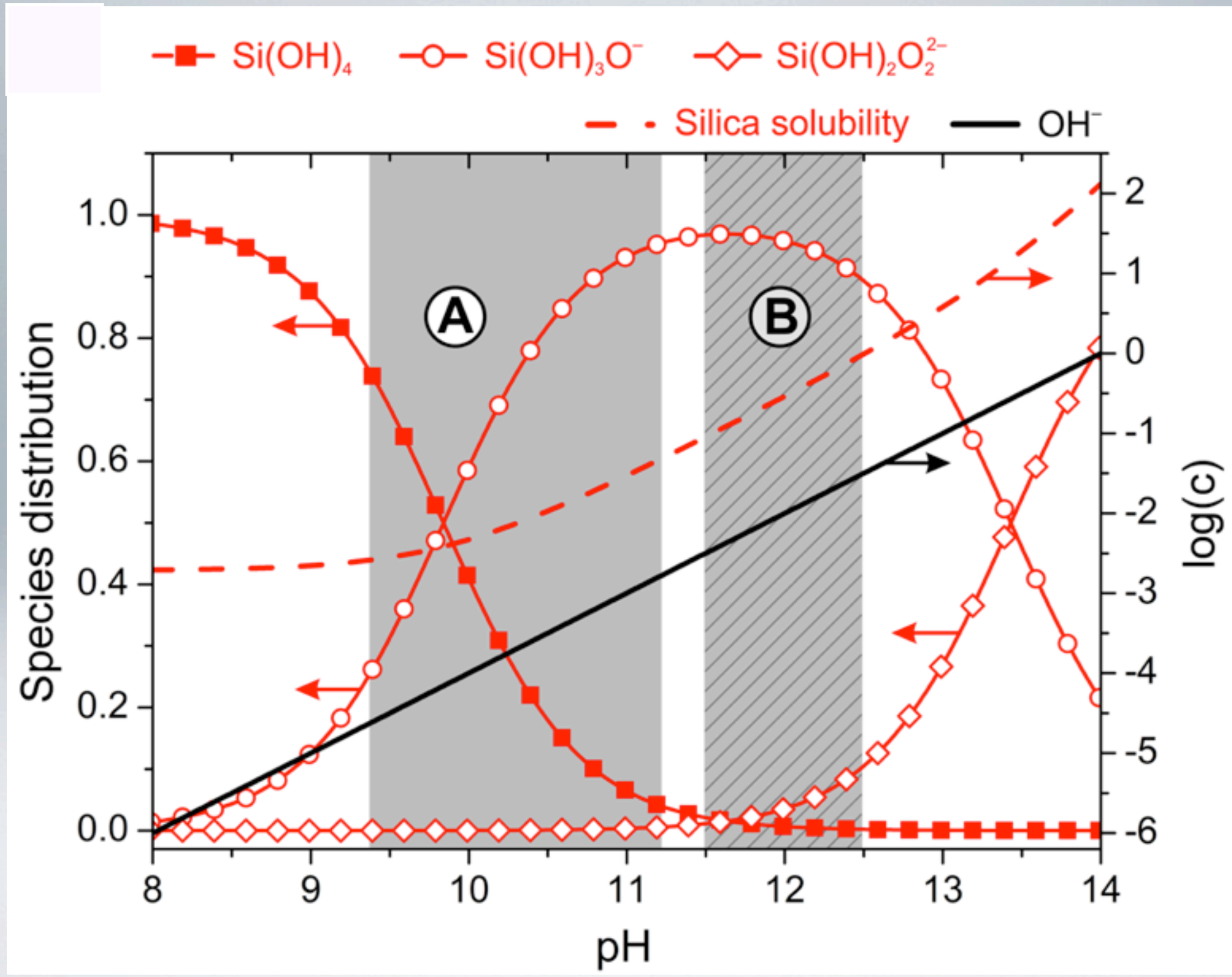

A: Silica Biomorphs B: Silica gardens

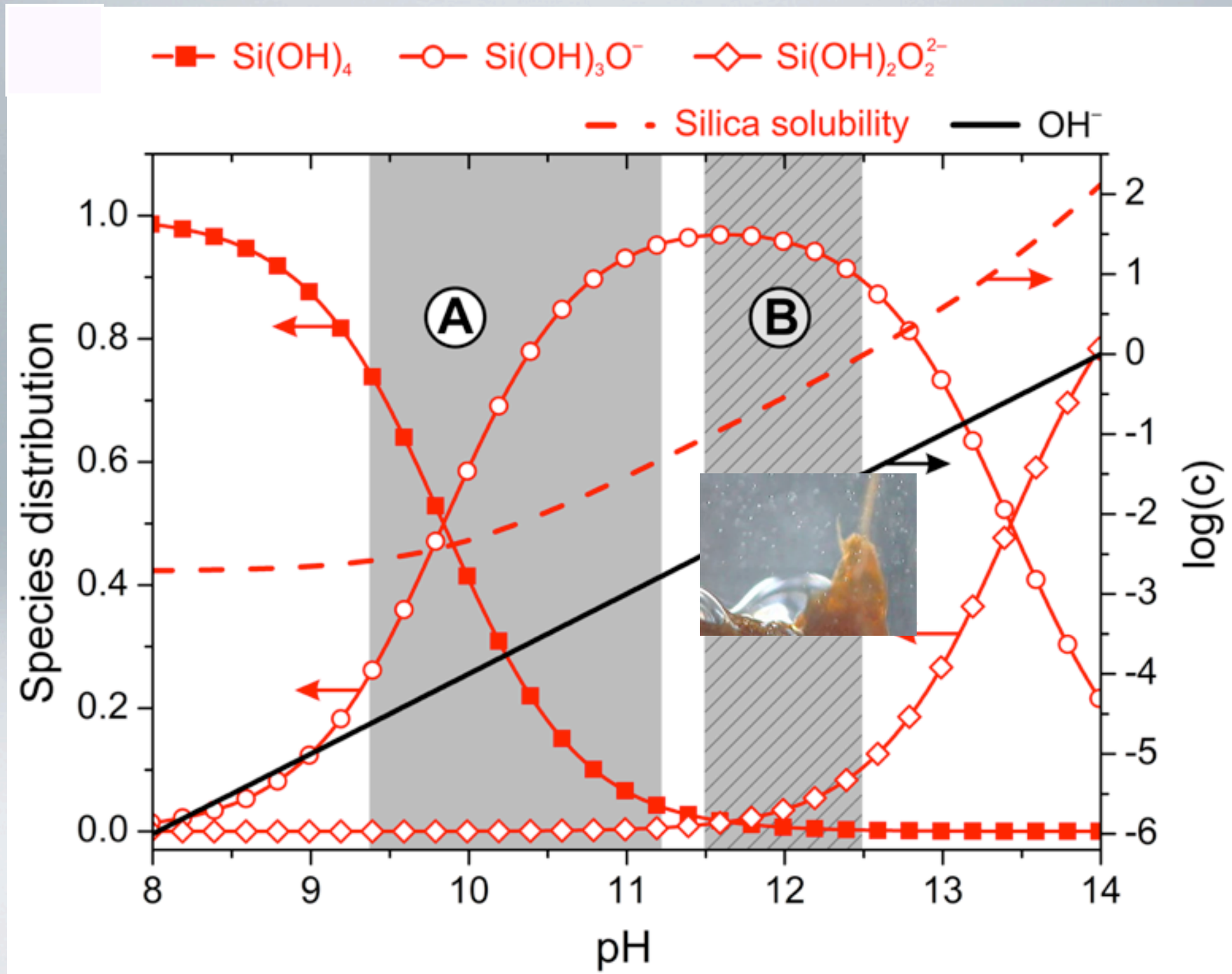

Iron^{2+} silica garden

A: Silica Biomorphs B: Silica gardens

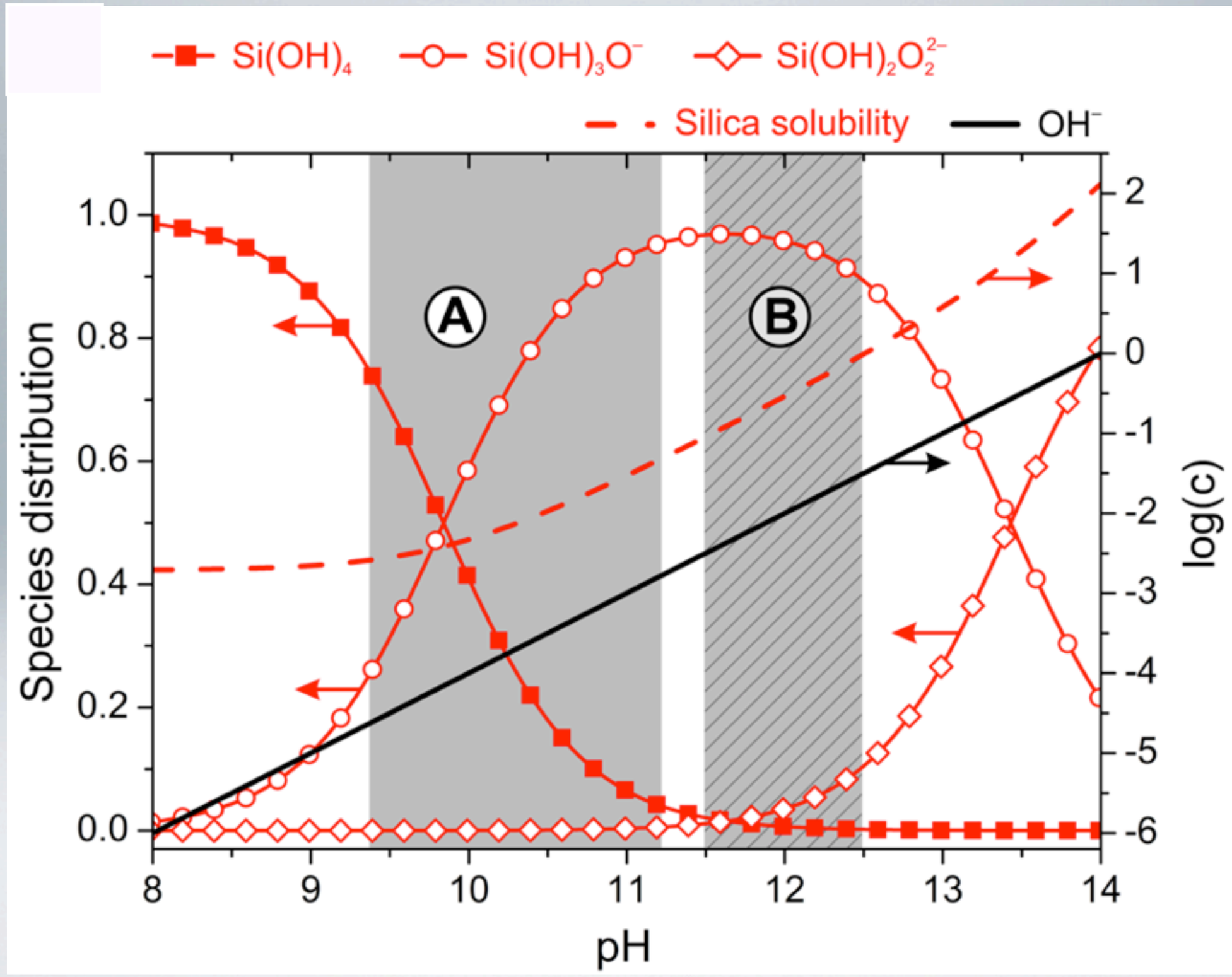

A: Silica Biomorphs B: Silica gardens

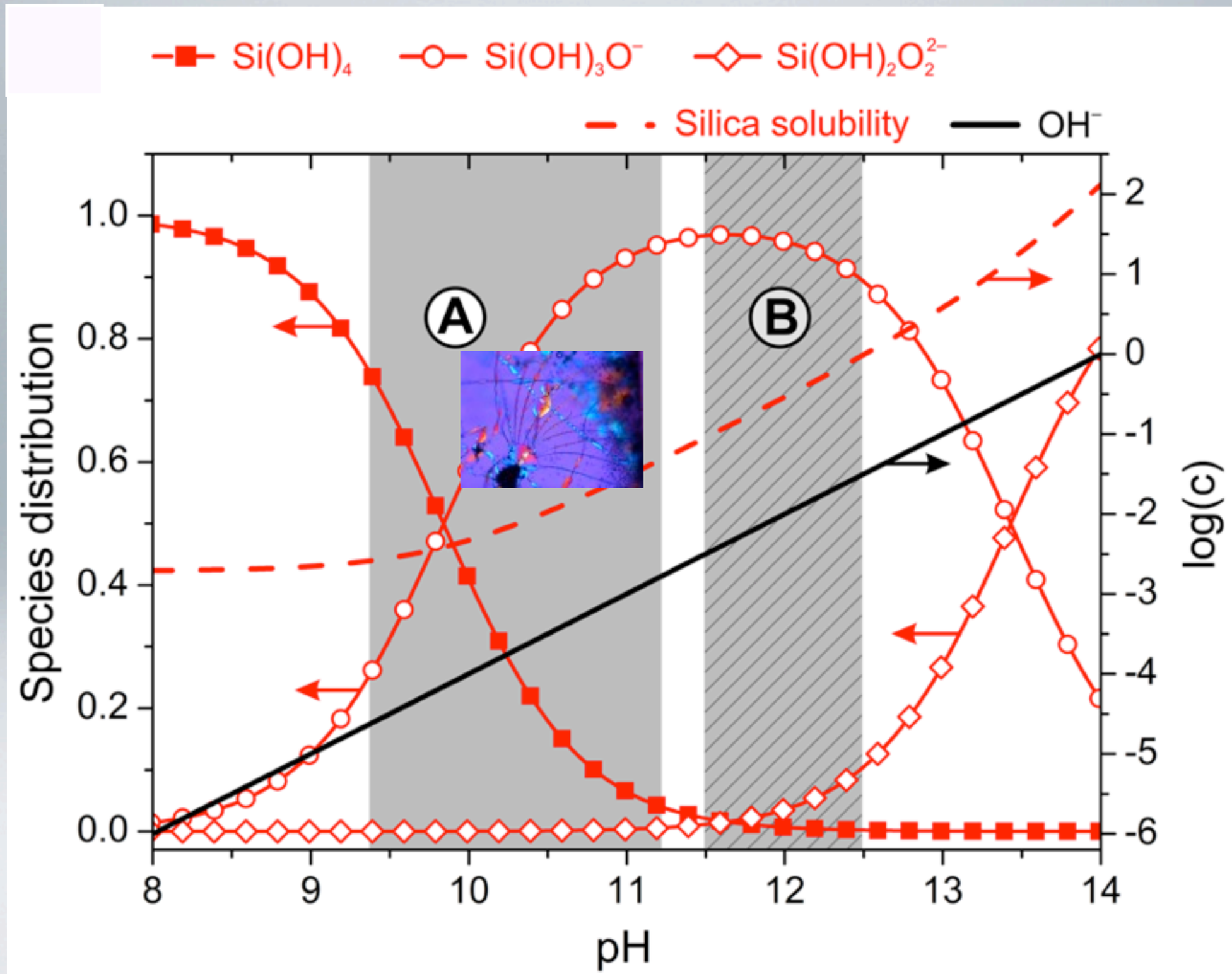

Preparation of silica/carbonate biomorphs

In solution

1:350 diluted waterglass at pH 11.3

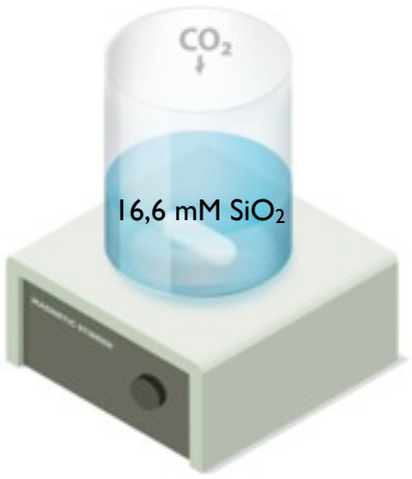

Add equal volume of $BaCl_2$ 0.01 M at pH 6.0. Final pH: 11.0

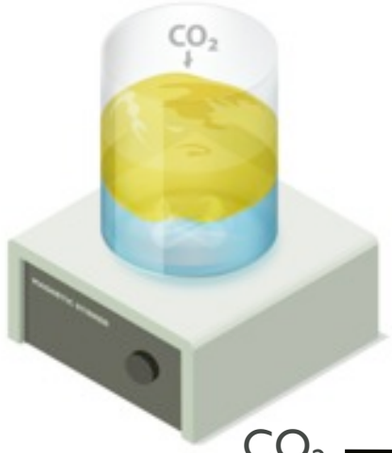

Barium carbonate biomorphs will appear on the water/solution interface and on the walls of the vessel

Room conditions
but they also form at higher pressure and temperature

$CO_2 \longrightarrow HCO_3$ and $CO_3^{=}$

In gels

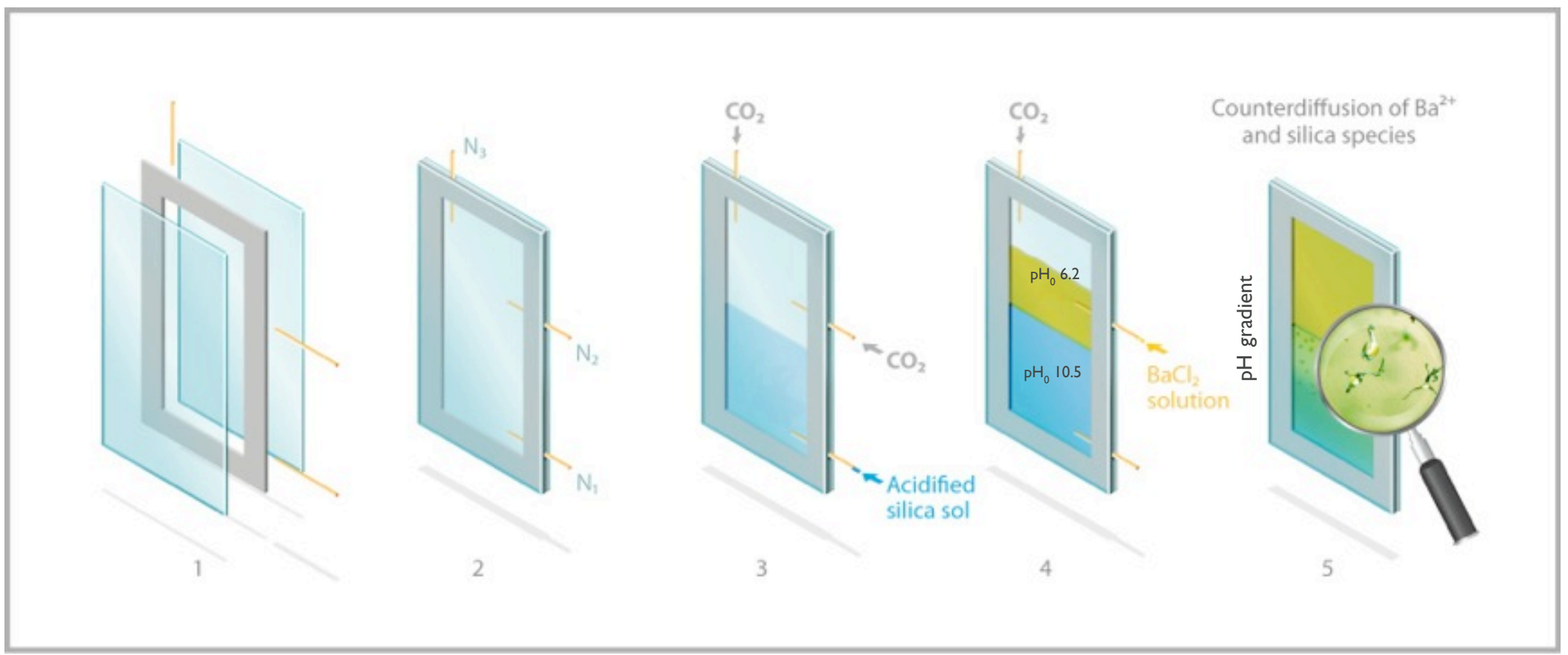

Silica/carbonate biomorphs

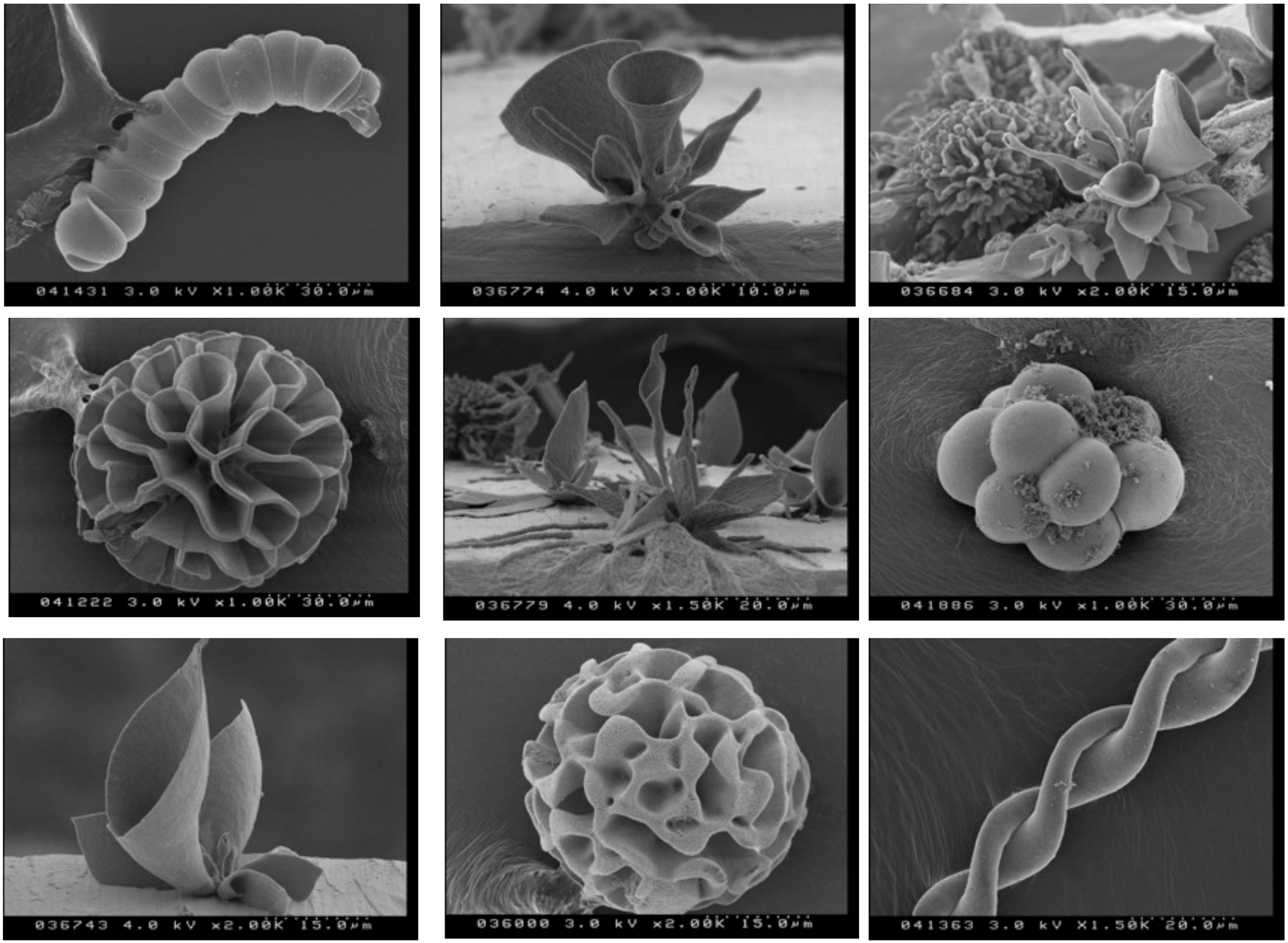

J.M. García-Ruiz, A. Carnerup, A. Christy, N. J. Welham, and S. Hyde, Astrobiology 2 (2002) 335

S.T. Hyde, A. M. Carnerup, A-K. Larsson, A.G. Christy, J.M. García-Ruiz, Physica A 339 (2004) 24

Silica/carbonate biomorphs

Silica/carbonate biomorphs are self-assembled nano-crystalline aggregates displaying differentiable morphologies of constant positive or negative Gaussian curvatures.

Silica/carbonate biomorphs, though abiotically produced, mimic remarkably the morphology of living organisms and the texture of biological skeletons.

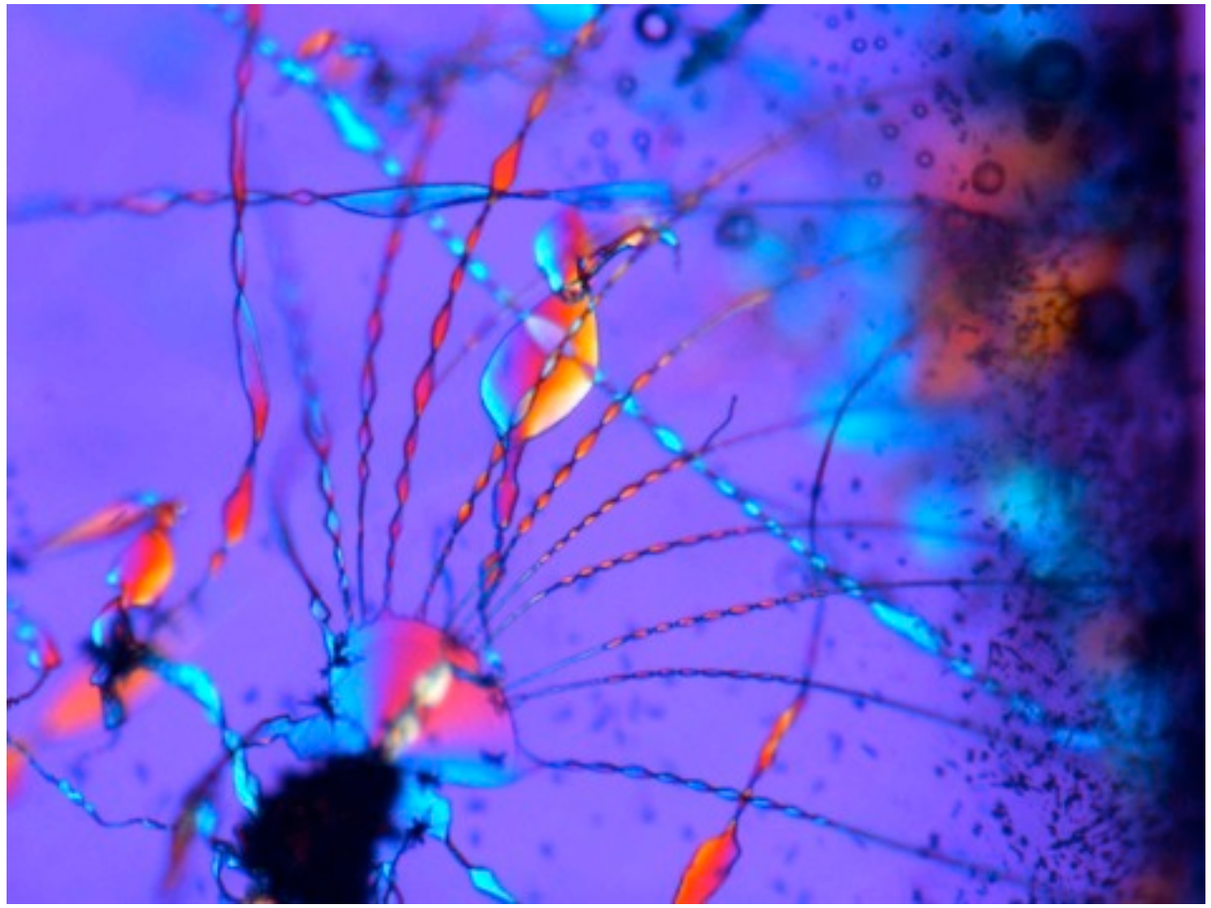

Facts

1. XRD and nfrared spectroscopy shows a composite material made of crystalline $BaCO_3$ and an amorphous phase of tetraedrically coordinated silica.
2. EDX-TEM and FESEM and dissolution experiments prove the existence of an outer silica layer covering the whole crystal aggregate. This silica skin appears after the formation of the crystal aggregates
3. The crystalline phase is made of nano-crystals
4. Morphology is pH dependent. At lower pH range fractal sheaf-of-wheat and globular cauliflower-like crystal aggregates. At higher pH range morphology displayed complex shapes, with positive and negative gaussian curvature, like cardioids and twisted ribbons
5. Morphogenesis is independent of fluid dynamics.
6. Growth kinetics is controlled by reaction
7. Only orthorhombic carbonates create morphologies beyond the fractal route

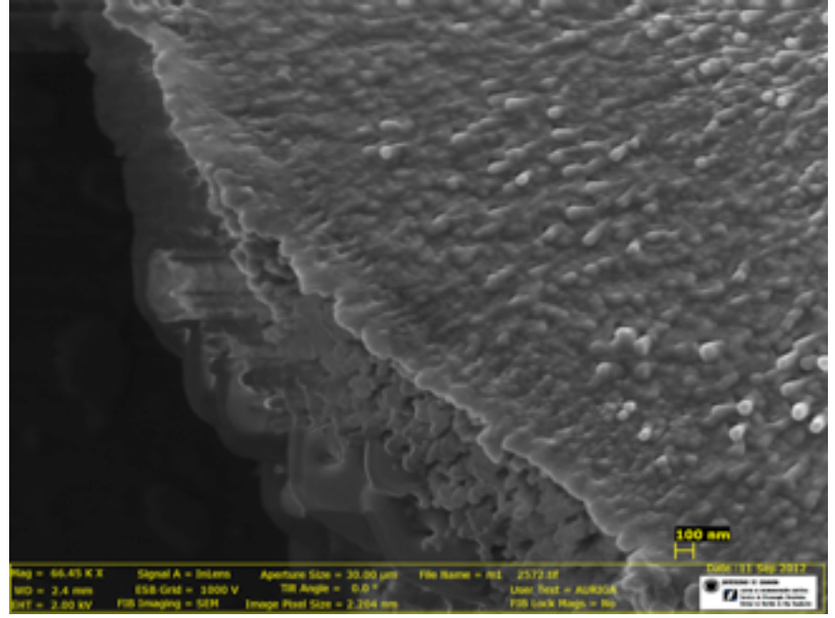

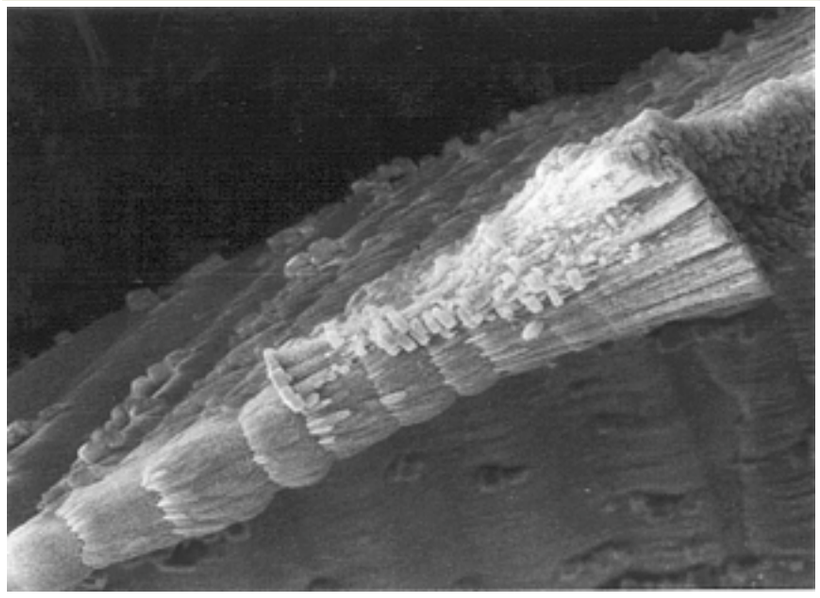

Facts

1. XRD and nfrared spectroscopy shows a composite material made of crystalline $BaCO_3$ and an amorphous phase of tetraedrically coordinated silica.
2. EDX-TEM and FESEM and dissolution experiments prove the existence of an outer silica layer covering the whole crystal aggregate. This silica skin appears after the formation of the crystal aggregates
3. The crystalline phase is made of nano-crystals
4. Morphology is pH dependent. At lower pH range fractal sheaf-of-wheat and globular cauliflower-like crystal aggregates. At higher pH range morphology displayed complex shapes, with positive and negative gaussian curvature, like cardioids and twisted ribbons
5. Morphogenesis is independent of fluid dynamics.
6. Growth kinetics is controlled by reaction
7. Only orthorhombic carbonates create morphologies beyond the fractal route

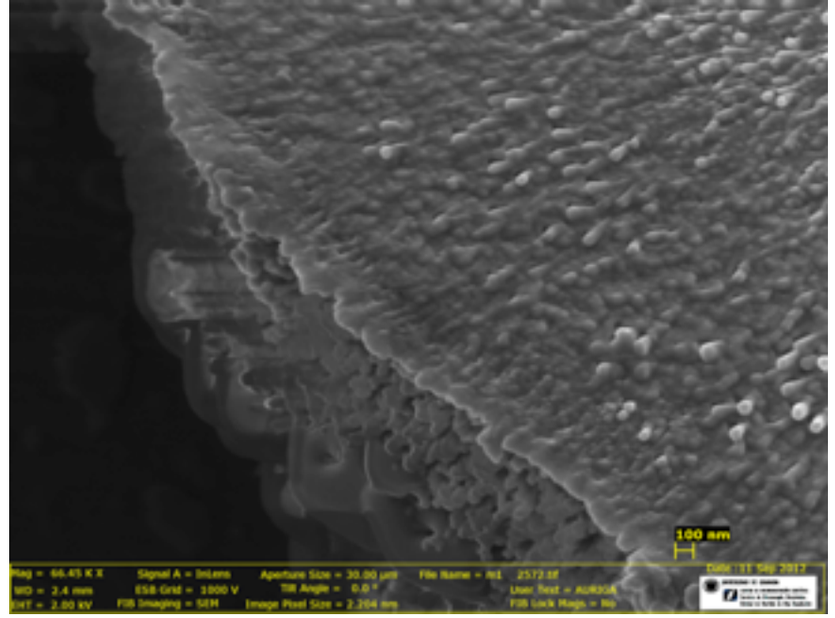

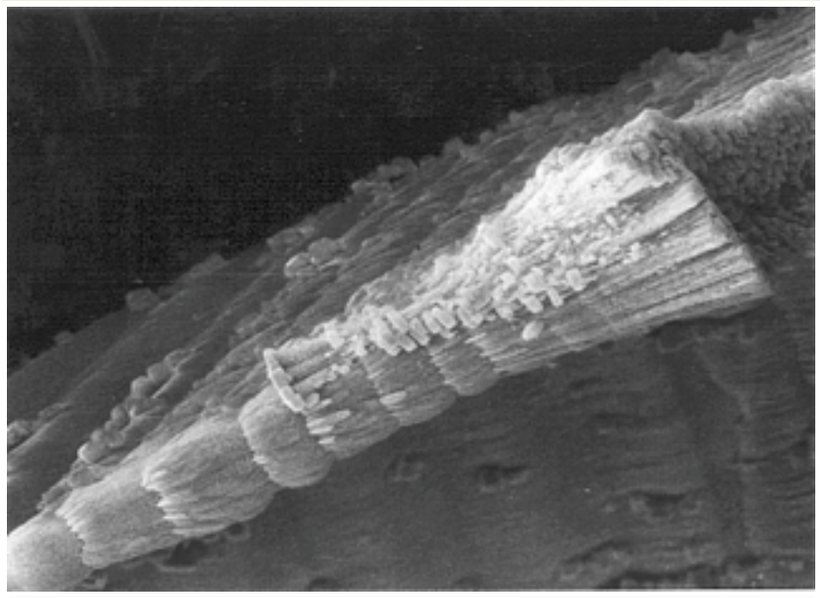

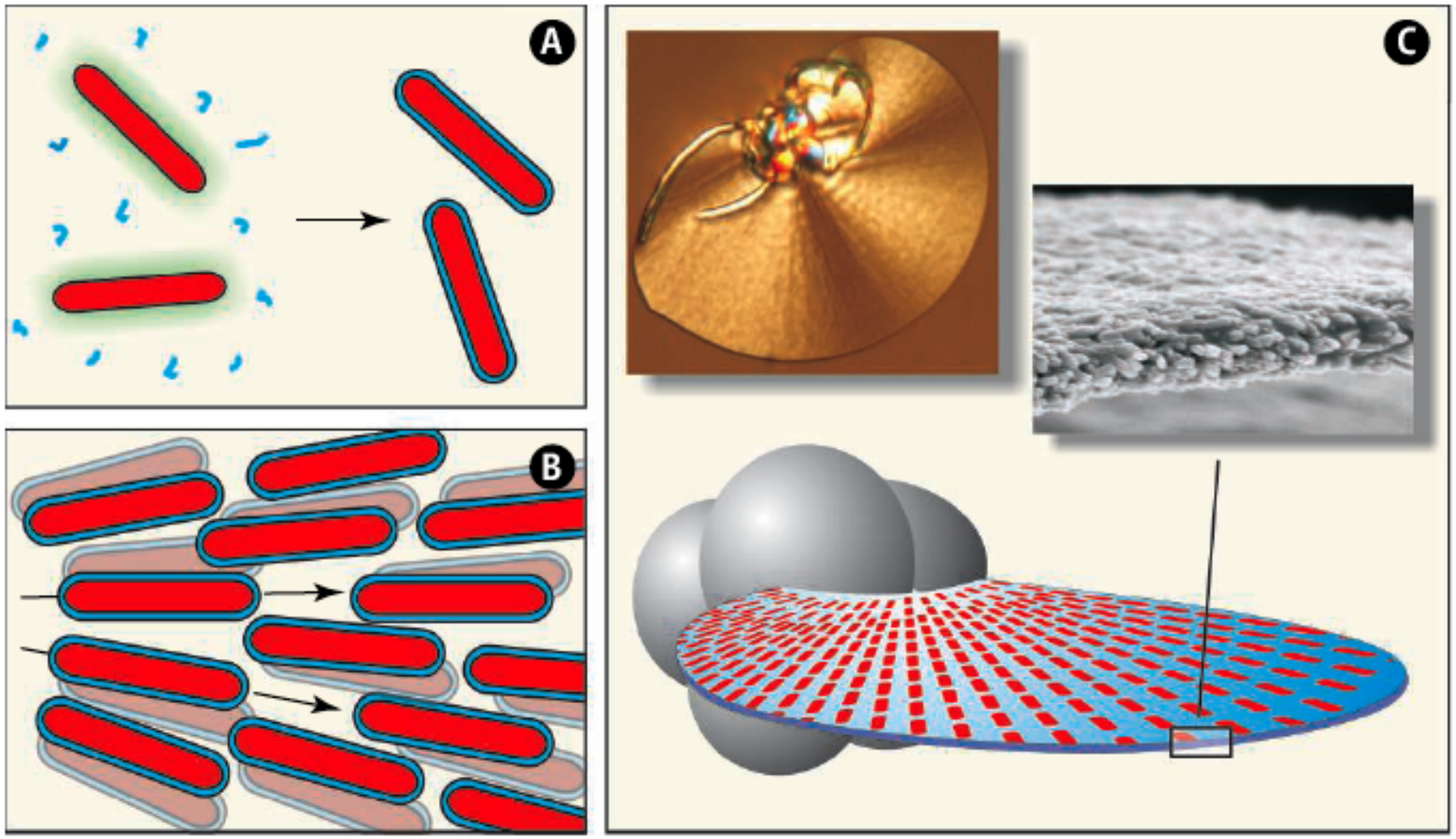

Self-assembled carbonate crystals coated/embedded in silica

M. Kellermeier and W. Kunz, Science 323 (2009) 344

Two consecutive morphological routes

The first of these routes goes from crystallographic towards dilation symmetry

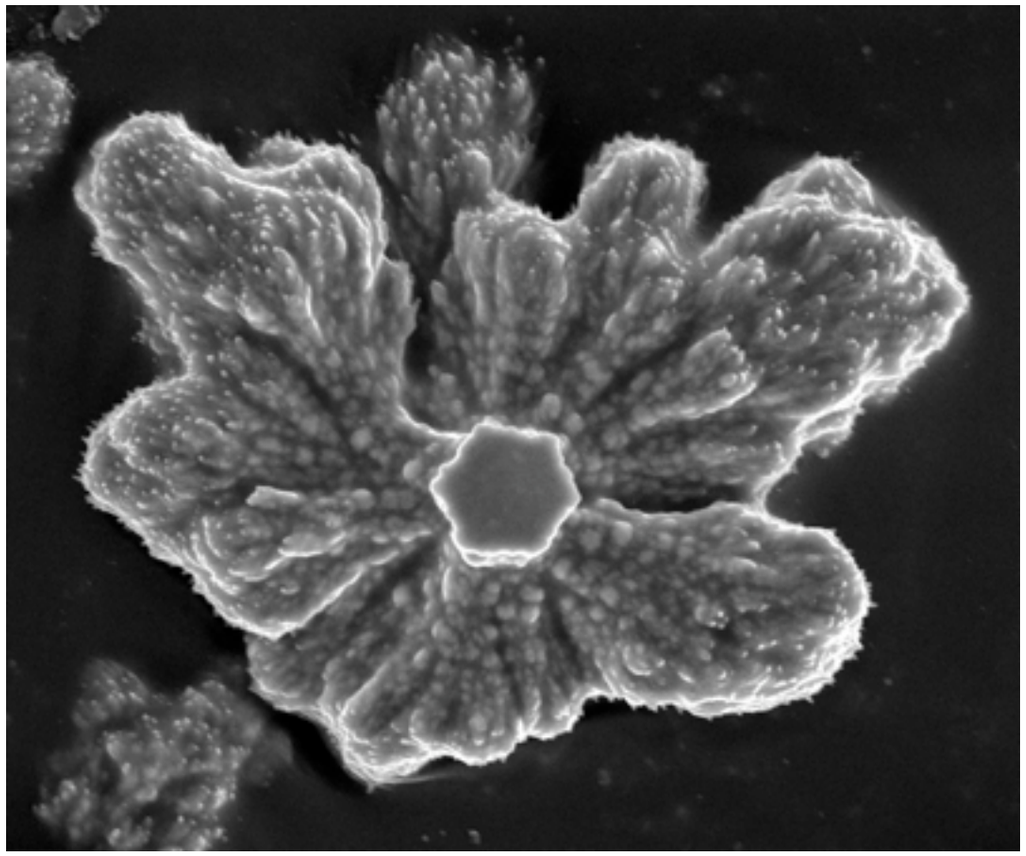

The second one continues towards rotational symmetry

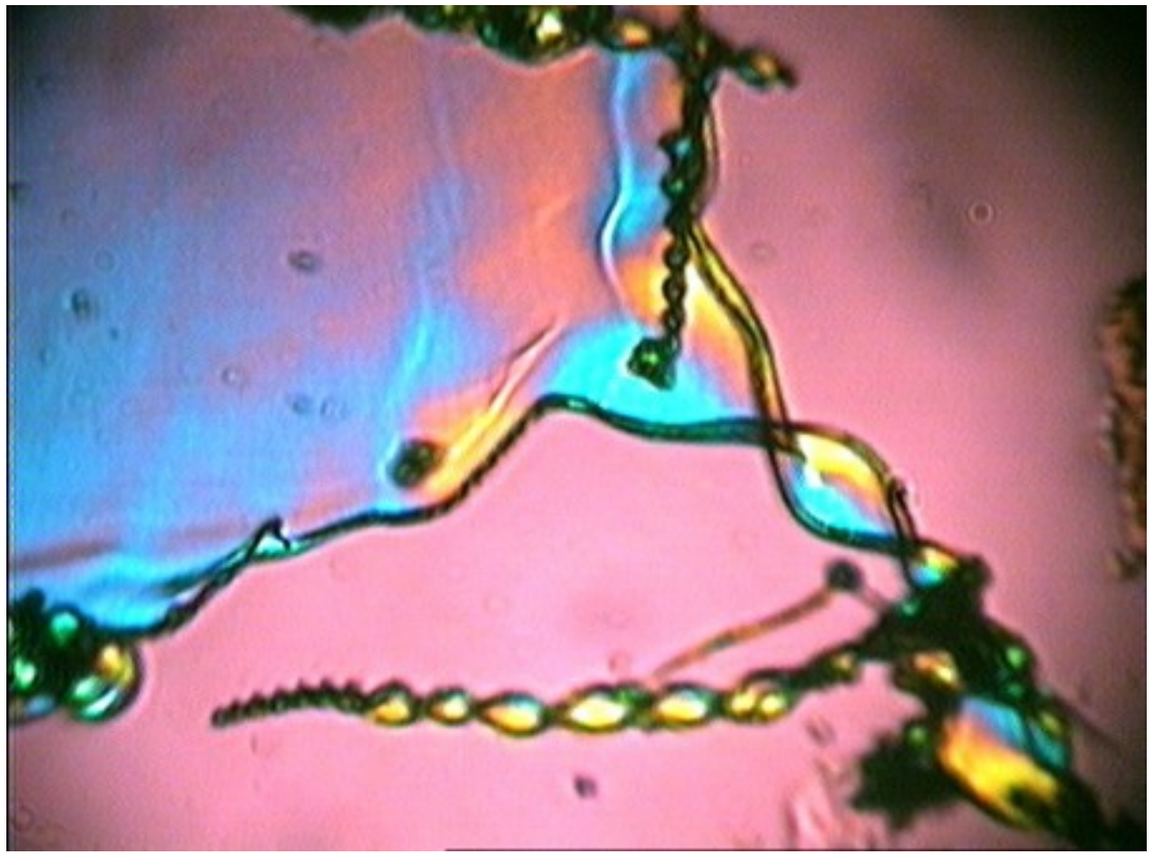

The first of these two routes goes from crystallographic towards dilation symmetry

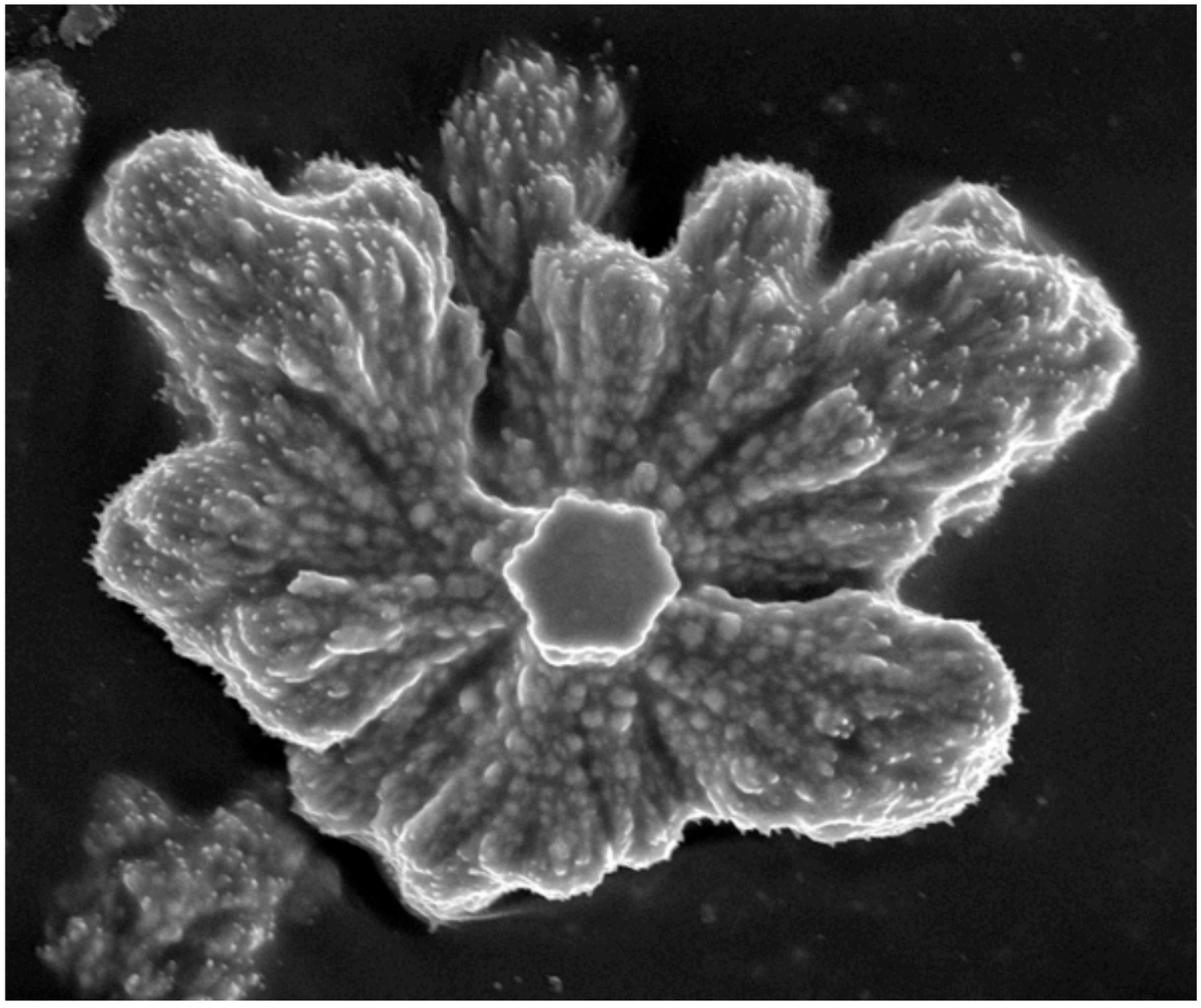

Silica/carbonate biomorphs arise from a single crystal.

As for biomineral skeletons, **the symmetry of the single crystal core must be broken to create shapes with non-crystallographic symmetry.**

The fractal route: from single crystal to fractal dendrites …

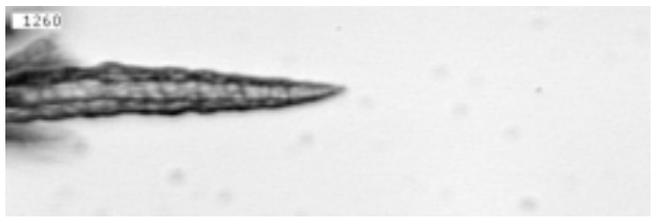

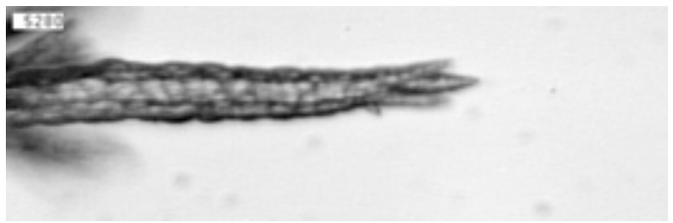

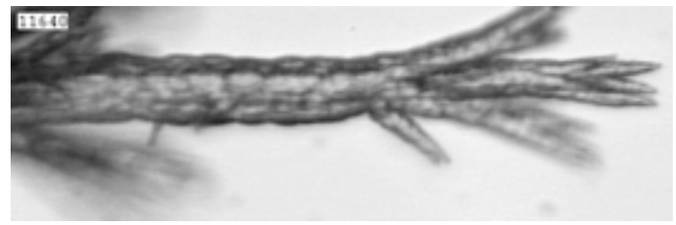

by continuous crystal splitting at non-crystallographic angles

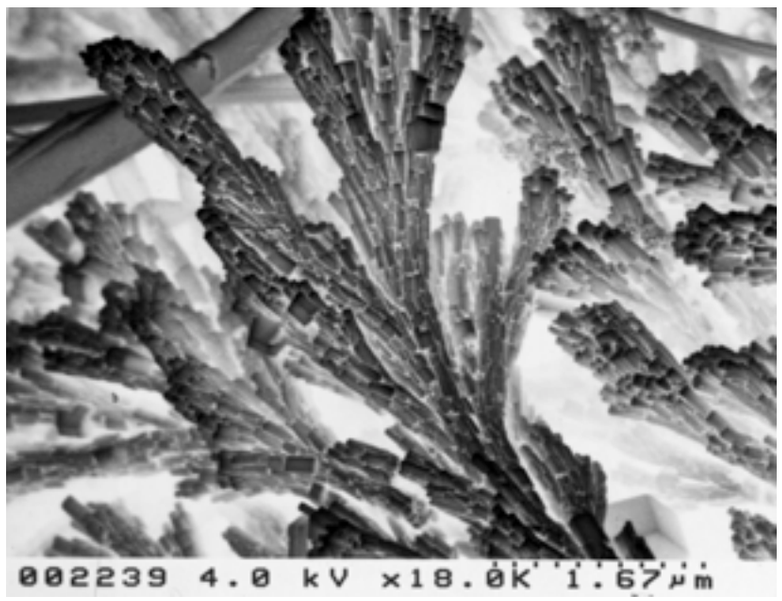

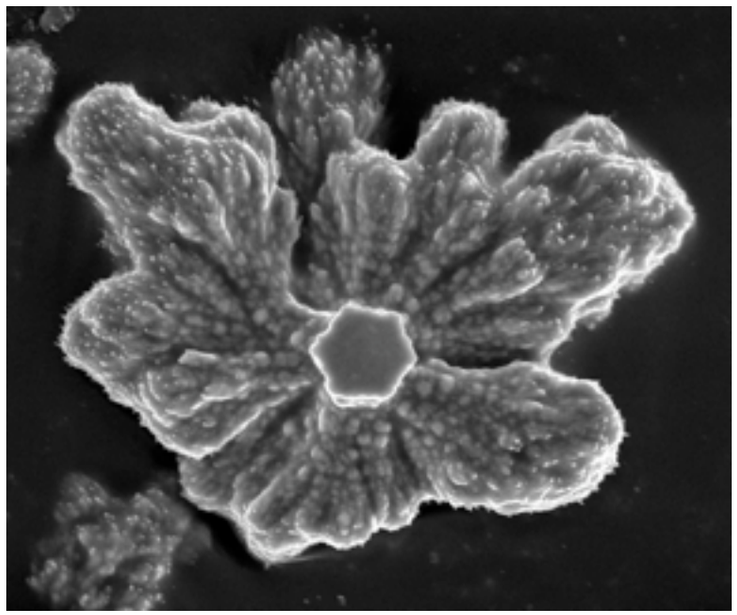

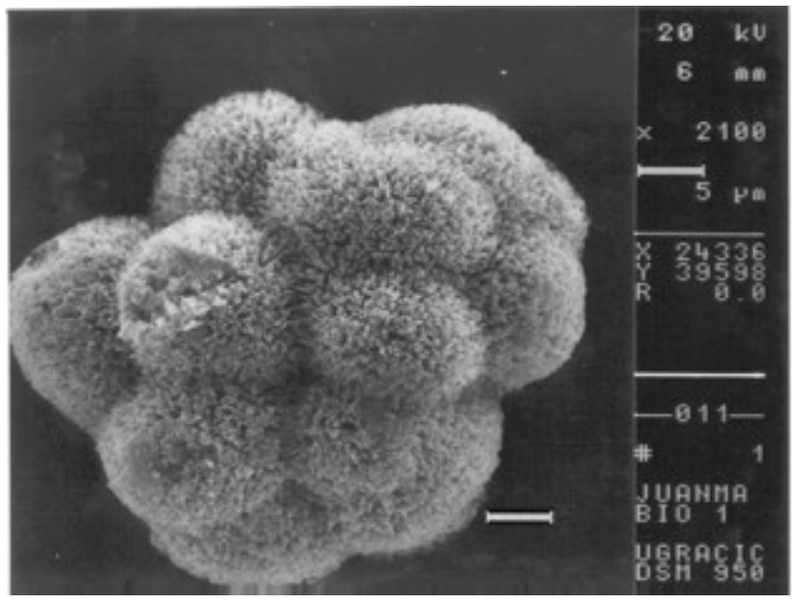

Explanation proposed by Keith & Padden (1963) theory based on the role of polymeric impurities

The fractal route: from single crystal to fractal dendrites …

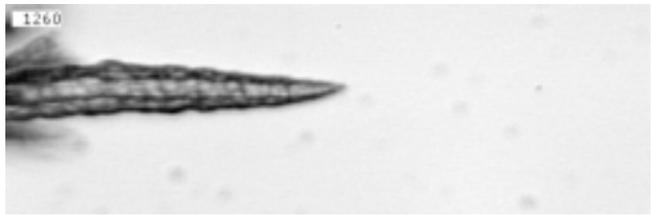

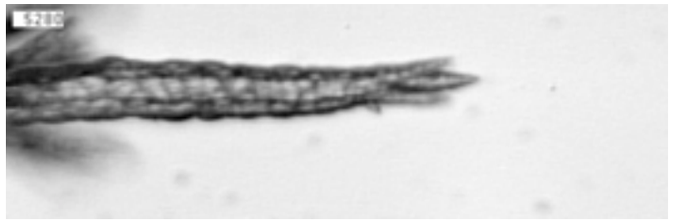

by continuous crystal splitting at non-crystallographic angles

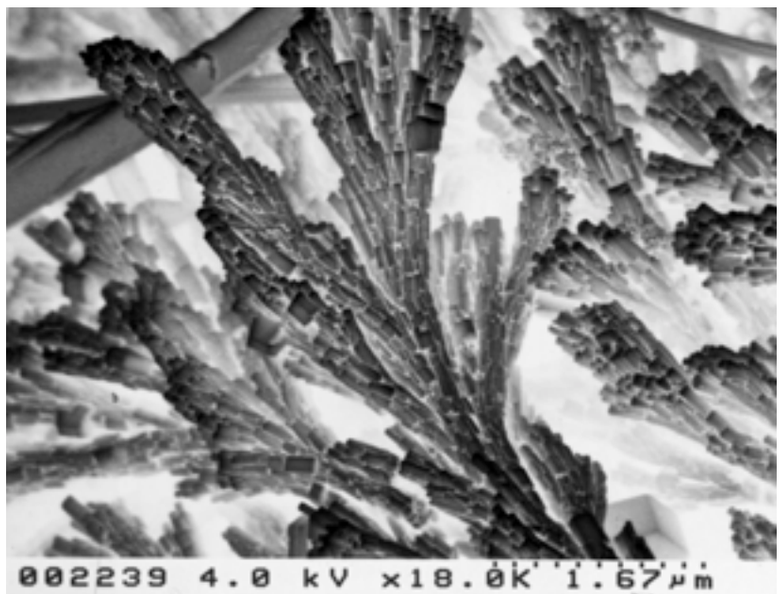

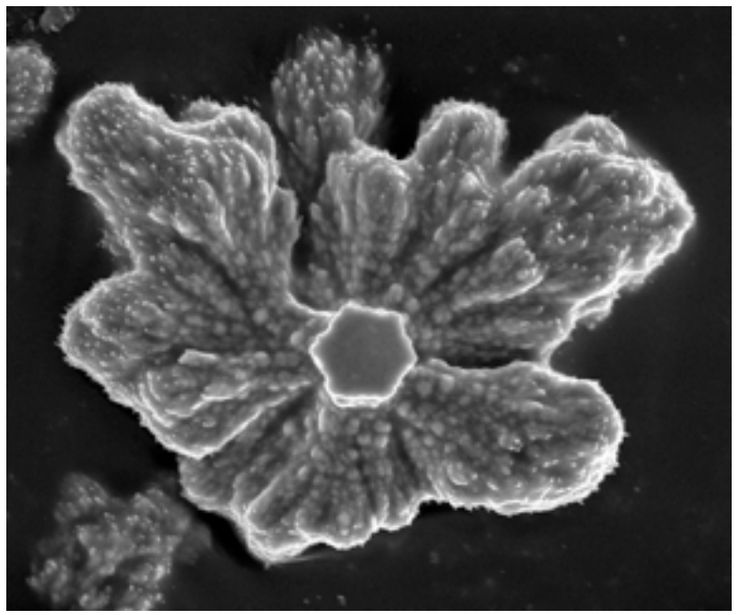

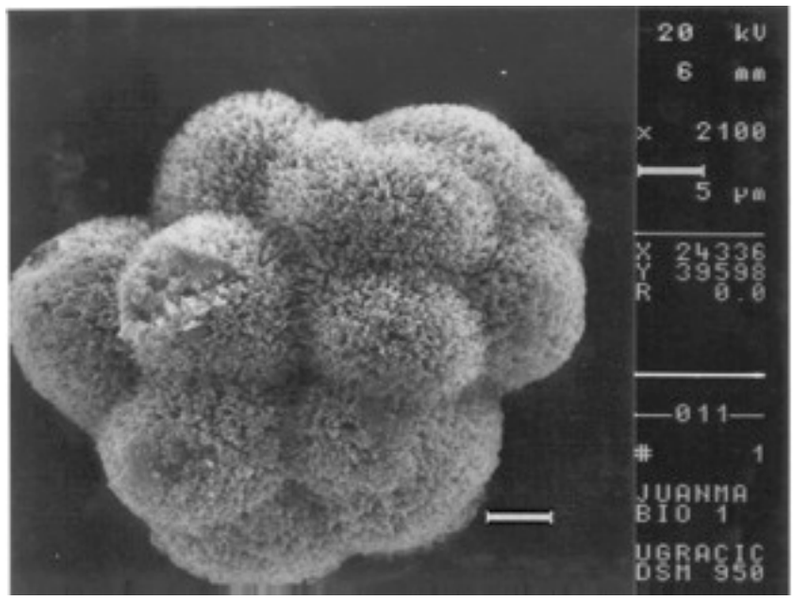

Explanation proposed by Keith & Padden (1963) theory based on the role of polymeric impurities

Fibrillation: the gate to complex shapes with continuous curvature

At higher pH, the silica supersaturation obtained by pH change can be important enough to provoke fibrillation, i.e. the transition from single crystal to a sheet-like polycrystalline material growing by oriented aggregation.

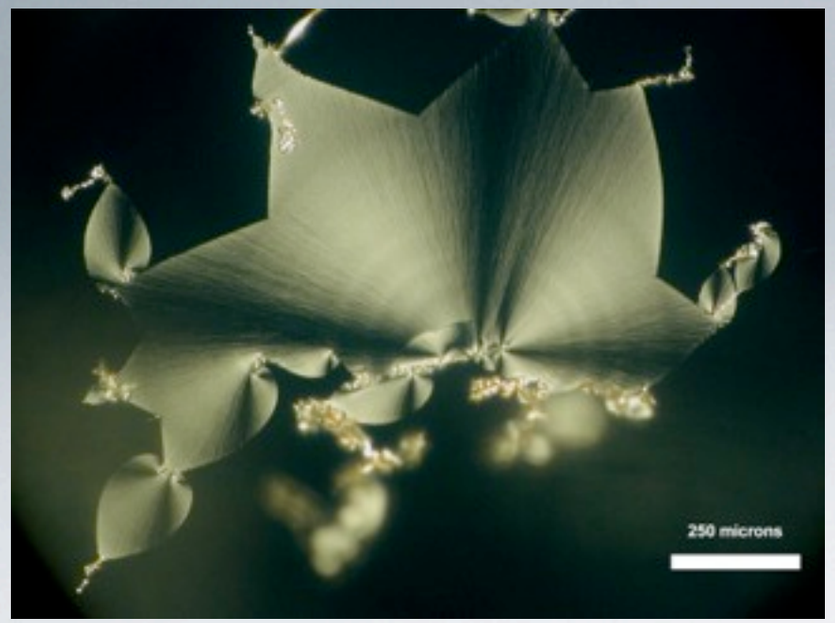

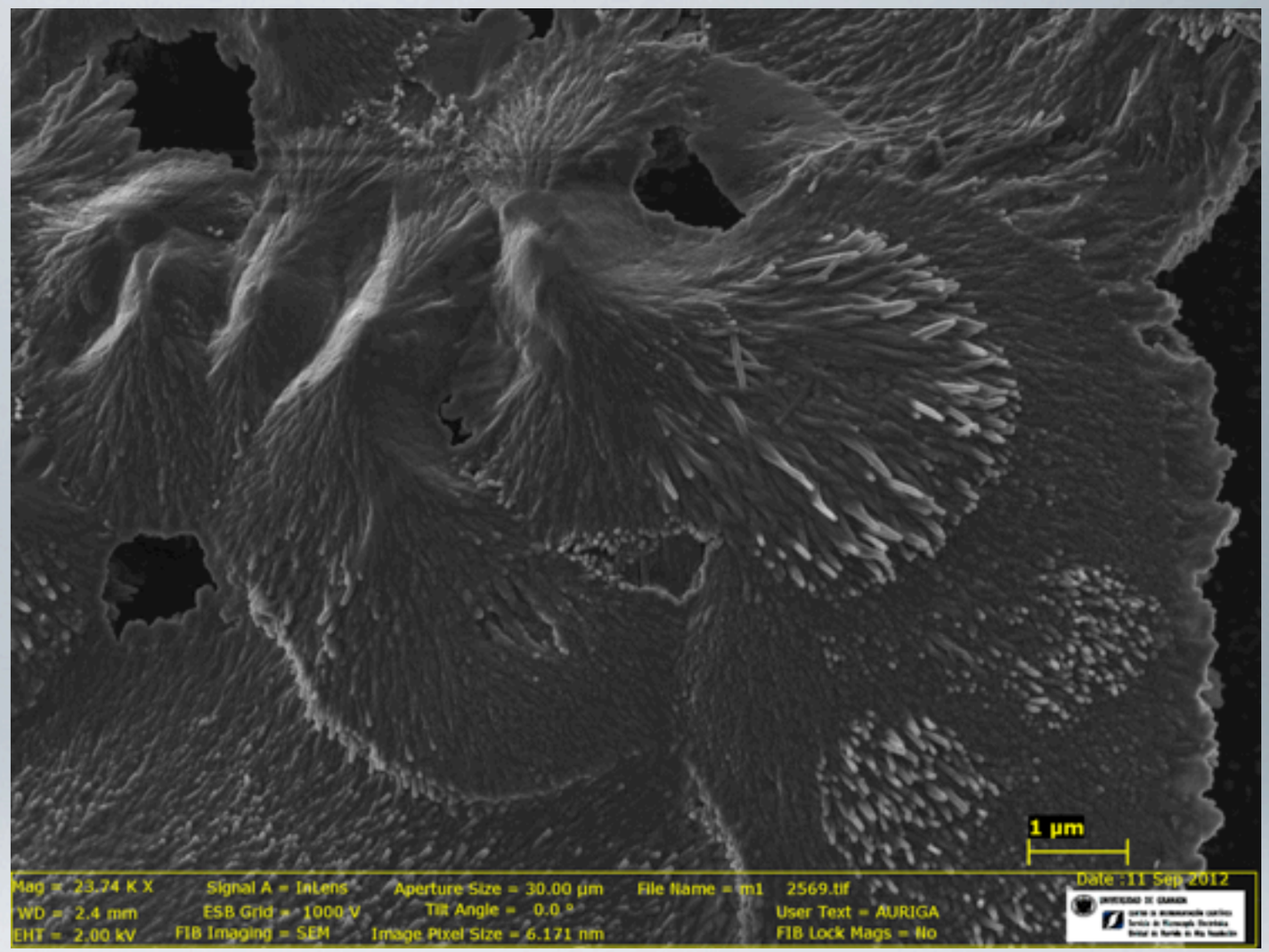

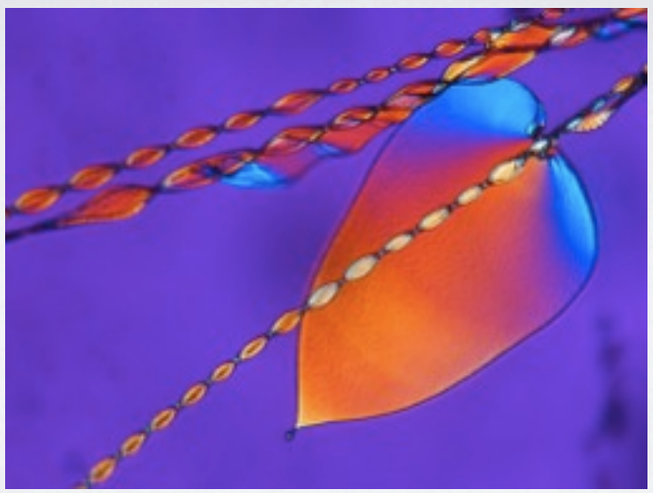

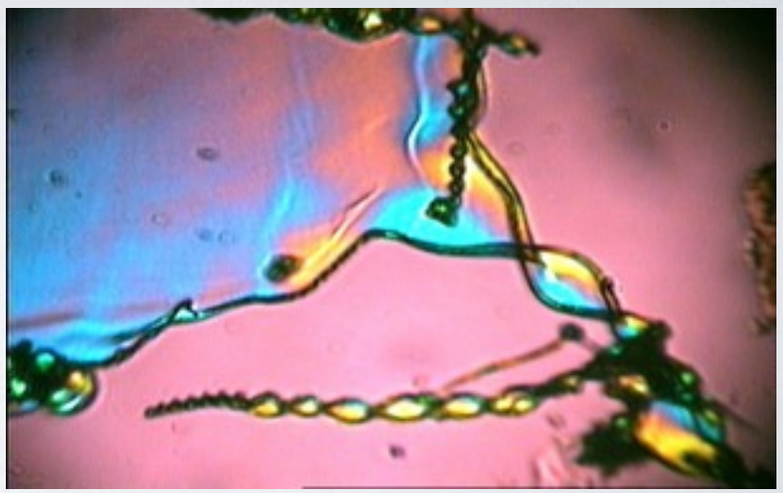

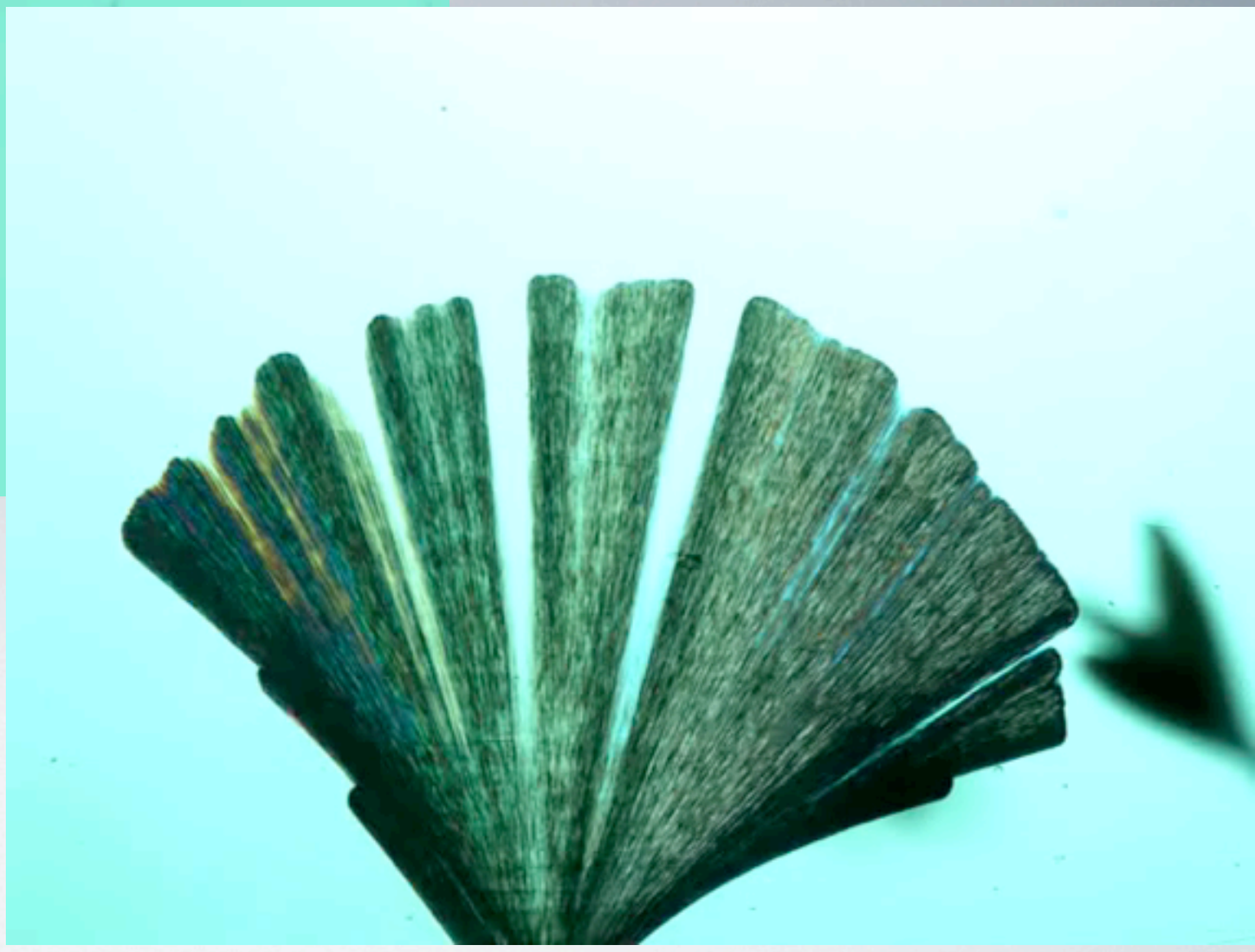

At higher pH, the silica supersaturation provoked by pH change can be important enough to provoke fibrillation, i.e. the transition from single crystal polycrystalline growth front that advance as a laminae.

The morphogenesis of a disk

Radial Growth with $V_\rho = K^{te}$

The morphogenesis of a disk

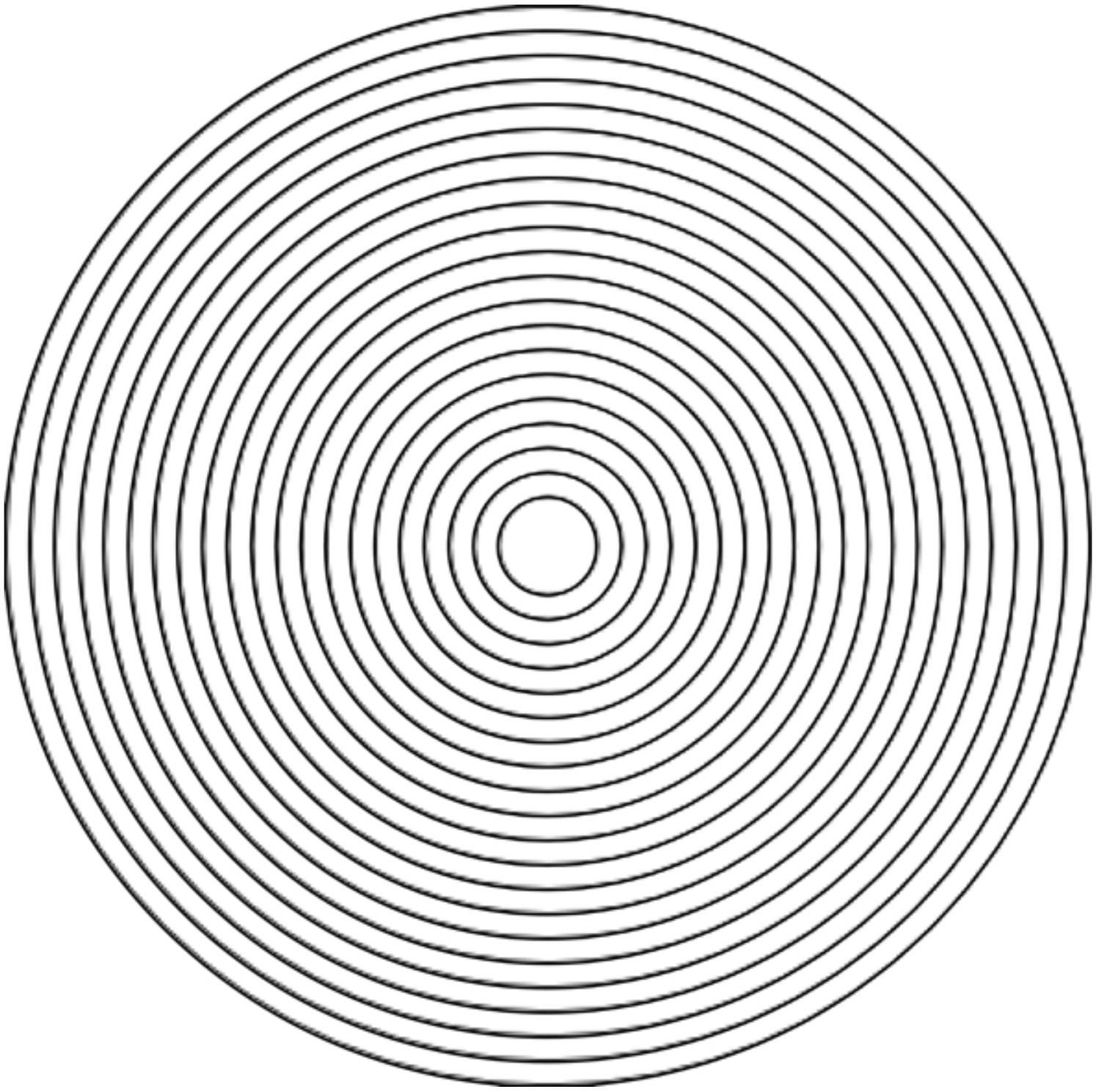

Radial Growth with $V_\rho = K^{te}$

The curling

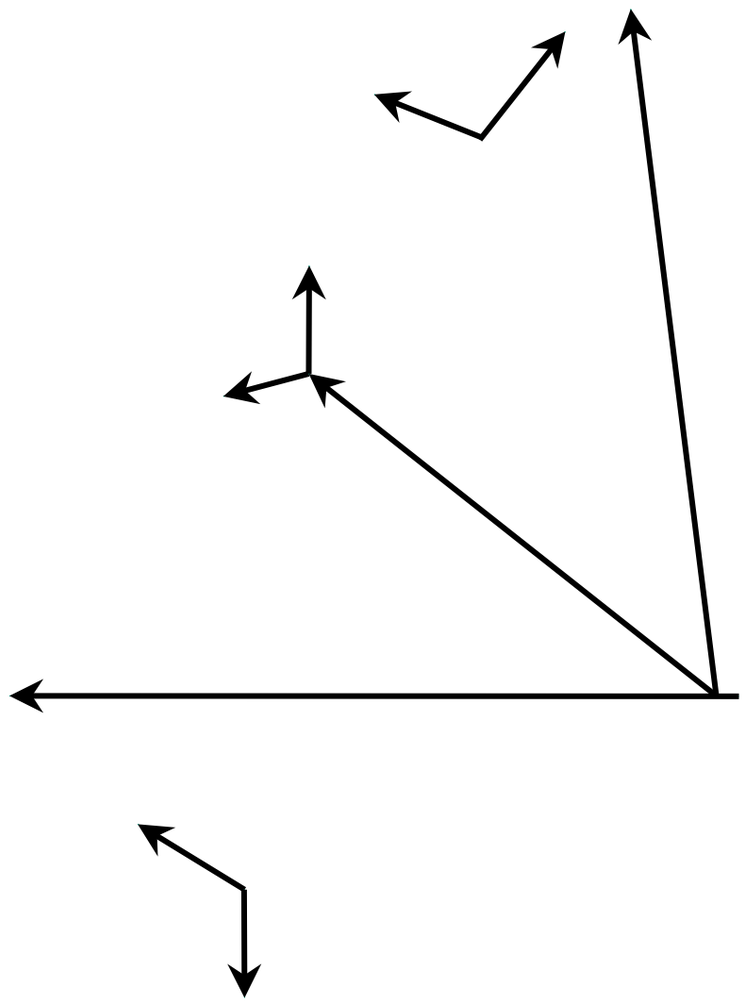

The curling

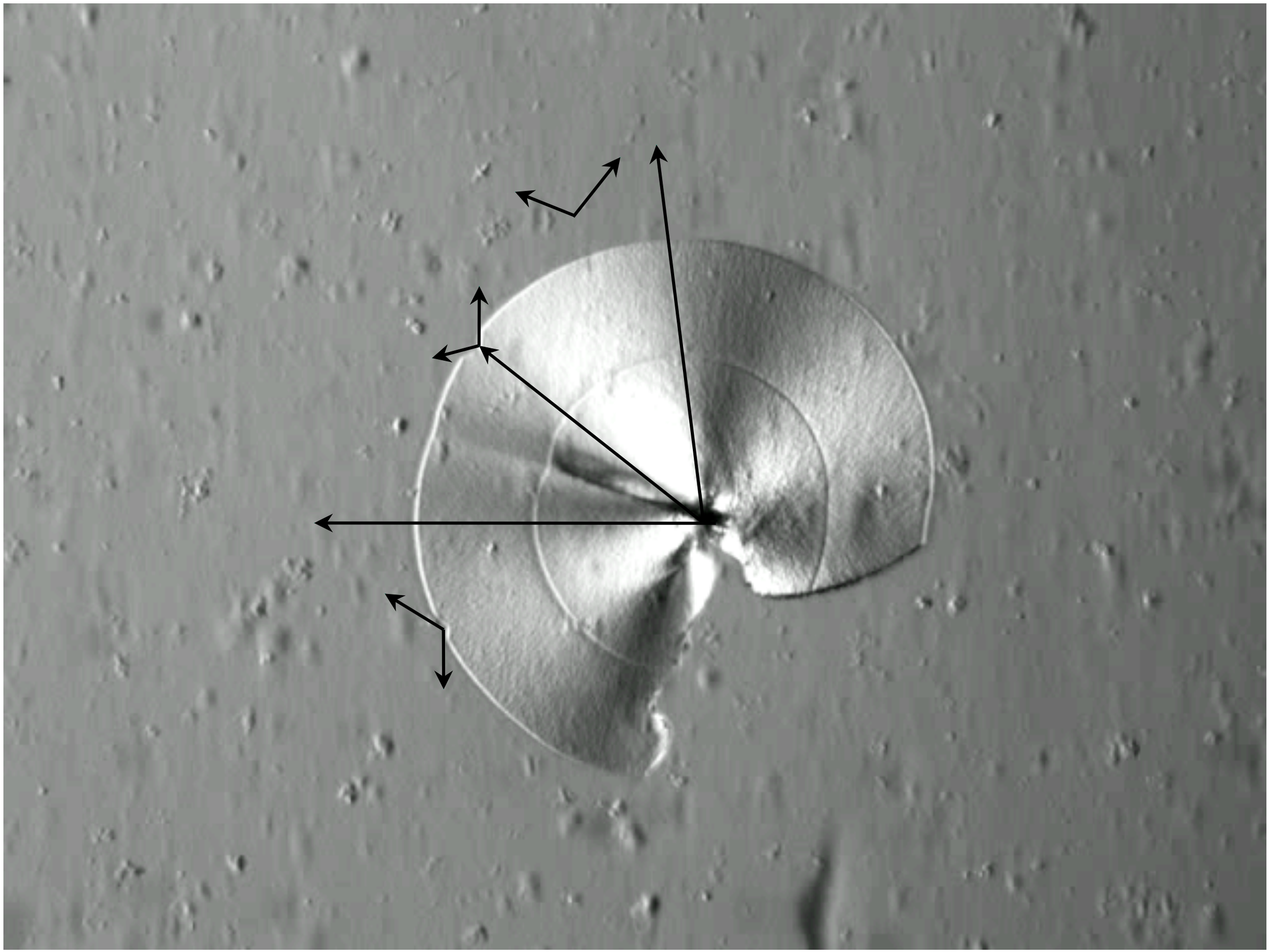

The curling

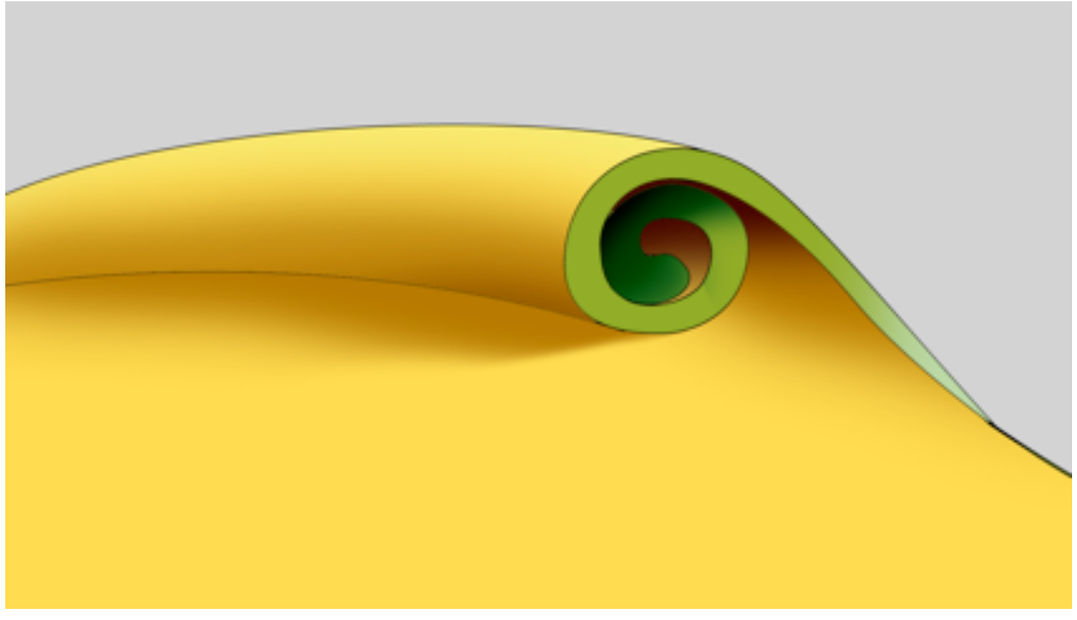

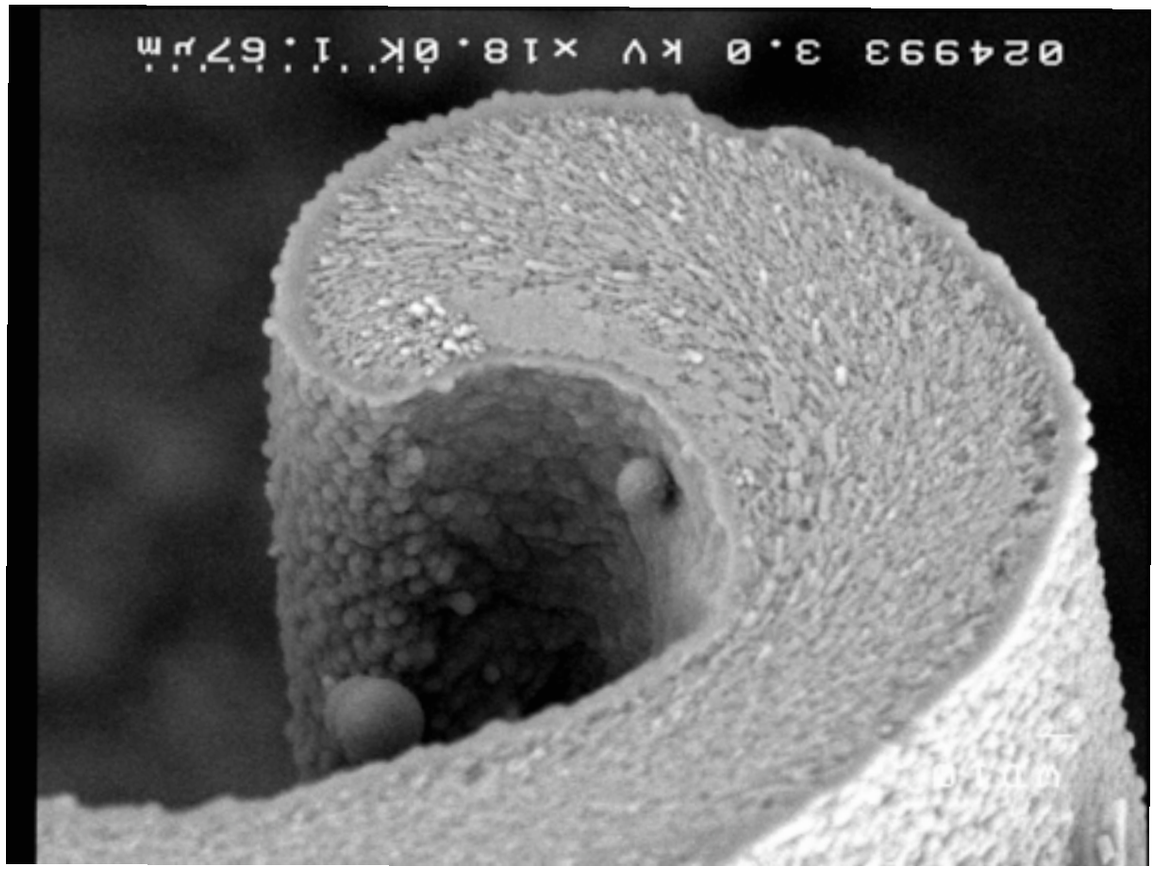

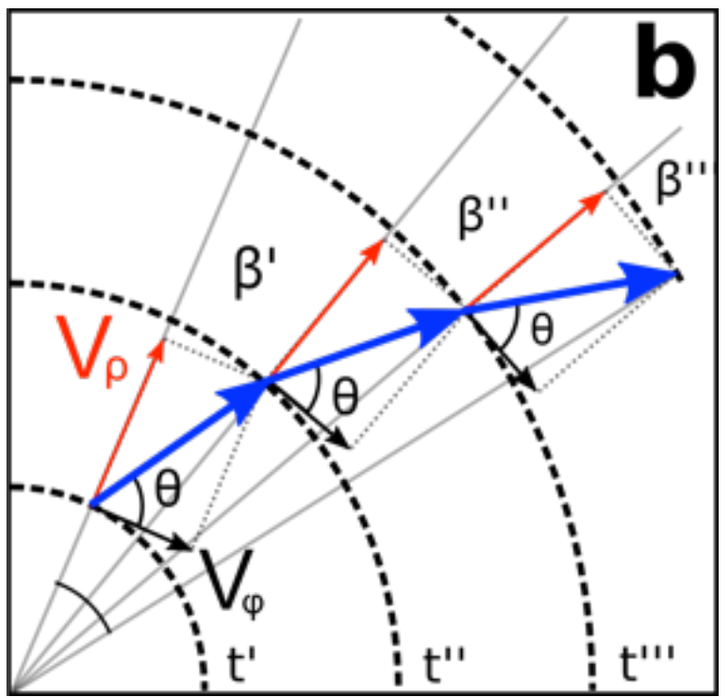

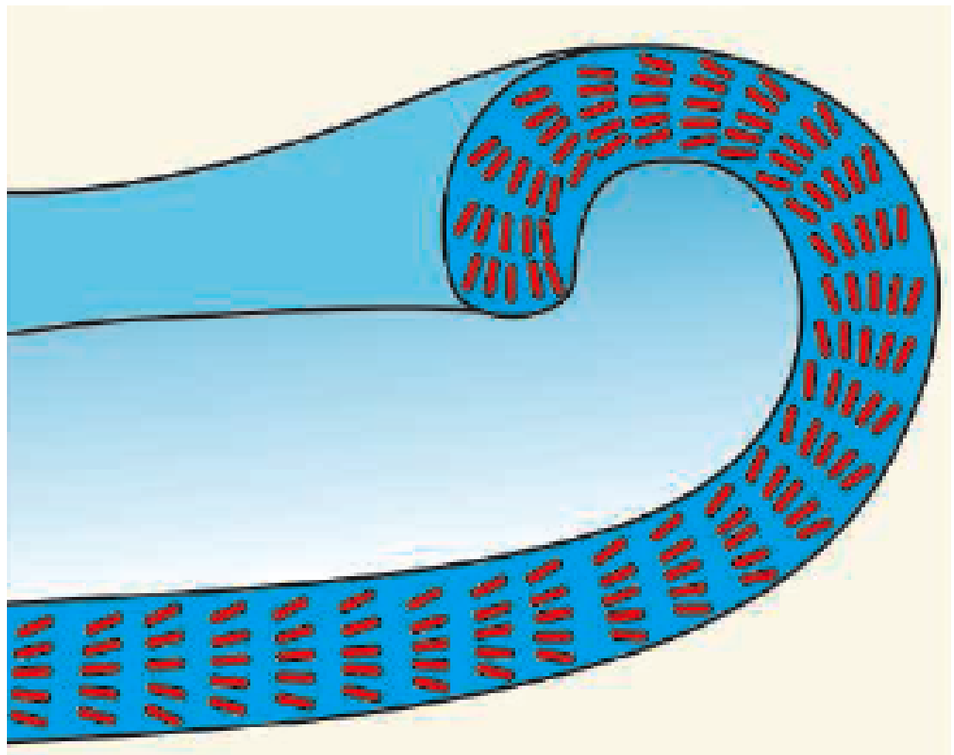

Three morphogenetical parameters

(L or D ; H_1 H_2 ; $V_{\varphi 1}$ $V_{\varphi 2}$ V_ρ

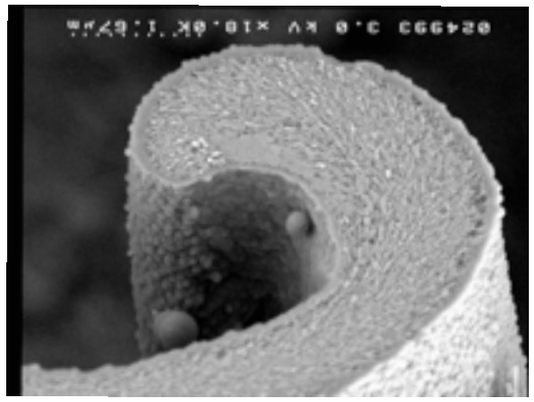

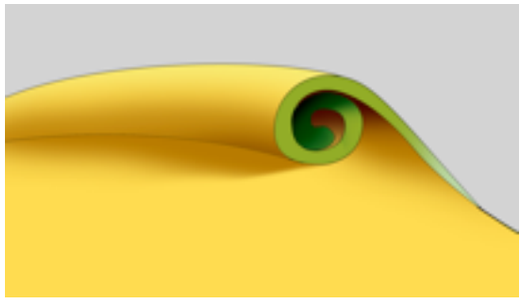

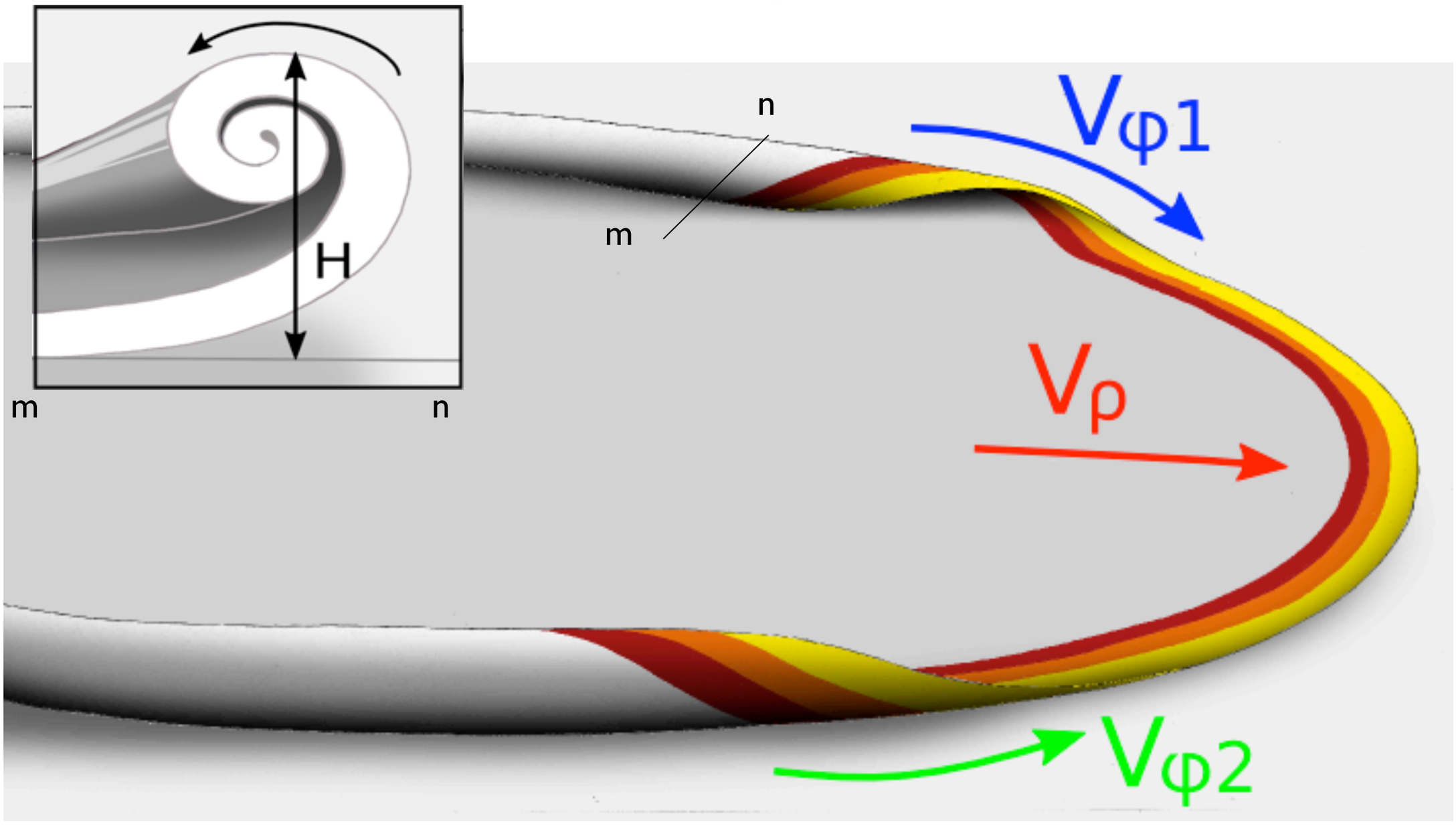

The curling

The morphogenesis of leave-like sheets

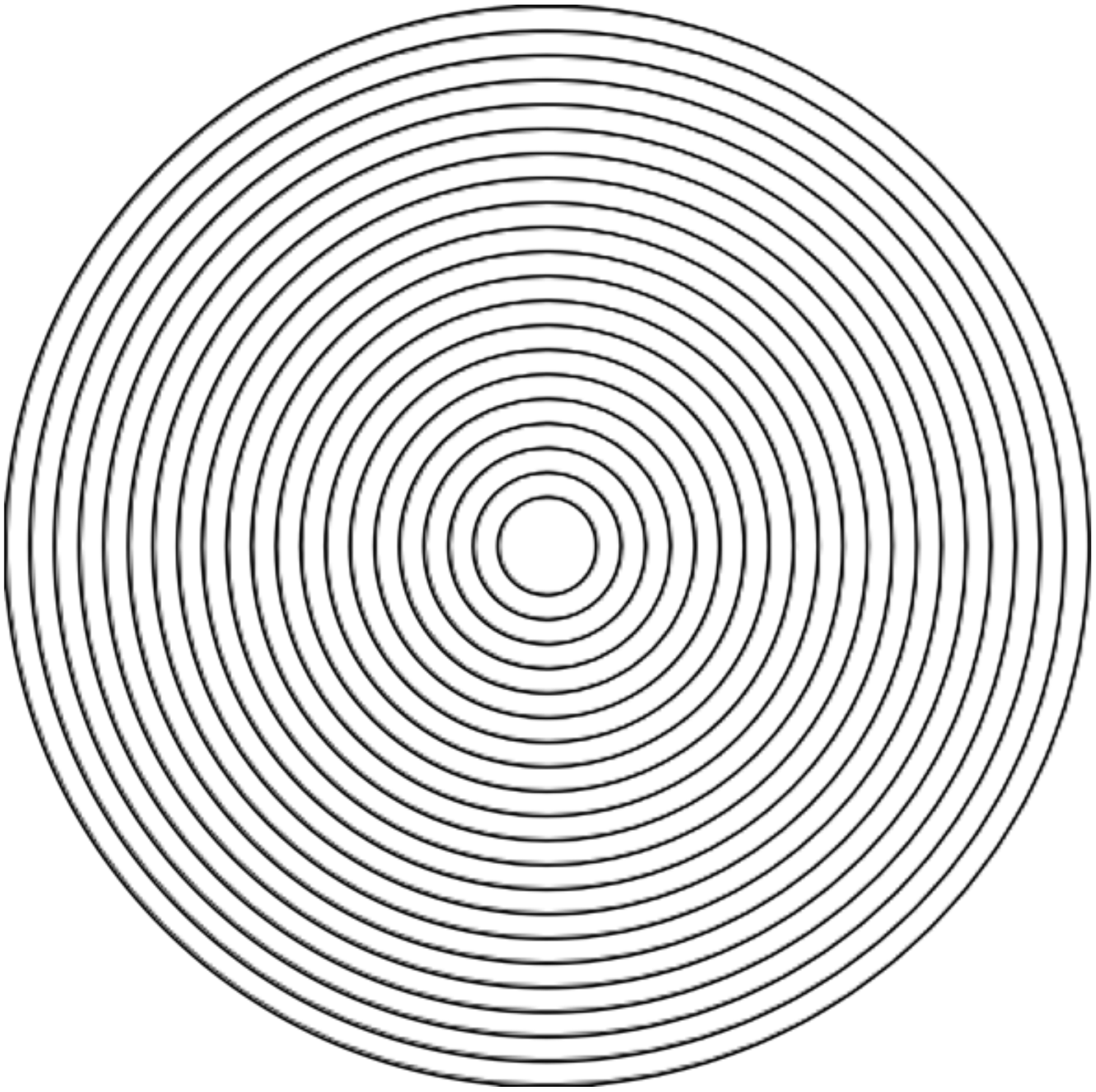

The morphogenesis of leave-like sheets

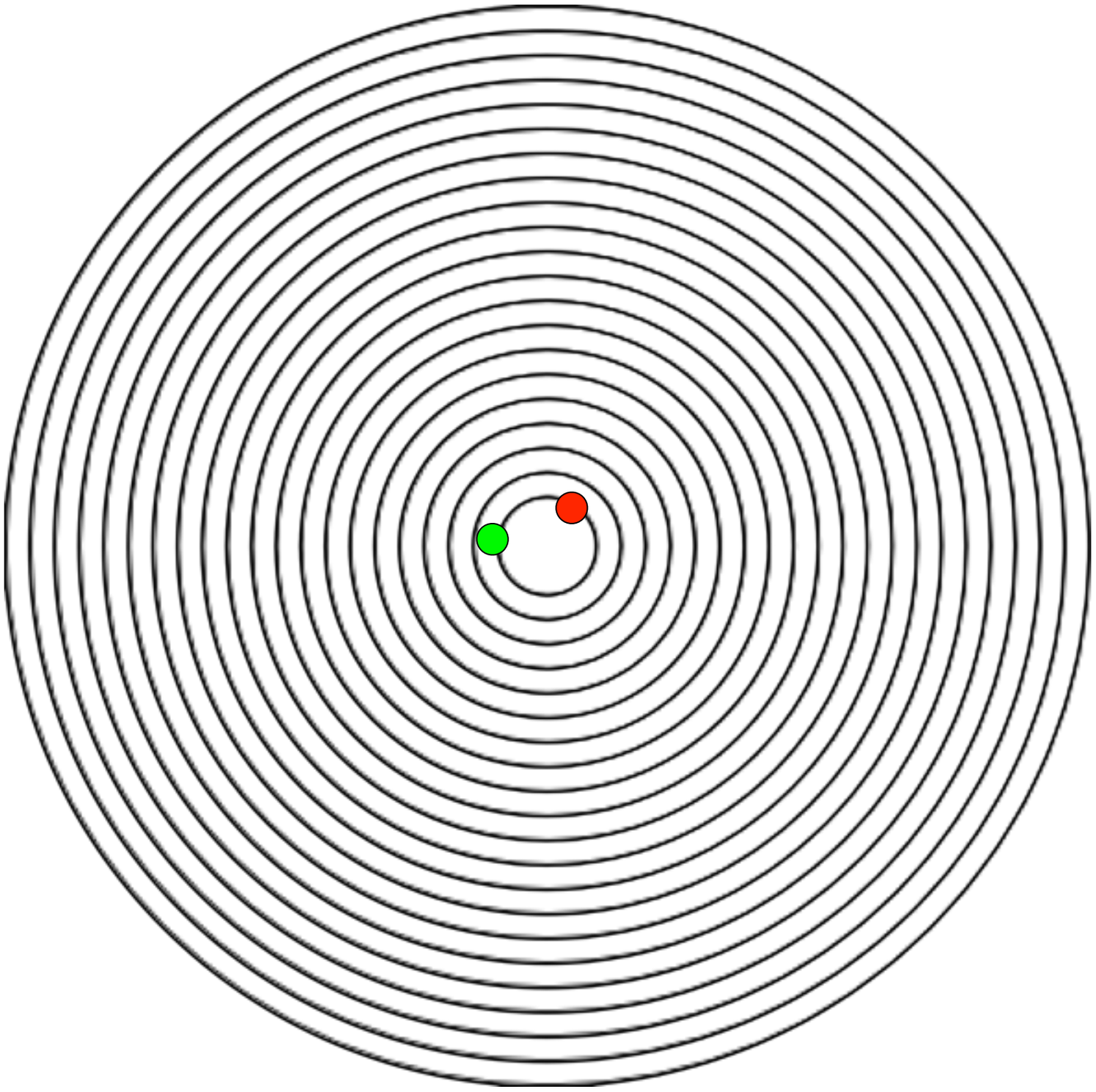

Two curling points

The morphogenesis of leave-like sheets

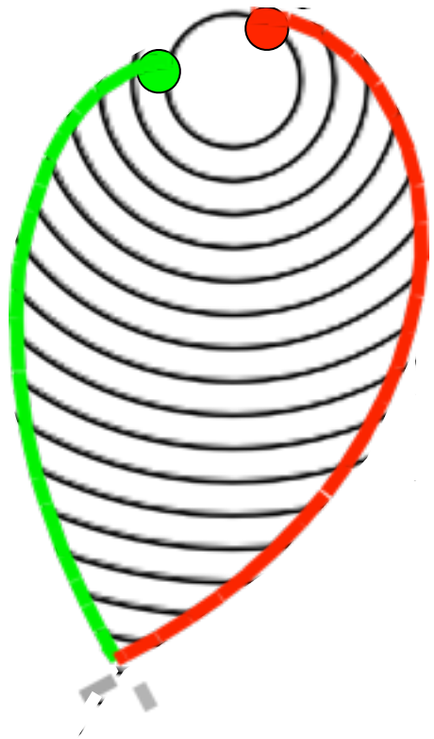

Two curling points

The power of curling

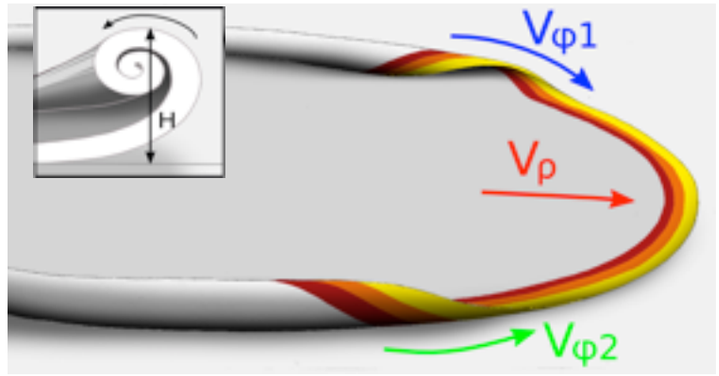

The morphogenesis of a helicoids of constant width
(L_1L_2 or D_1D_2 ; $H_1 = H_2$; $V_{\varphi 1} \approx V_{\varphi 2} \approx V_\rho$):

The morphogenesis of the leaf-like shape
(L_1D_2 or D_1L_2 ; $H_1 = H_2$; $V_{\varphi 1}$ $V_{\varphi 2}$ V_ρ) :

The morphogenesis of the braid
(L_1L_2 or D_1D_2 ; $H_1 \approx H_2$; $V_{\varphi 1} \approx V_{\varphi 2} > V_\rho$):

The morphogenesis of worm like structures
(L_1L_2 or D_1D_2 or L_1D_2 ; $H_1 >> H_2$; $V_{\varphi 1}$; $V_{\varphi 2}$; V_ρ):

The power of curling

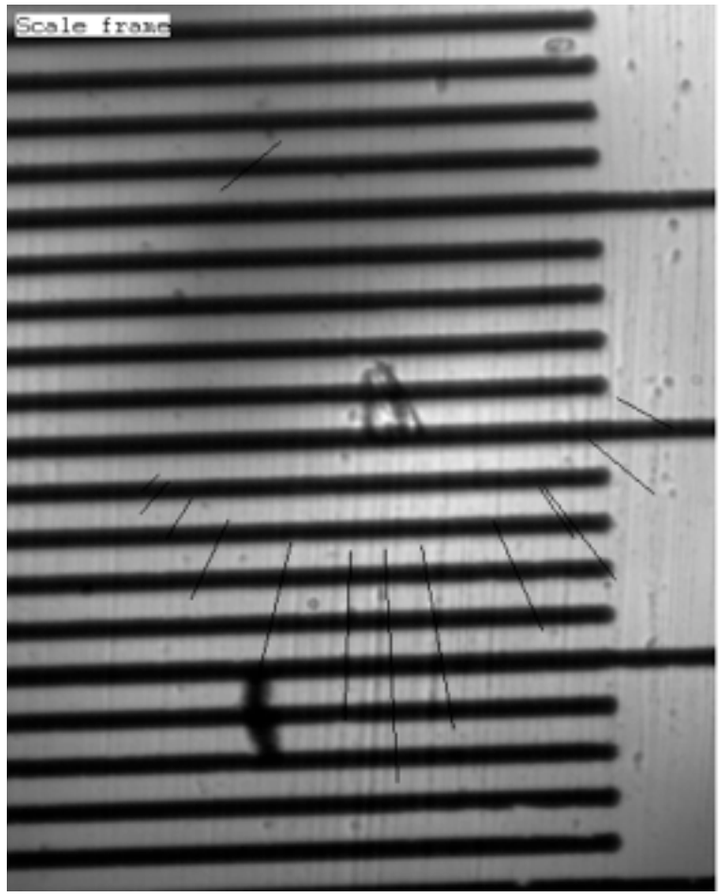

The morphogenesis of the leaf-like shape
(L_1D_2 or D_1L_2 ; $H_1 = H_2$;$V_{\varphi 1}$ $V_{\varphi 2}$ V_ρ) :

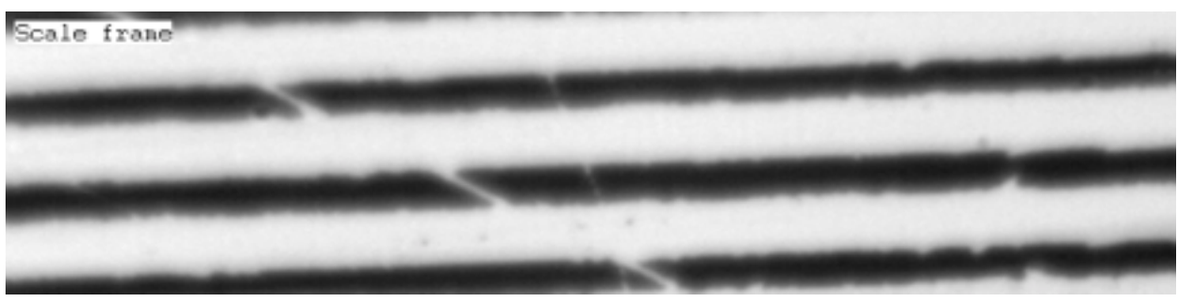

The morphogenesis of the braid
(L_1L_2 or D_1D_2 ; $H_1 \approx H_2$;$V_{\varphi 1} \approx V_{\varphi 2} > V_\rho$):

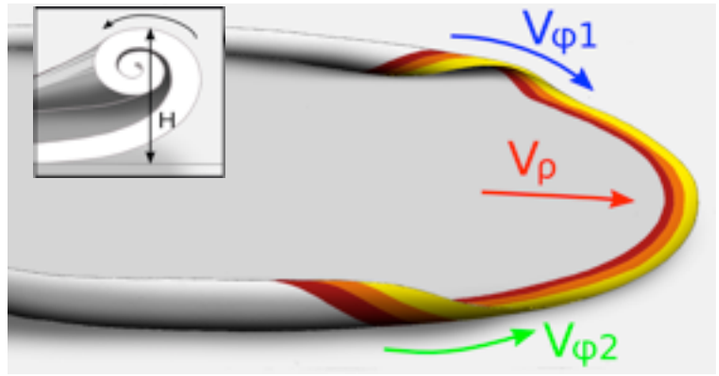

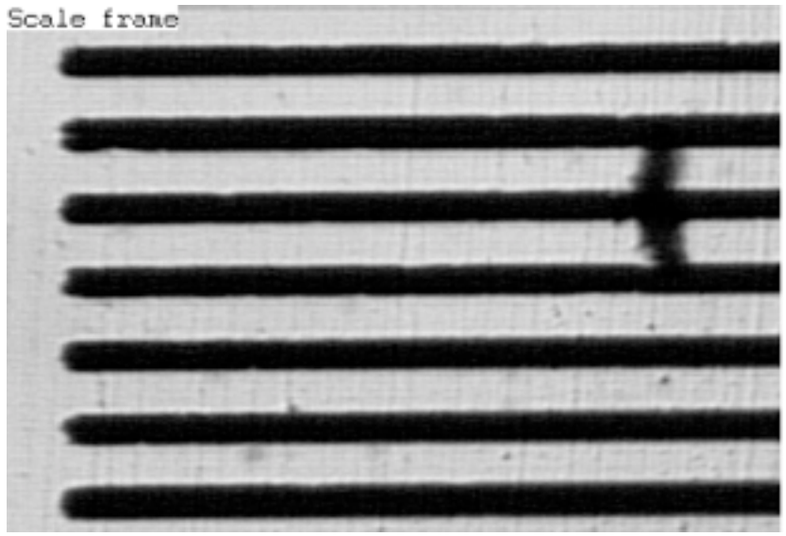

The morphogenesis of a helicoids of constant width
(L_1L_2 or D_1D_2 ; $H_1 = H_2$;$V_{\varphi 1} \approx V_{\varphi 2} \approx V_\rho$):

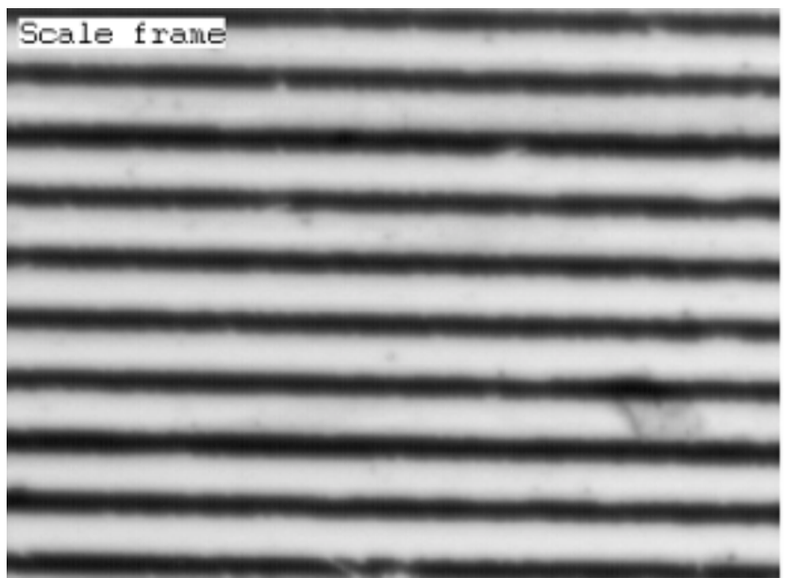

The morphogenesis of worm like structures
(L_1L_2 or D_1D_2 or L_1D_2 ; $H_1 >> H_2$;$V_{\varphi 1}$;$V_{\varphi 2}$;V_ρ):

The power of curling

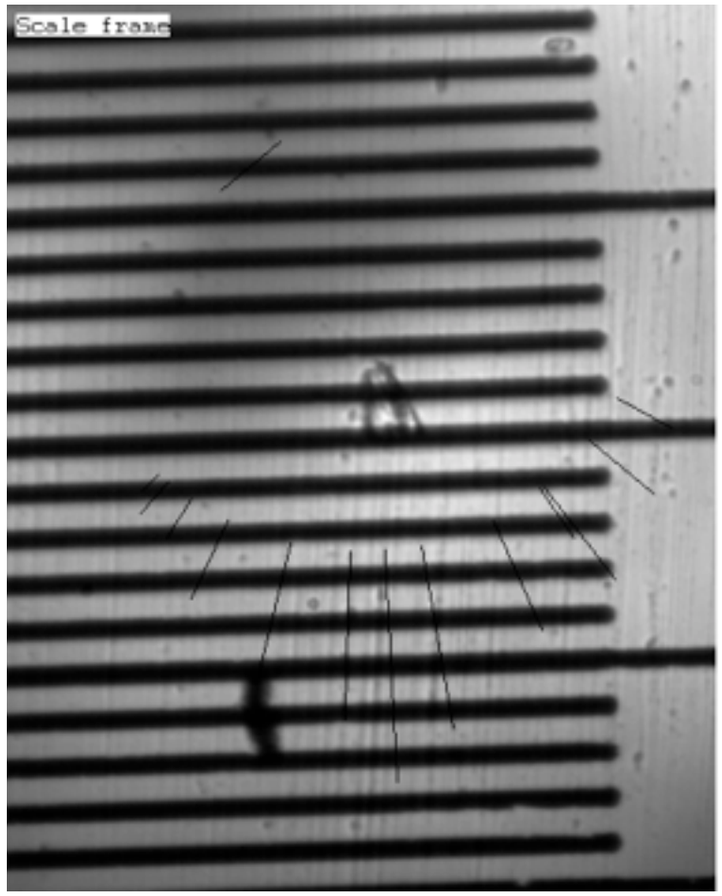

The morphogenesis of the leaf-like shape
(L_1D_2 or D_1L_2 ; $H_1 = H_2$;$V_{\varphi 1}$ $V_{\varphi 2}$ V_ρ) :

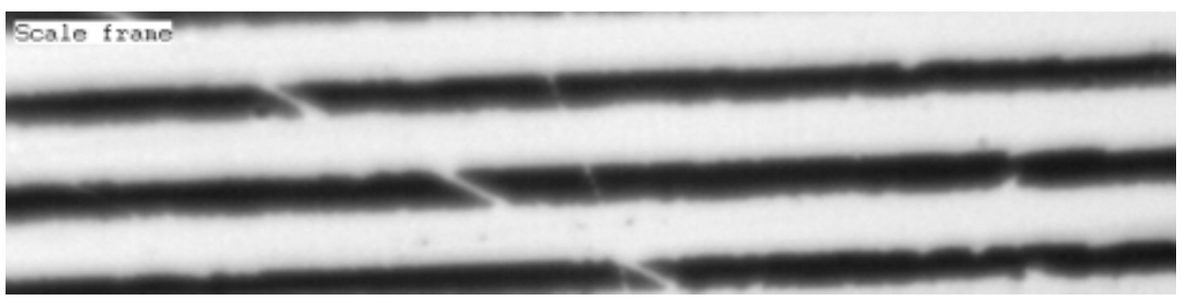

The morphogenesis of the braid
(L_1L_2 or D_1D_2 ; $H_1 \approx H_2$;$V_{\varphi 1} \approx V_{\varphi 2} > V_\rho$):

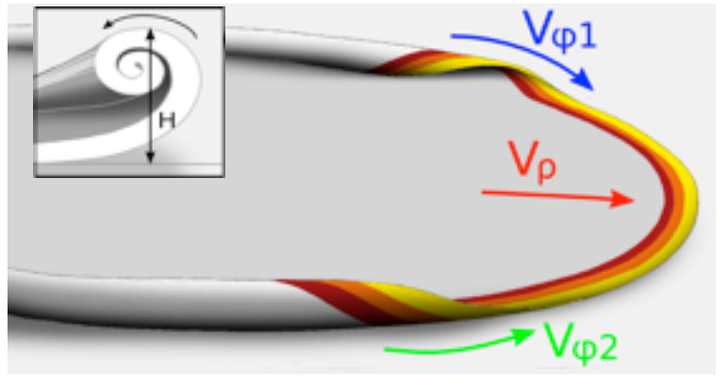

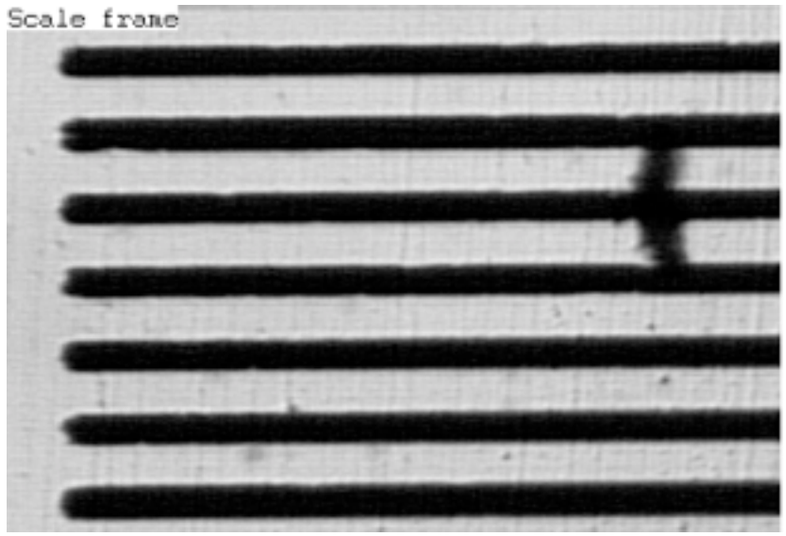

The morphogenesis of a helicoids of constant width
(L_1L_2 or D_1D_2 ; $H_1 = H_2$;$V_{\varphi 1} \approx V_{\varphi 2} \approx V_\rho$):

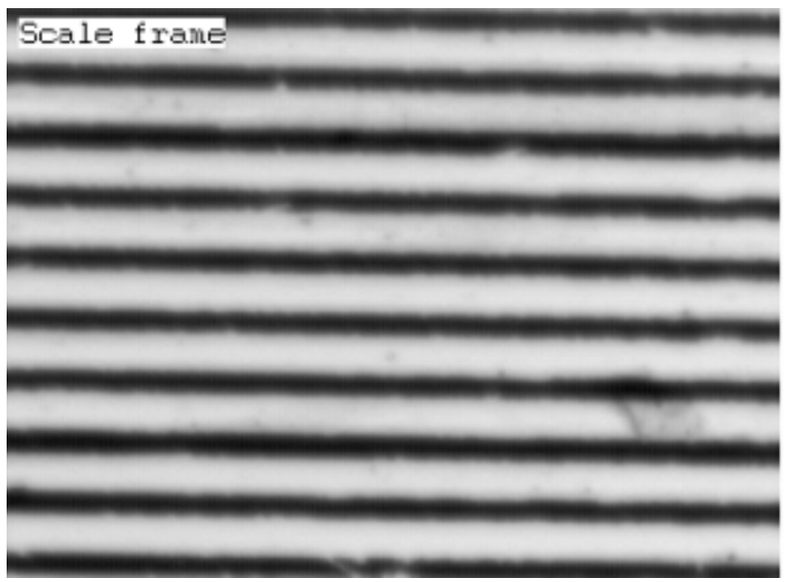

The morphogenesis of worm like structures
(L_1L_2 or D_1D_2 or L_1D_2 ; $H_1 >> H_2$;$V_{\varphi 1}$;$V_{\varphi 2}$;V_ρ):

The power of curling

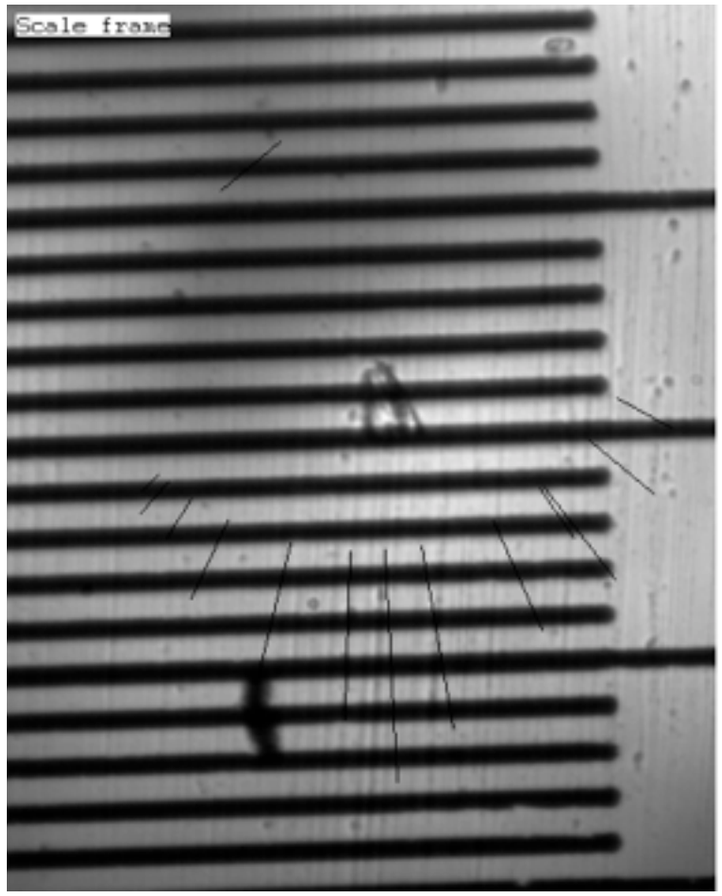

The morphogenesis of the leaf-like shape
(L_1D_2 or D_1L_2 ; $H_1 = H_2$;$V_{\varphi 1}$ $V_{\varphi 2}$ V_ρ) :

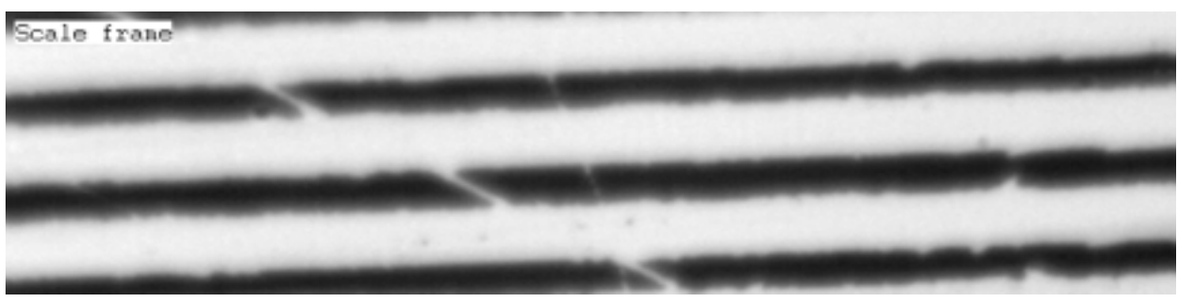

The morphogenesis of the braid
(L_1L_2 or D_1D_2 ; $H_1 \approx H_2$;$V_{\varphi 1} \approx V_{\varphi 2} > V_\rho$):

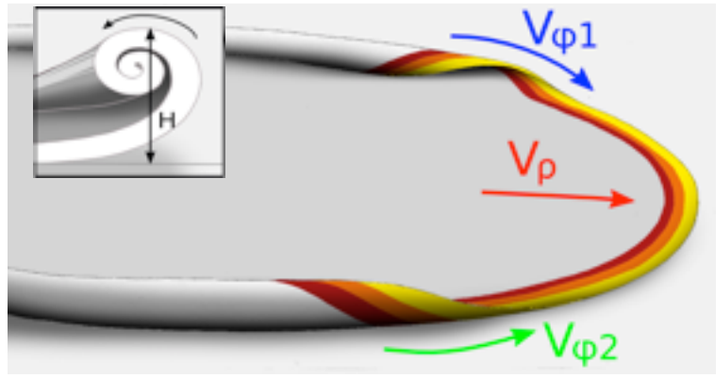

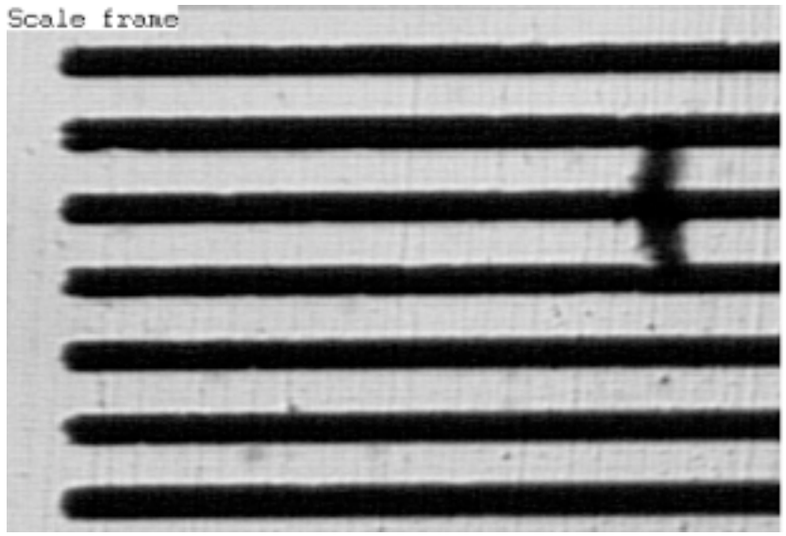

The morphogenesis of a helicoids of constant width
(L_1L_2 or D_1D_2 ; $H_1 = H_2$;$V_{\varphi 1} \approx V_{\varphi 2} \approx V_\rho$):

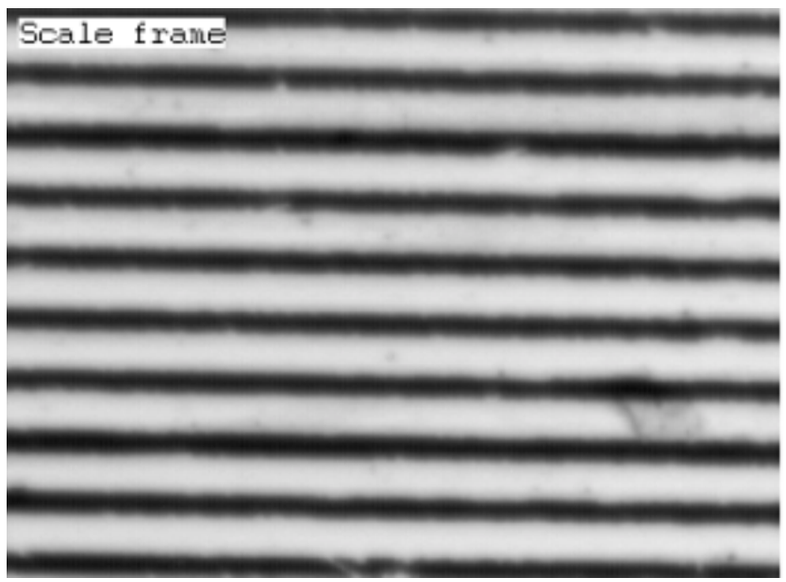

The morphogenesis of worm like structures
(L_1L_2 or D_1D_2 or L_1D_2 ; $H_1 >> H_2$;$V_{\varphi 1}$;$V_{\varphi 2}$;V_ρ):

The power of curling

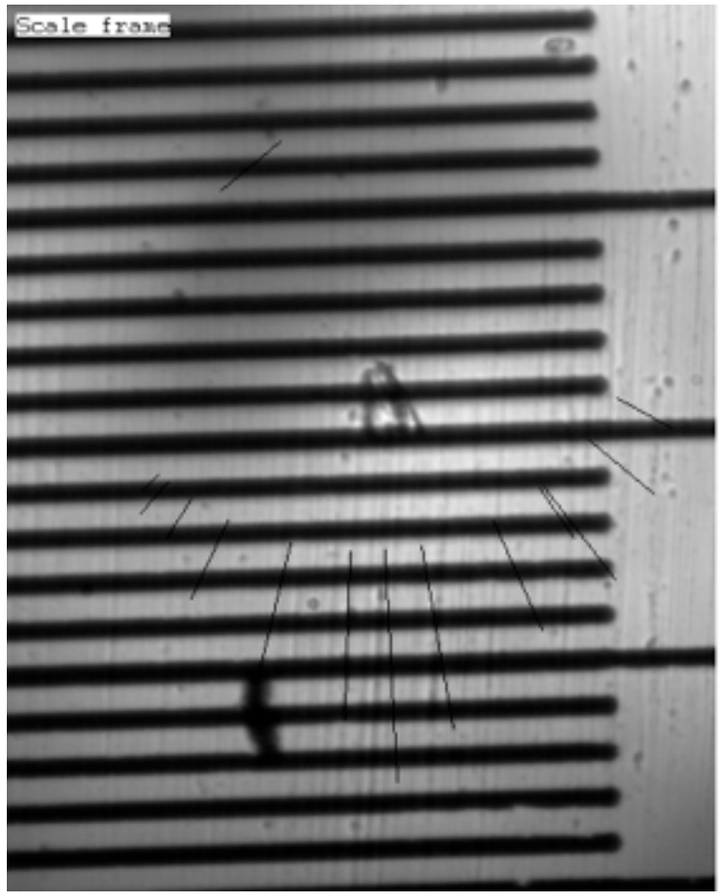

The morphogenesis of the leaf-like shape
(L_1D_2 or D_1L_2 ; $H_1 = H_2$;$V_{\varphi 1}$ $V_{\varphi 2}$ V_ρ) :

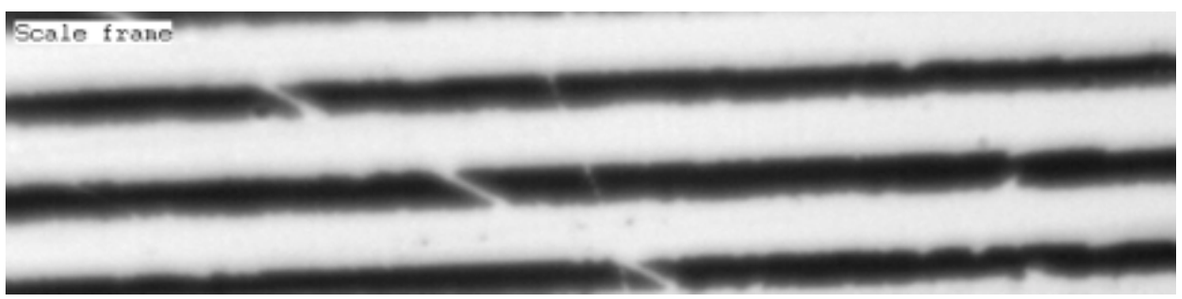

The morphogenesis of the braid
(L_1L_2 or D_1D_2 ; $H_1 \approx H_2$;$V_{\varphi 1} \approx V_{\varphi 2} > V_\rho$):

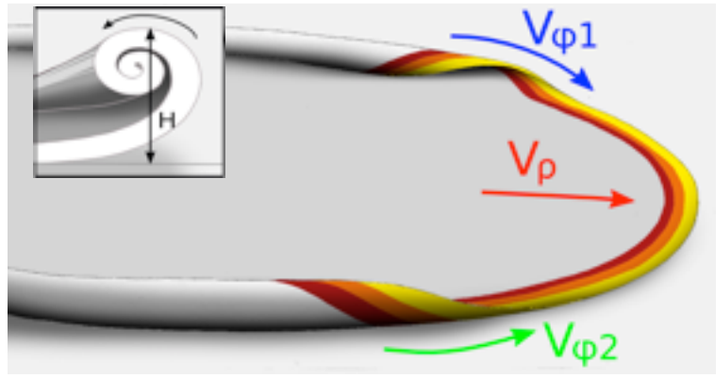

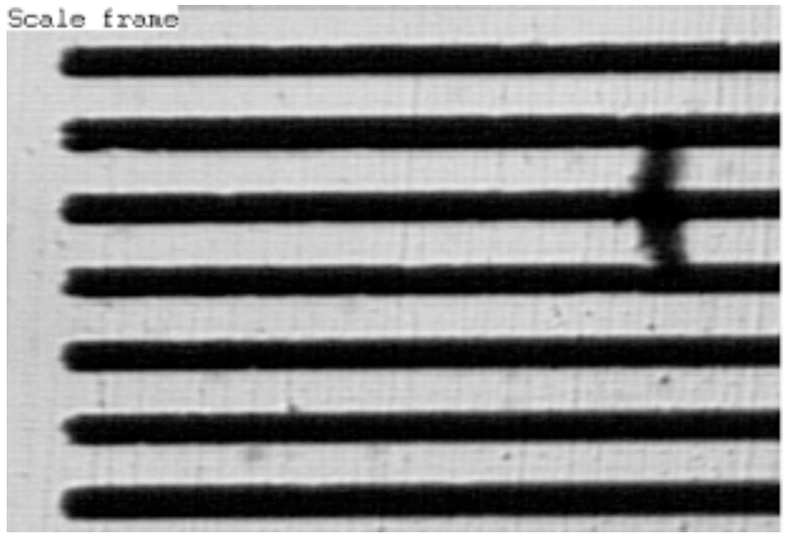

The morphogenesis of a helicoids of constant width
(L_1L_2 or D_1D_2 ; $H_1 = H_2$;$V_{\varphi 1} \approx V_{\varphi 2} \approx V_\rho$):

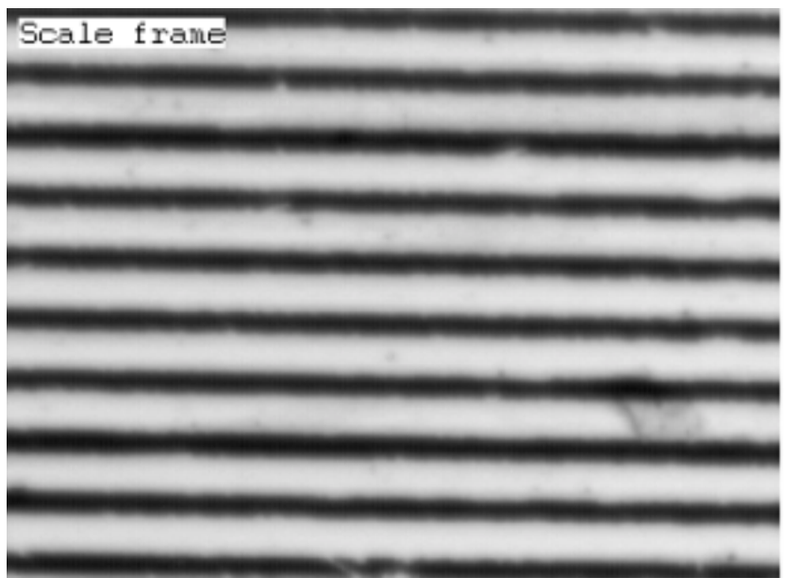

The morphogenesis of worm like structures
(L_1L_2 or D_1D_2 or L_1D_2 ; $H_1 >> H_2$;$V_{\varphi 1}$;$V_{\varphi 2}$;V_ρ):

The chemical driven force

The structure and growth of laminae is proposed to result from a coupled co-precipitation of amorphous silica and (barium) carbonate taking place locally at the growing front

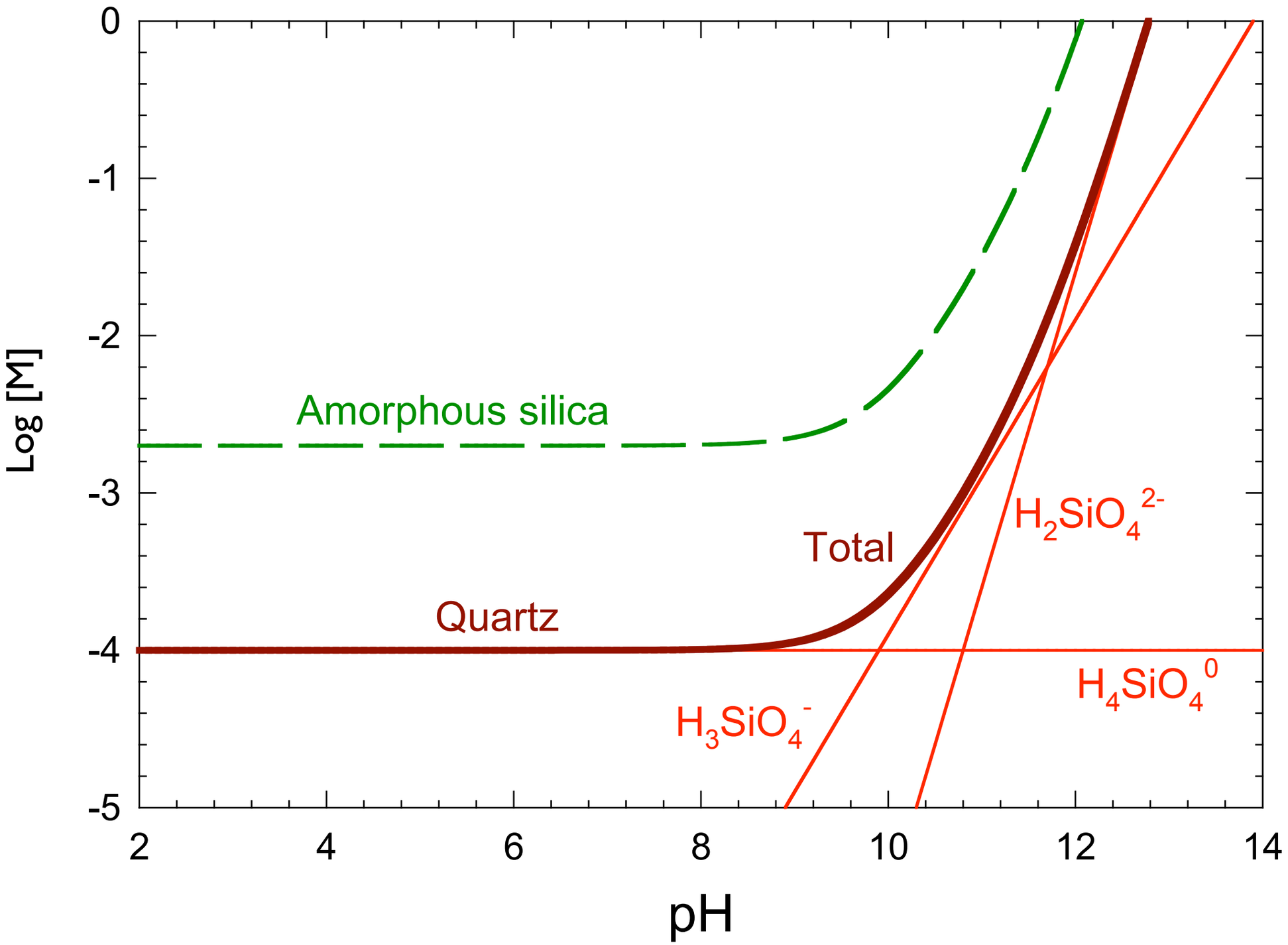

J.M. Garcia-Ruiz, E. Melero, S. Hyde, Science 323 (2009) 362

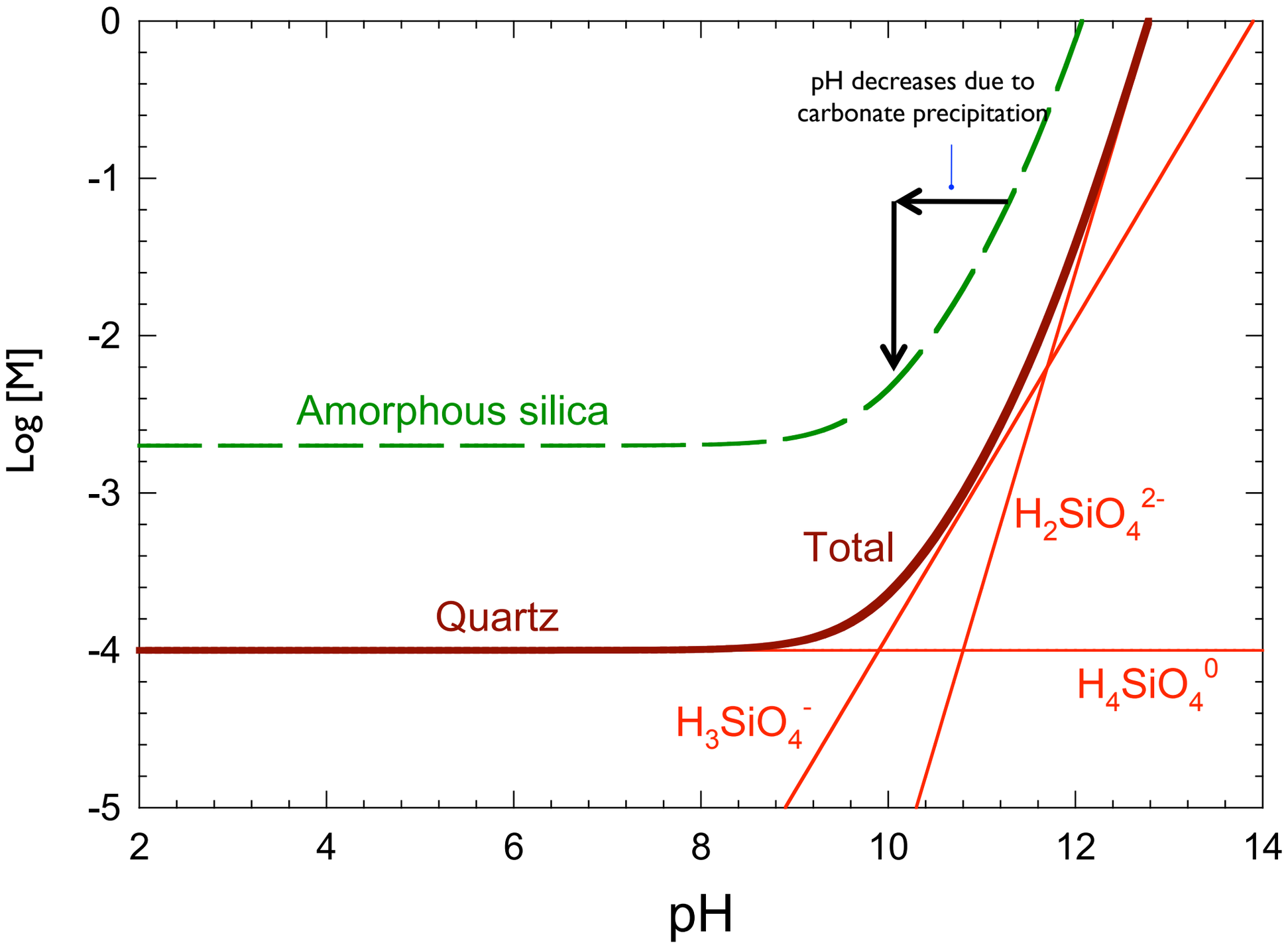

J.M. Garcia-Ruiz, E. Melero, S. Hyde, Science 323 (2009) 362

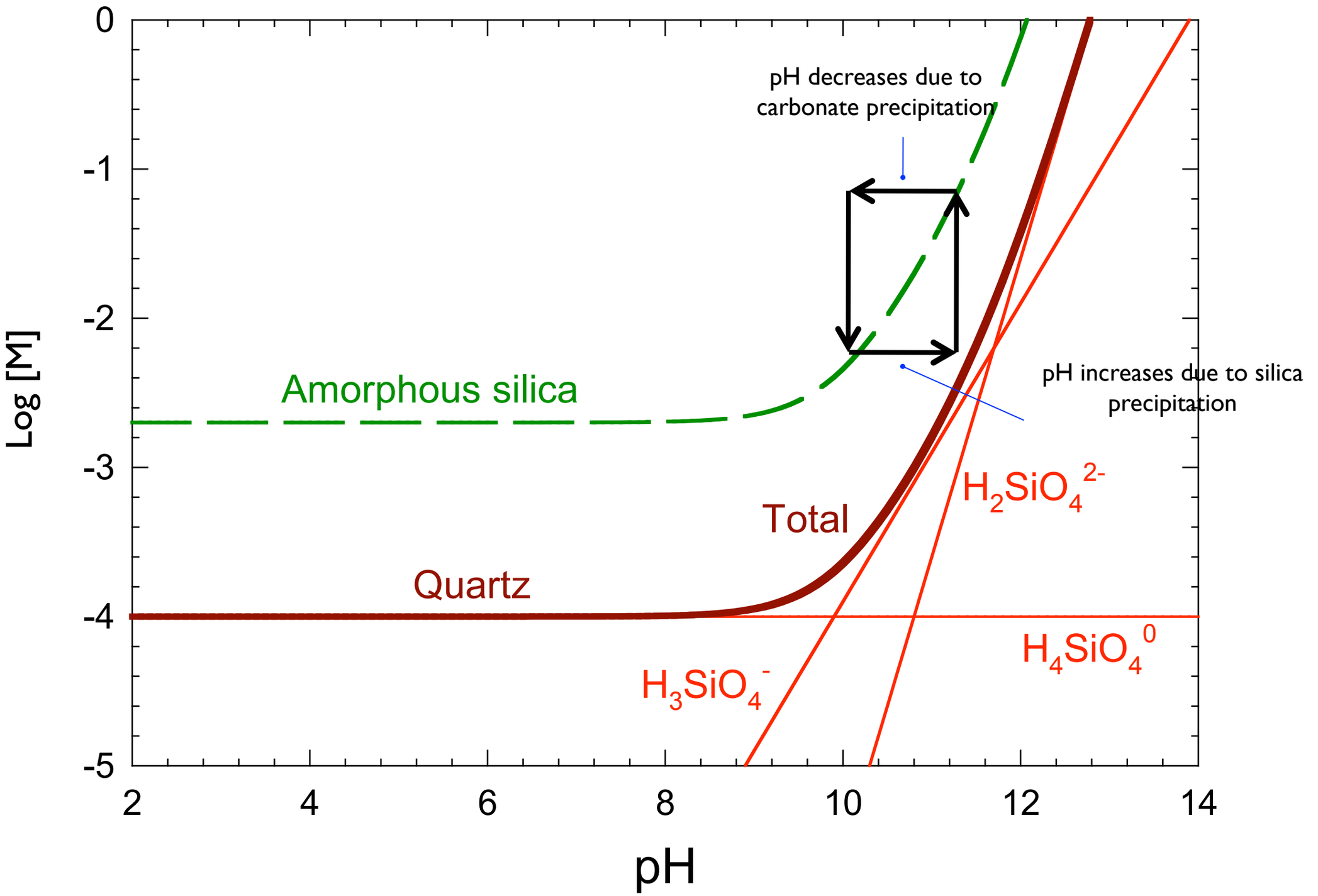

J.M. Garcia-Ruiz, E. Melero, S. Hyde, Science 323 (2009) 362

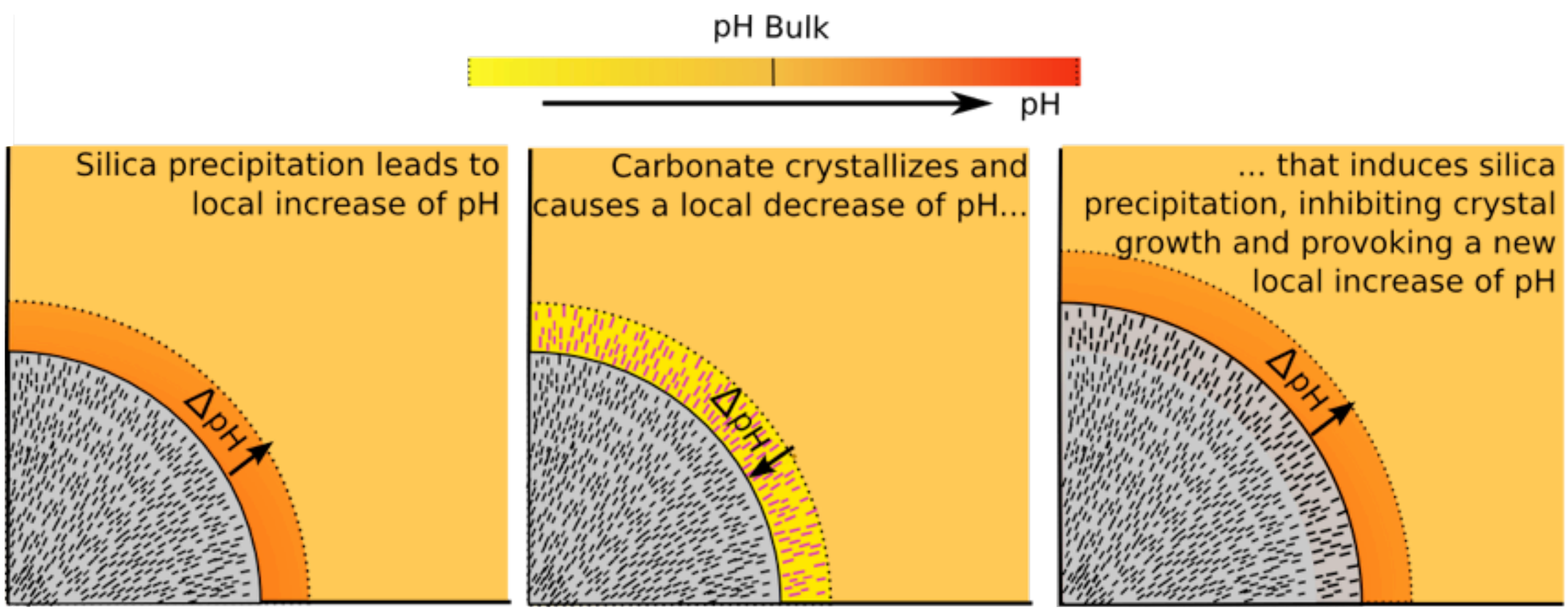

Silica precipitation

This feedback mechanisms provokes a continuous self-feeding of impurities. Beyond splitting it causes fibrillation of the growth front leading to the formation of laminar structures of silica-carbonate composite.

J.M. Garcia-Ruiz, E. Melero, S. Hyde, Science 323 (2009) 362

M. Kellermeier, E. Melero-García, W. Kunz, J. M. García-Ruiz. Journal of Colloid and Interface Science, 380 (2012) 1-7.

M. Kellermeier, H. Cölfen, and J.M. García-Ruiz, European Journal of Inorganic Chemistry (2012) 5123–5144

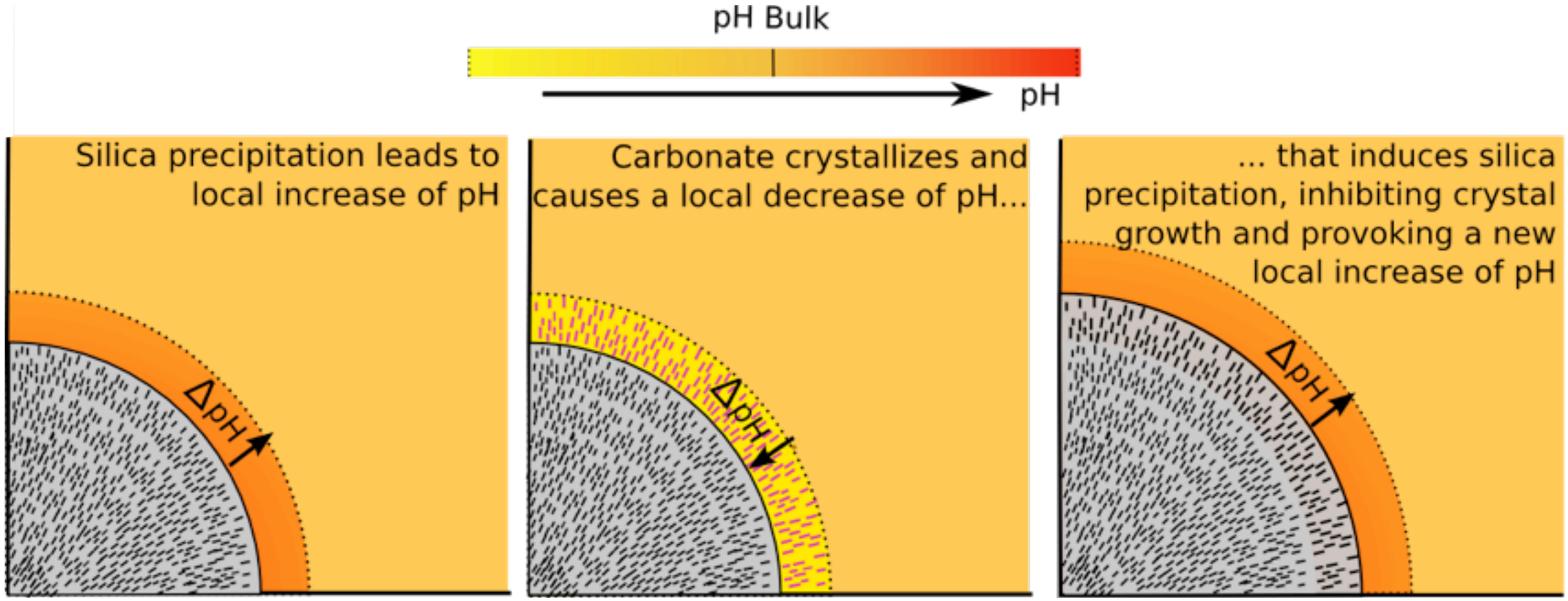

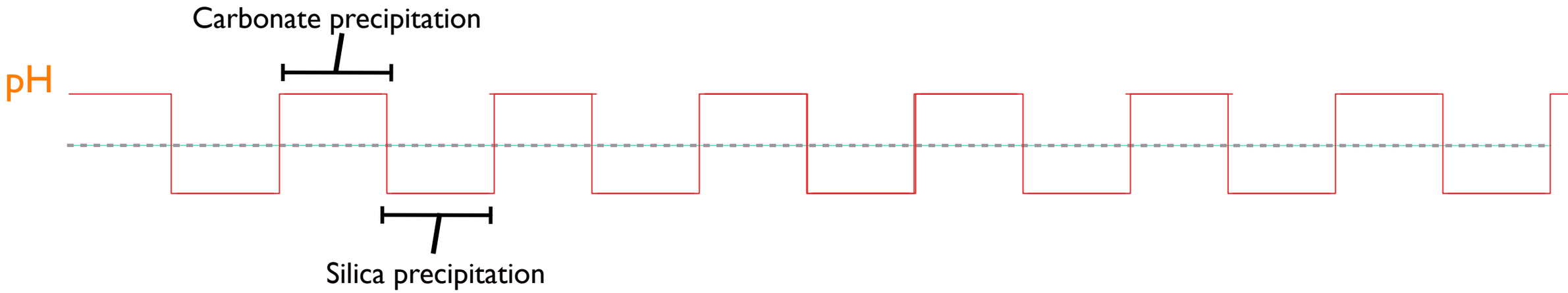

This feedback mechanisms provokes a continuous self-feeding of impurities.
Beyond splitting it causes fibrillation of the growth front leading to the formation of laminar structures of silica-carbonate composite.

J.M. Garcia-Ruiz, E. Melero, S. Hyde, Science 323 (2009) 362

M. Kellermeier, E. Melero-García, W. Kunz, J. M. García-Ruiz. Journal of Colloid and Interface Science, 380 (2012) 1-7.

M. Kellermeier, H. Cölfen, and J.M. García-Ruiz, European Journal of Inorganic Chemistry (2012) 5123–5144

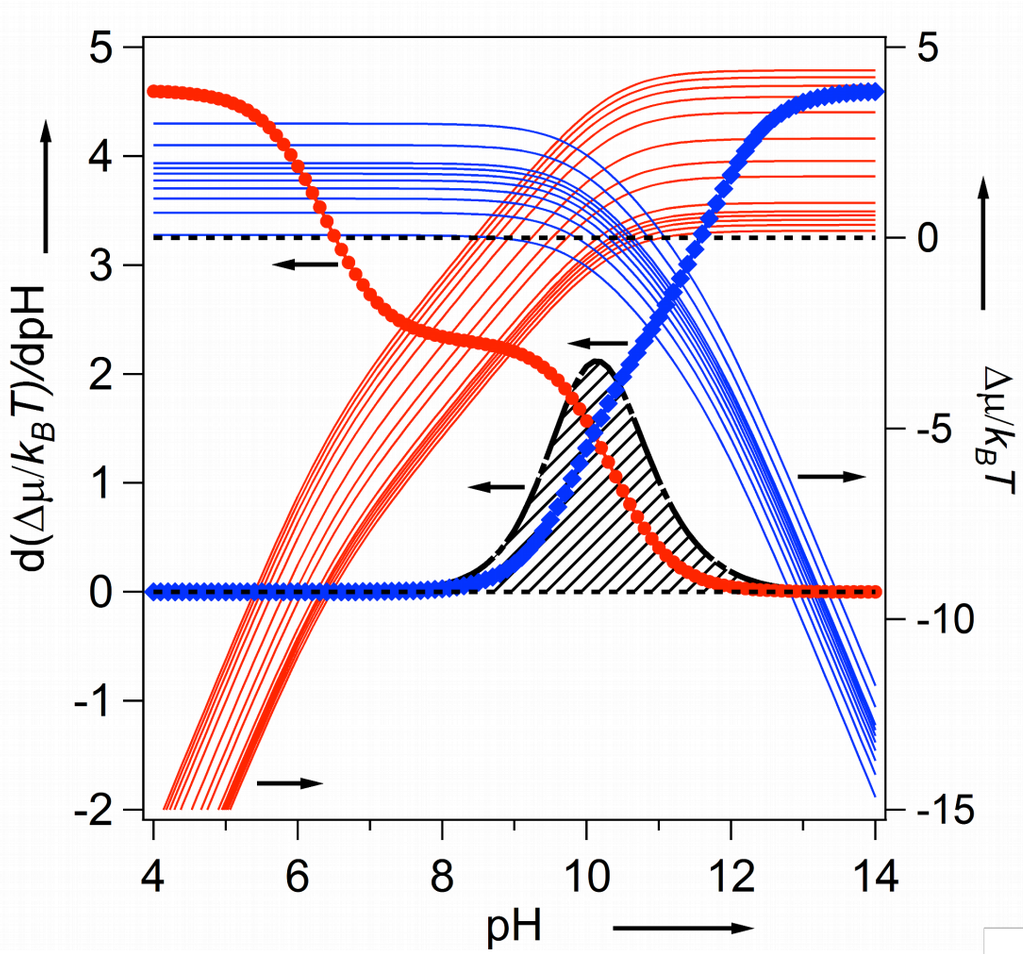

$$\frac{[HCO_3^-][H^+]}{[H_2CO_3]} = K_1^C = 10^{-6.35}; \quad \frac{[SiO(OH)_3^-][H^+]}{[Si(OH)_4]} = K_1^{Si} = 10^{-9.9};$$

$$\frac{[CO_3^{2-}][H^+]}{[HCO_3^-]} = K_2^C = 10^{-10.33}; \quad \frac{[SiO_2(OH)_2^{2-}][H^+]}{[SiO(OH)_3^-]} = K_2^{Si} = 10^{-11.7};$$

$$\Delta\mu_C^* = \ln\left(\frac{TCO_2}{K_{sp}}\frac{[Ba^{2+}]}{\alpha(H^+)}\right);$$

$$\alpha(H^+) = \left([H^+]^2/K_1^C K_2^C\right) + \left([H^+]/K_2^C\right) + 1;$$

$$\Delta\mu_{Si}^* = \ln\left(\frac{TSiO_2}{K_{Si}}\frac{1}{\beta(H^+)}\right);$$

$$\beta(H^+) = \left(K_1^{Si}K_2^{Si}/[H^+]^2\right) + \left(K_1^{Si}/[H^+]\right) + 1;$$

$$\frac{d\Delta\mu_C^*}{dpH} = \overline{\Delta\mu_C^*} = -\frac{\overline{\alpha(pH)}}{\alpha(pH)};$$

$$\frac{d\Delta\mu_{Si}^*}{dpH} = \overline{\Delta\mu_{Si}^*} = -\frac{\overline{\beta(pH)}}{\beta(pH)};$$

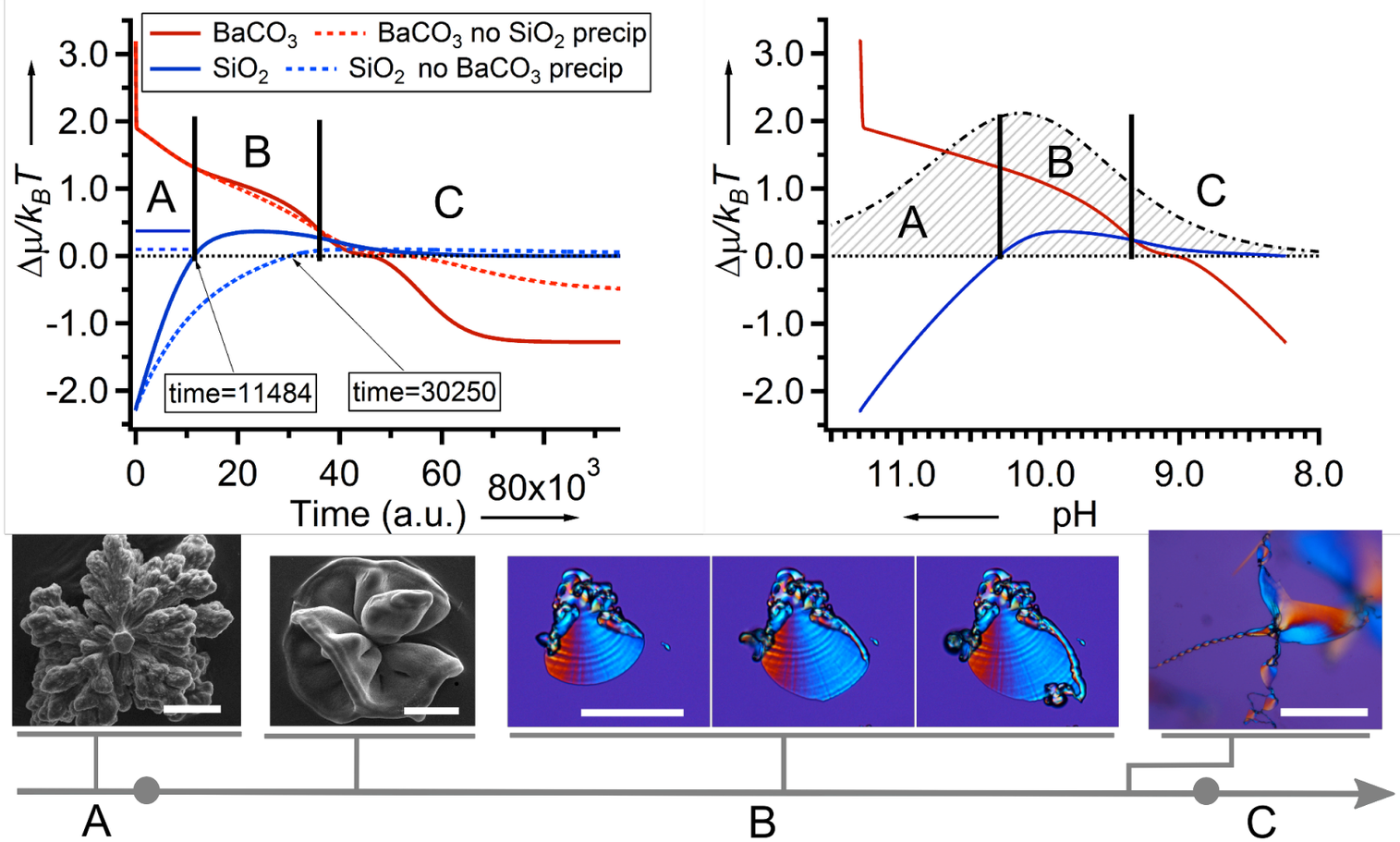

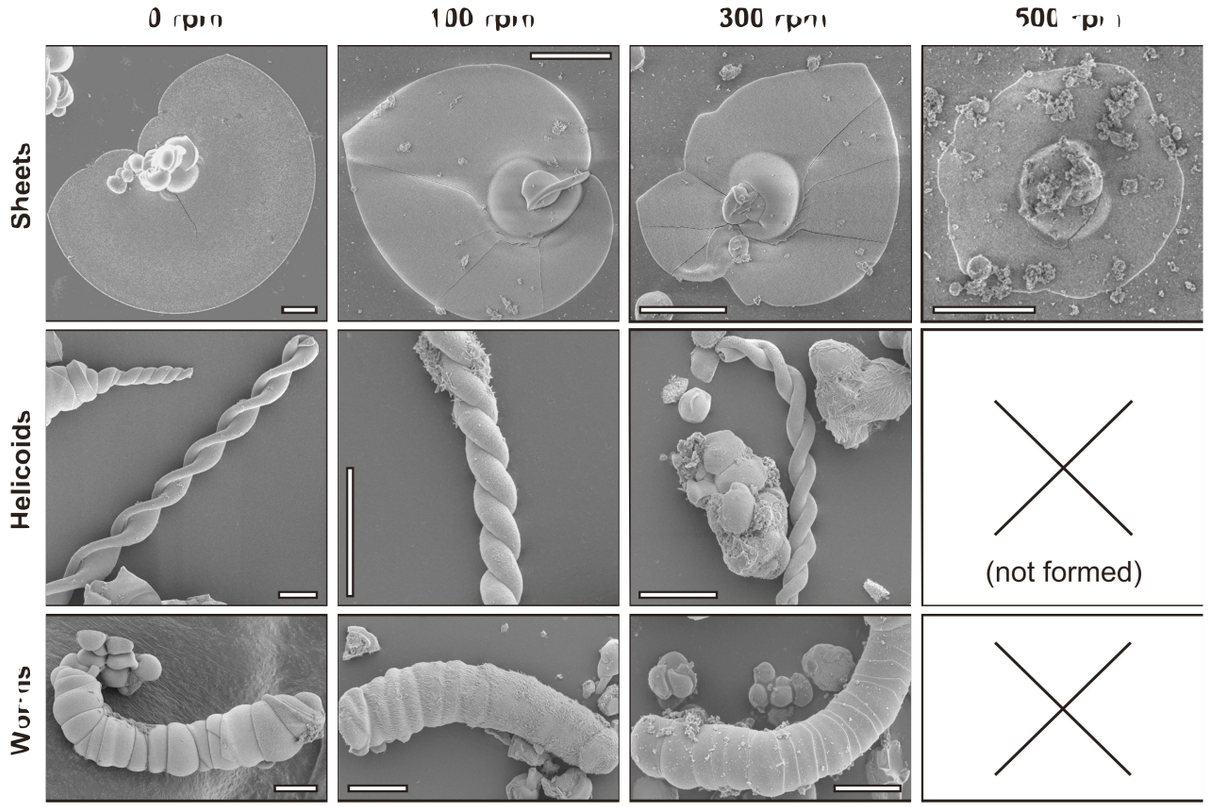

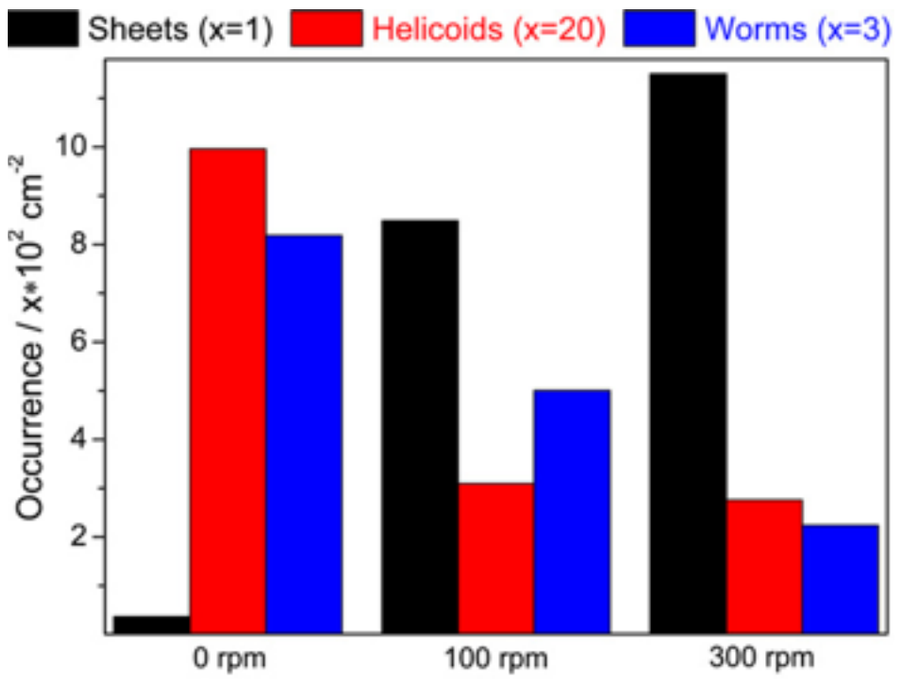

M. Kellermeier, E. Melero-García, W. Kunz, J. M. García-Ruiz, J. Colloid Interface Sci. 2012, 380, 1.

Proof of localness of the growth process

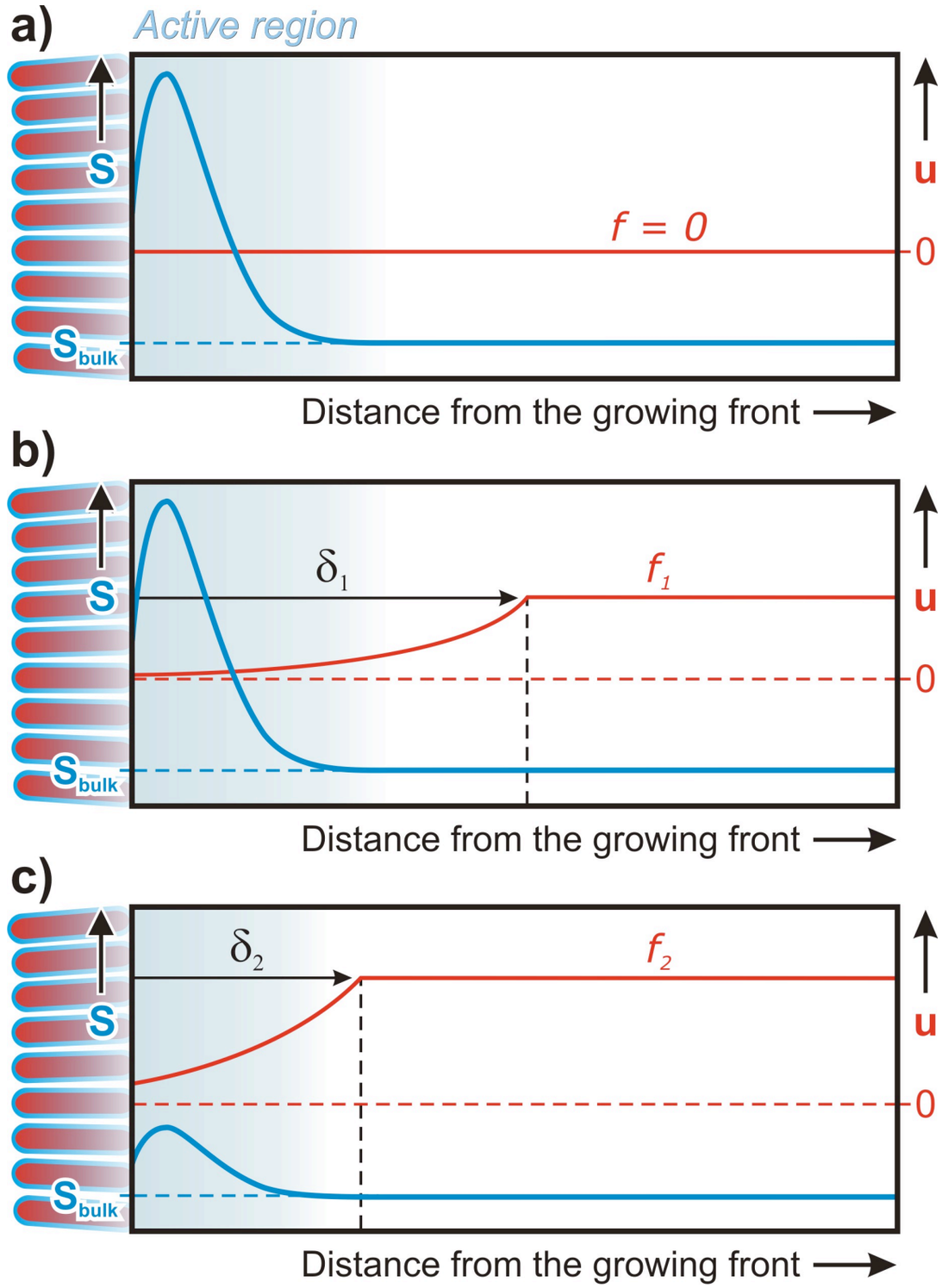

Detecting pH changes at high (time and space) resolution

-emission color different from excitation color $(\lambda_{em} > \lambda_{exc})$

Excitation can be eliminated by optical filtering

-local detection possible (a volume of 50 µl can be selectevily observed)

Only the region of the sample which is simultaneously excited and observed is detected

-Very fast process (10^{-9} s time delay between excitation and emission)

molecular diffusion is negligeable in this time range

-allow to determine the local concentration of the fluorophore S

Intensity is proportional to $\varepsilon(\lambda_{exc}), \alpha(\lambda_{em})$ *and to the local fluorophore concentration*

Very sensitive (10-12 M with standard equipment)

On going work with

Marco Montalti, Damiano Genovese, Giuseppe Falini
Dipartimento di Chimica "G. Ciamician", Università di Bologna, Italy

Gan Zhang,
Instituto Andaluz de Ciencias de la Tierra (CSIC-UGR), Granada, España

ACRIDINE ORANGE IS AN OFF/ON pH SENSOR

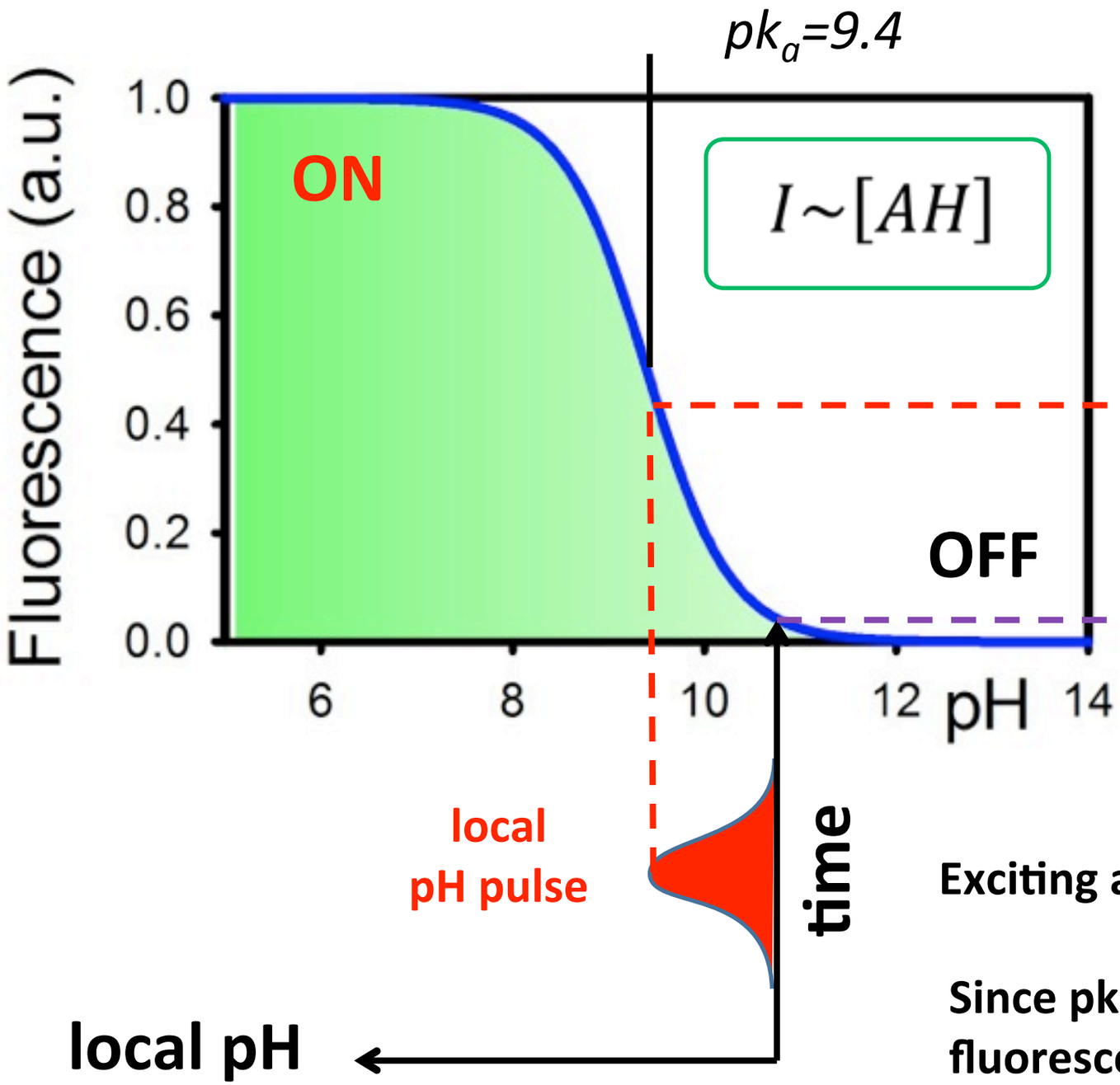

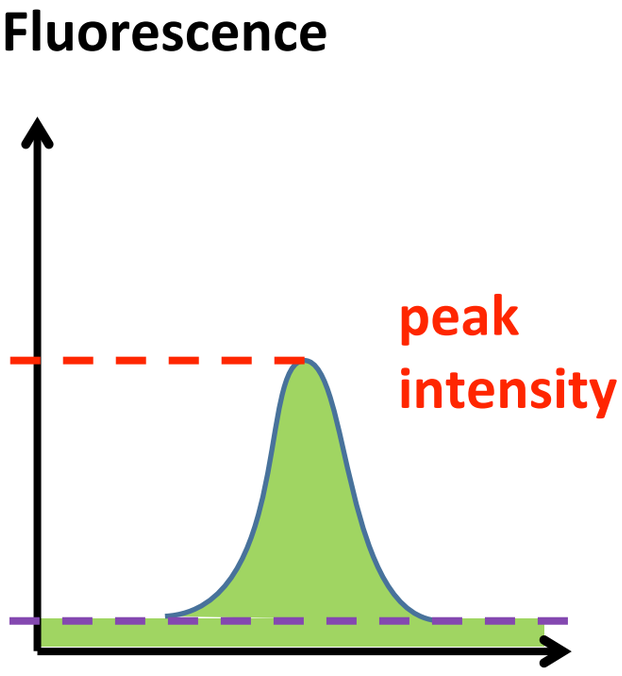

Exciting at 488 nm ε_A=0 and A is not fluorescent

Since pka=9.7 and the bulk pH is 10.3 the fluorescence of the bulk is very weak and a large increase of intensity results from small pH decreases.

Bulk pH (10.4)

Set up

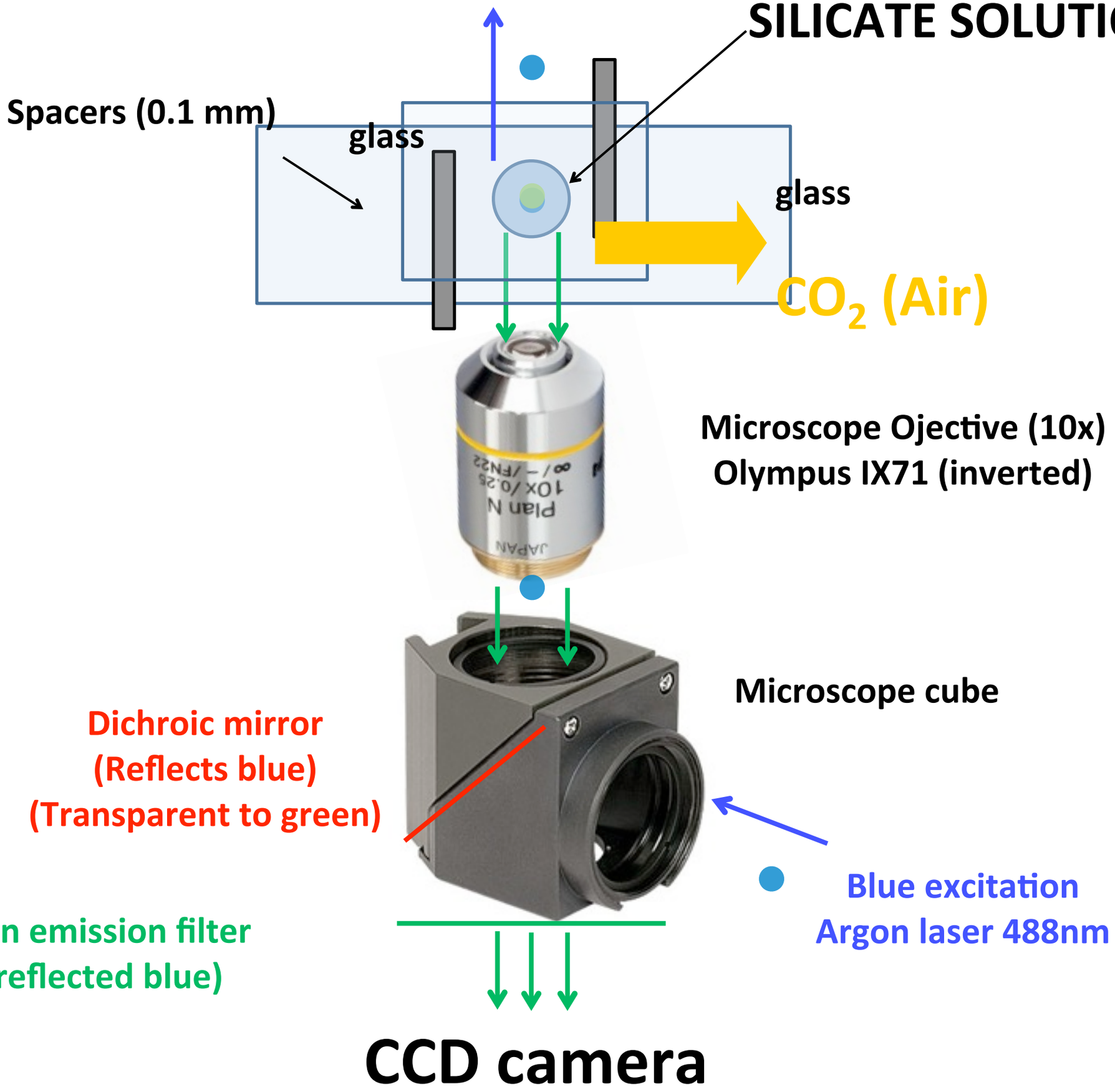
SILICATE SOLUTION
Spacers (0.1 mm)
glass
glass
CO_2 (Air)
Microscope Ojective (10x)
Olympus IX71 (inverted)
Microscope cube
Dichroic mirror
(Reflects blue)
(Transparent to green)
Blue excitation
Argon laser 488nm
Green emission filter
(cut reflected blue)
CCD camera

Growth of a biomorph in the presence of the pH probe

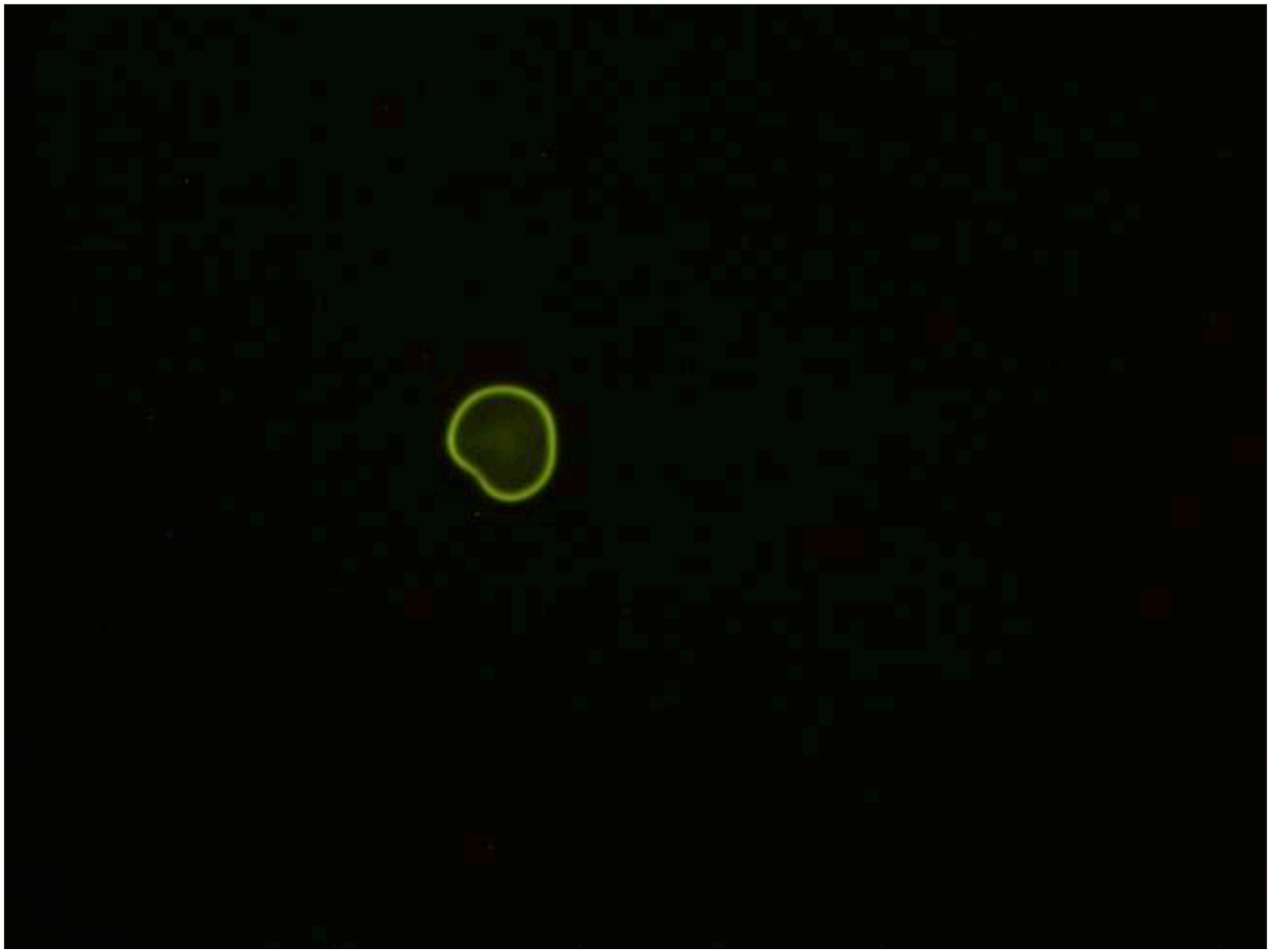

Results

The emission of the probe in the bulk (solution) is very weak

A strong increase of the fluorescence is observed in the proximity of the front of growth indicating a local decrease of the pH.

The local pH perturbation roughly moves along with the front of growth

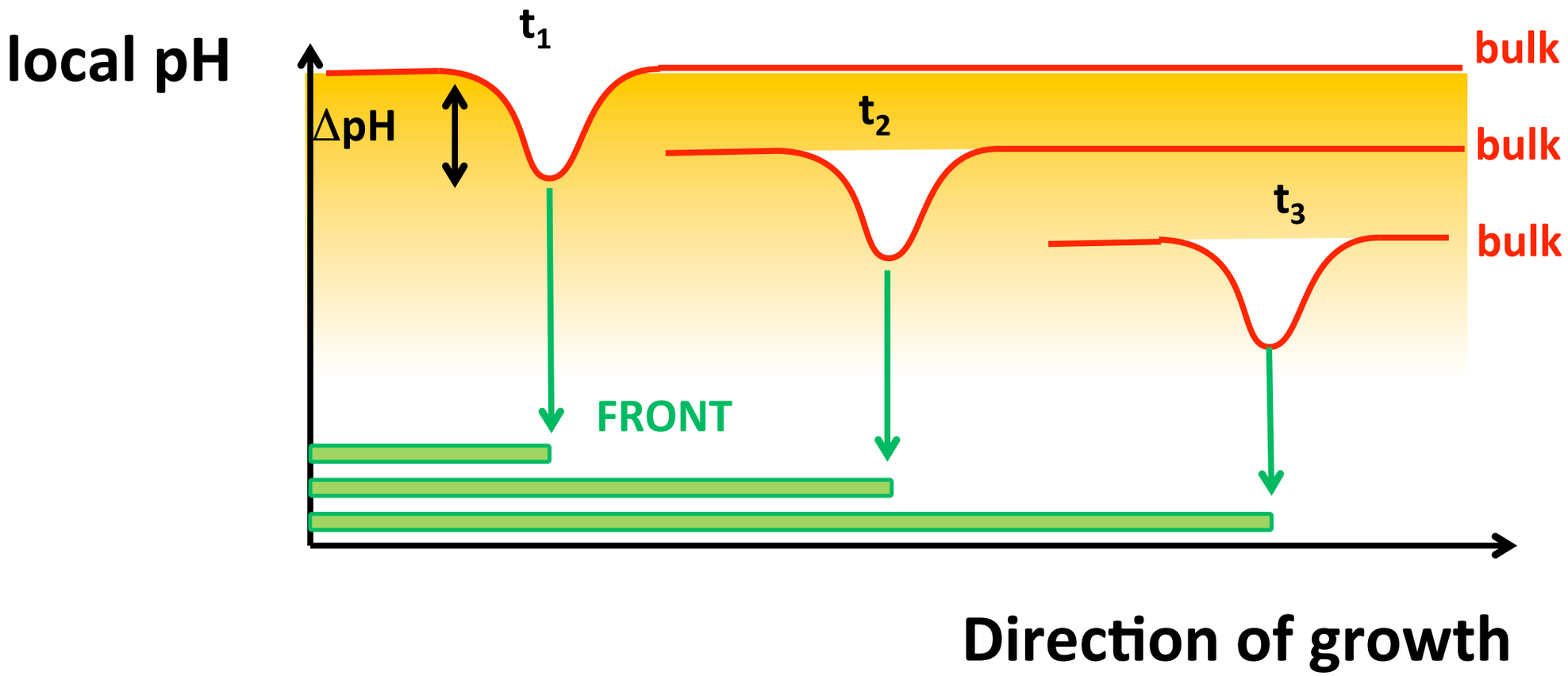

SOME QUESTIONS

Is the maximum local pH decrease (∆pH) constant during the time?

Does the peaks moves linearly?

ANALISYS (circular growth)

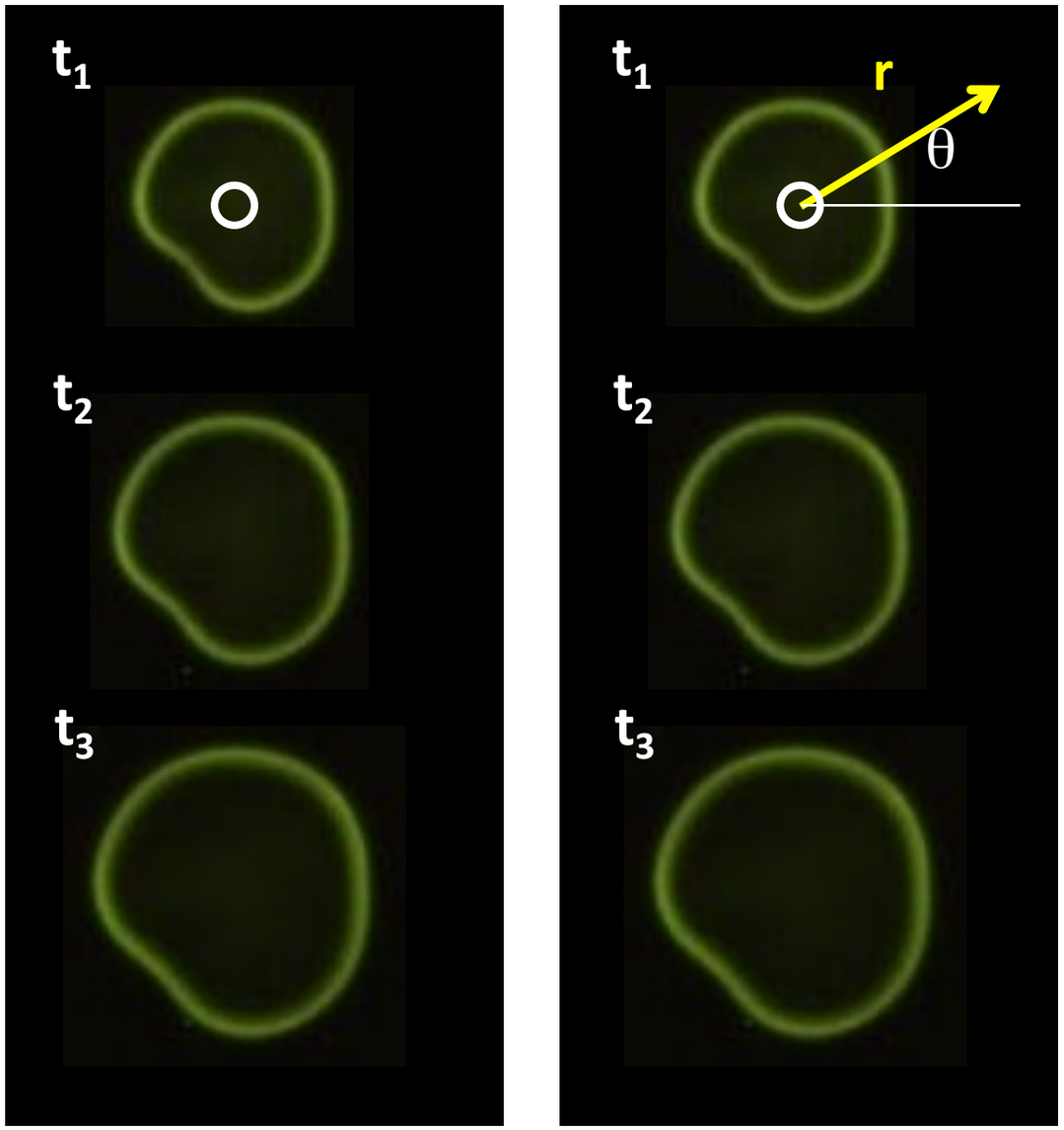

1 Find the centre C (in the first frame)

2 Choose a direction (angle θ)

3 Plot an intensity map As a function of time and of the distance r from C

4 Recalculate the map For different value of θ

INTENSITY MAP (FALSE COLORS)

INTENSITY MAP (FALSE COLORS)

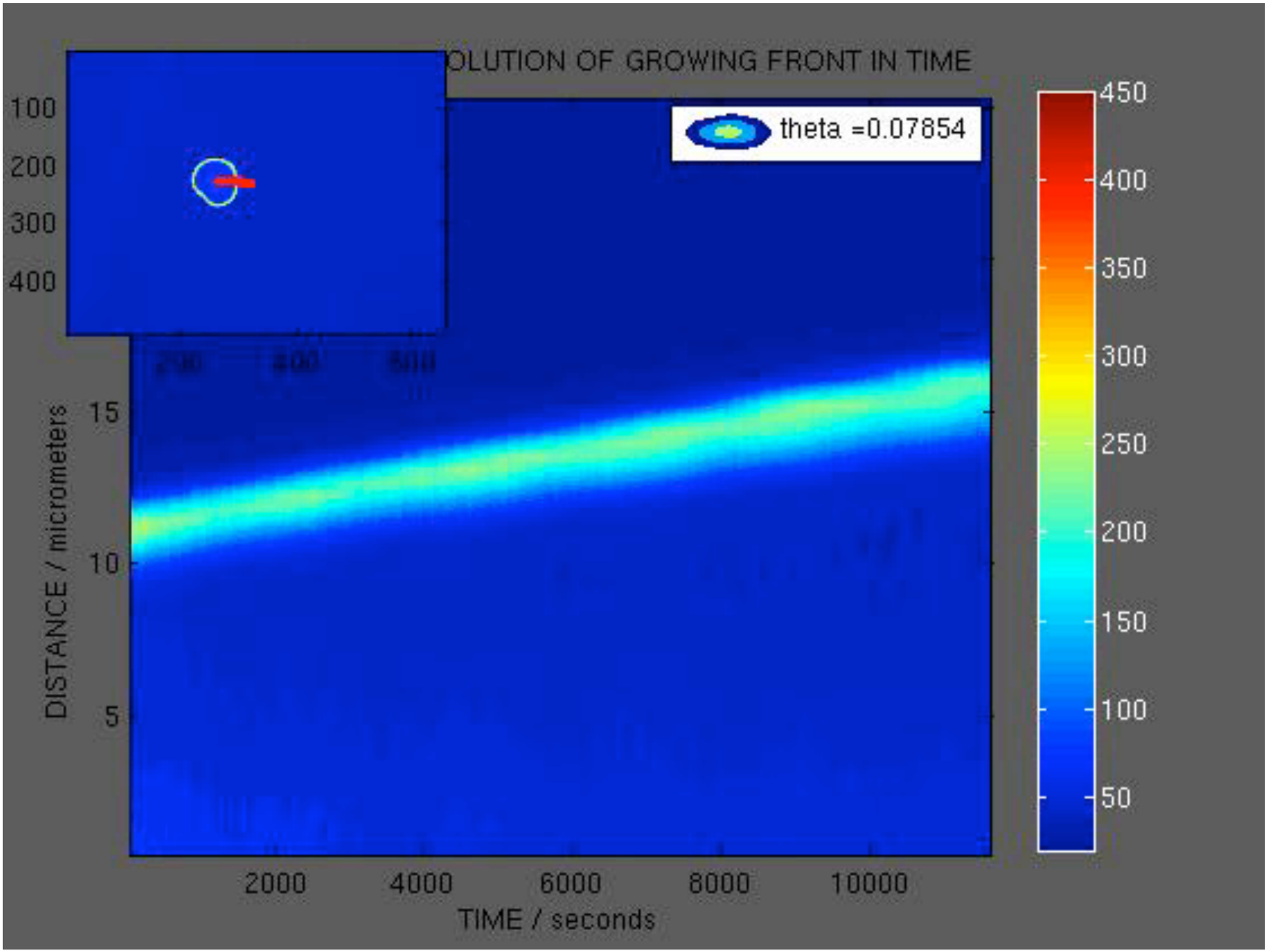

INTENSITY MAP (FALSE COLORS)

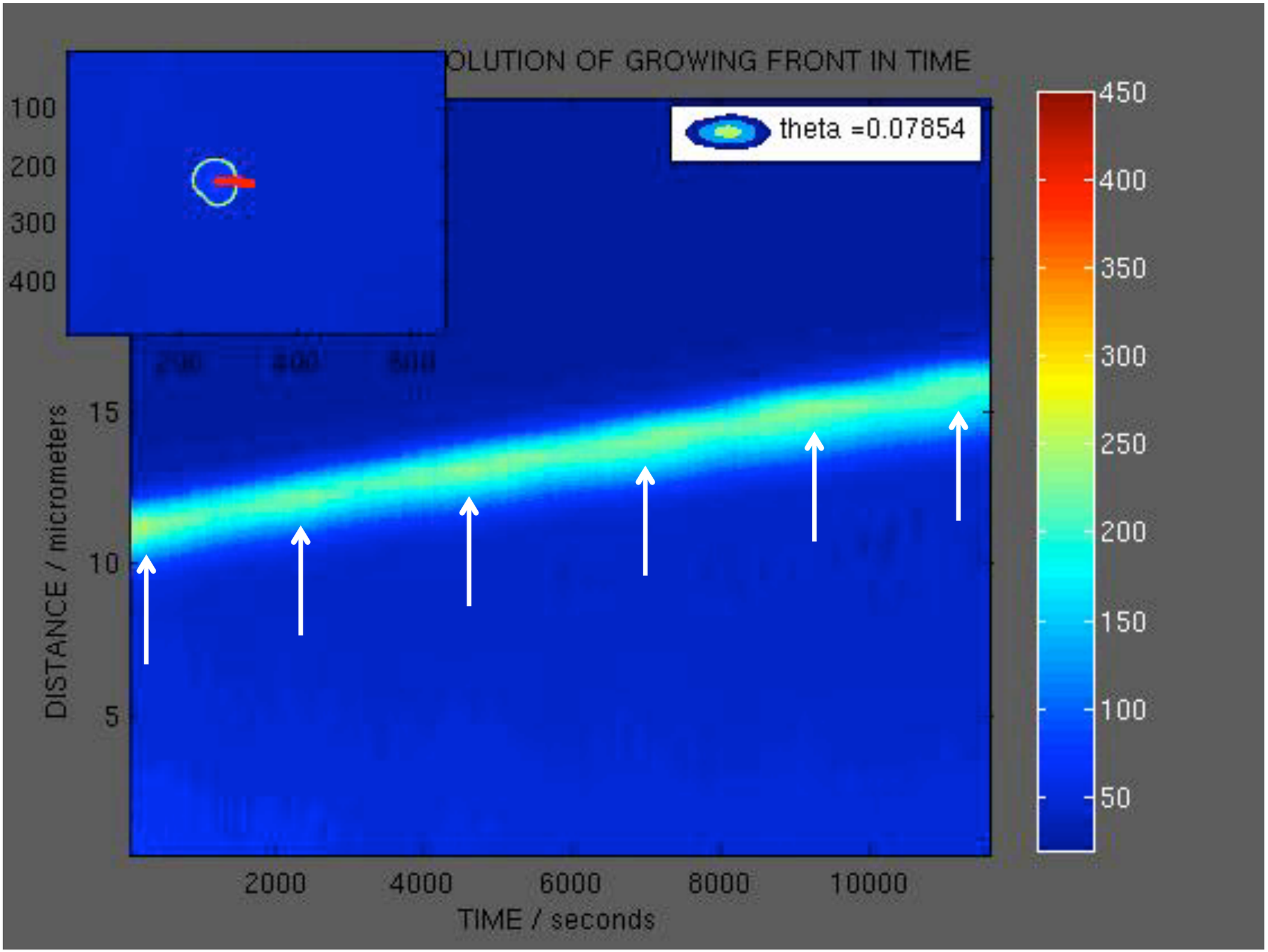

The power of curling

This novel morphogenetic mechanism explains :

1. The leaf–shape, so characteristic of silica biomorphs, is an inevitable result of two opposing and mutually interacting surfing curls.

2. ‘Regular’ forms, with uniform curvature distributions over their surface (such as twisted spheres and generic twisted surfaces) are less common than irregular shapes since geometric regularity in this sense requires fixed growth rates ratios over extended times.

3. This mechanism also explains the absence of chirality in silica biomorphs since the handedness of the helical structures depends on the relative sign of curl, which is arbitrary.

4. It also explains the failure to induce chirality in silica biomorphs using chiral molecules: the origin of the curling is at a much larger length scale to that of the molecular world and is therefore uncoupled from molecular chemistry.

5. Over all, this novel mechanism of morphogenesis explains the whole panoply of morphologies so far described for silica/carbonate biomorphs.

6. It is noticeable that life do not use the curling mechanism

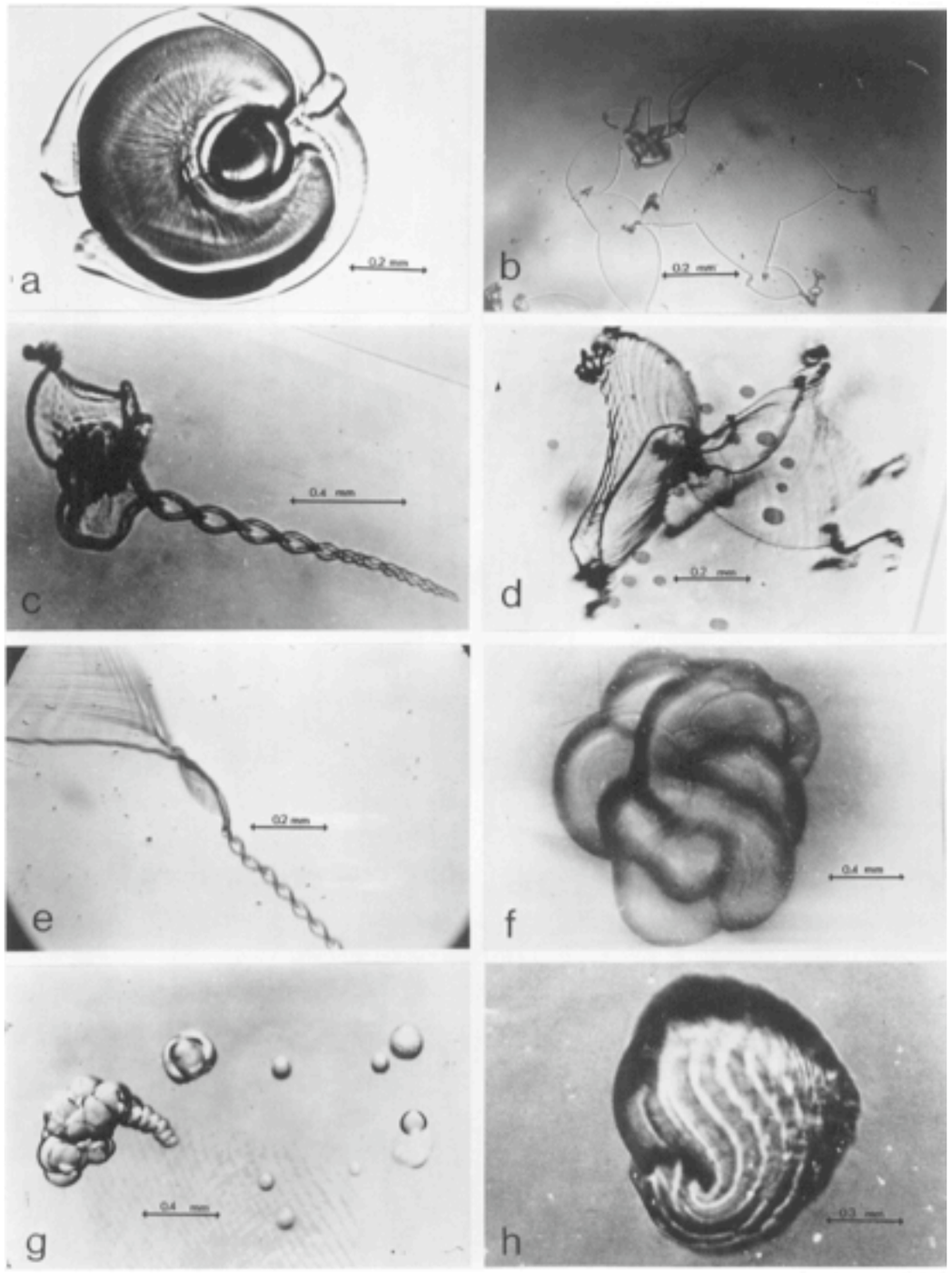

Main conclusions

1. Nano-crystalline materials displaying shapes with constant curvature can be made by self-organization (no scaffolds, no templates, no molds).
2. To make them it is required a self-feeding mechanism for continuous supply of a polymeric "impurity" provoking fibrilation and then laminar structures.
3. The route to produce similar self-organized materials is finding two compounds, one polymeric and other one crystalline, with reverse solubility with respect to some physicochemical parameter, such as pH, T, Eh, etc... (or biochemical).
4. Fluorescence microscopy has been succesfully used to detect pH changes at local scale
5. The results clearly show:
   - 5.1. A decrease of pH at the growth front with respect to the bulk solution
   - 5.2. An oscillatory behaviour of the pH value at the growth front

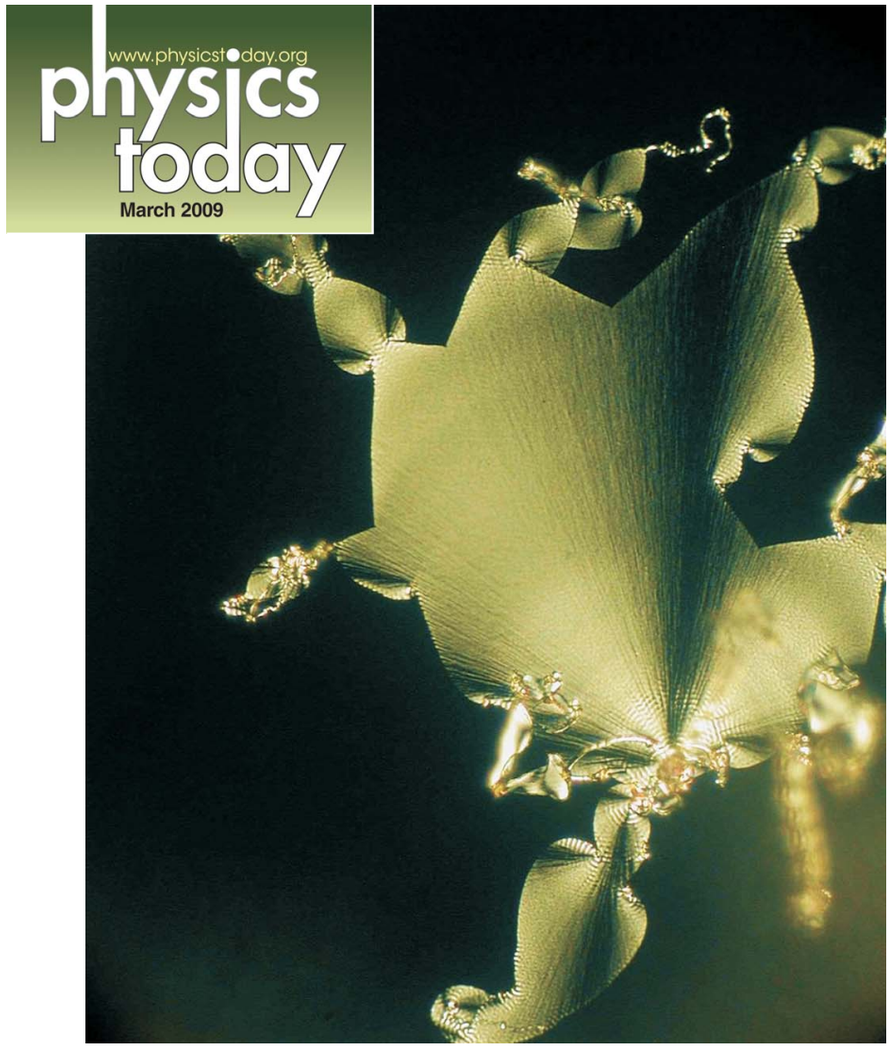

Complex shapes from simple chemistry

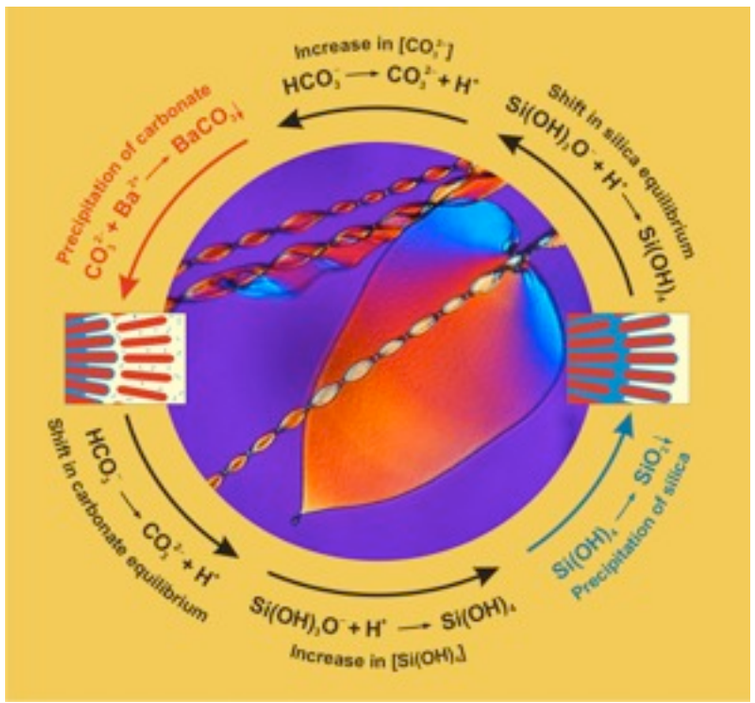

Morphology does not contain genetic information

The case of mineral fractal dendrites

Morphological convergence of silica biomorphs with primitive life forms

Some structures found in Precambrian rocks (cherts) which are interpreted as fossils remnants of primitive life and its laboratory made silica/carbonate counterparts

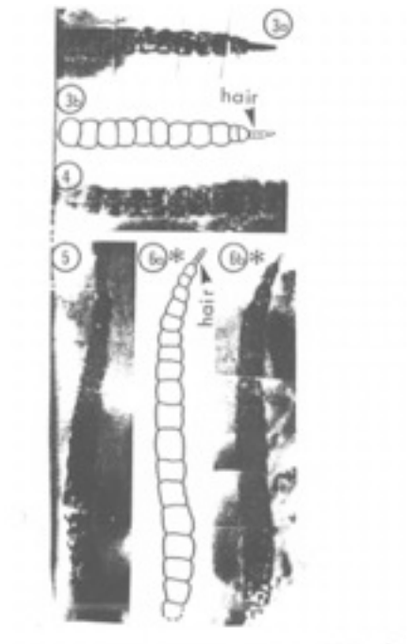

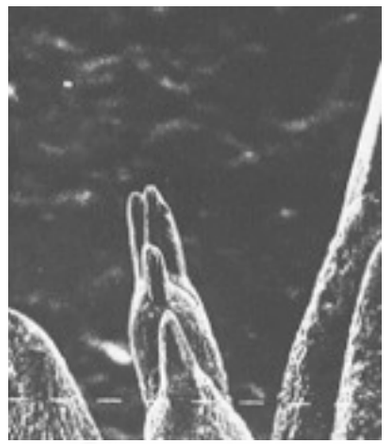

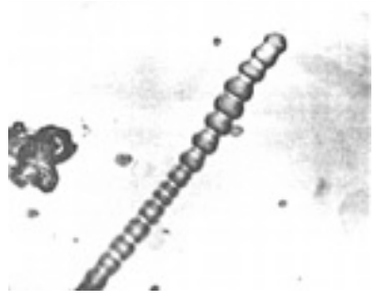

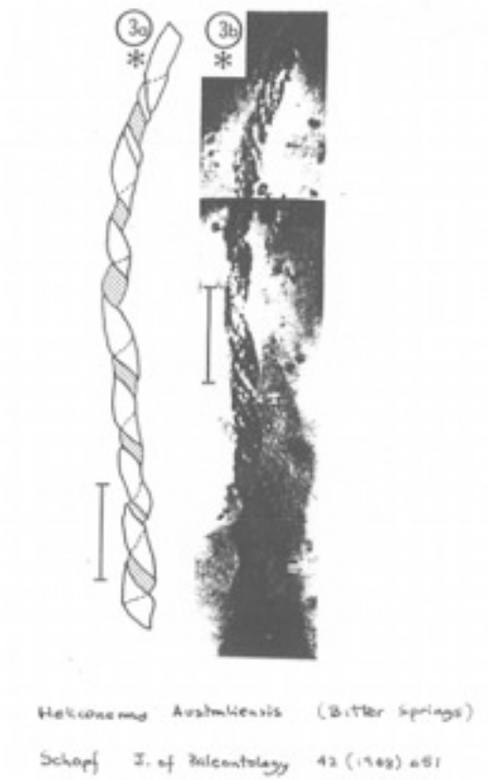

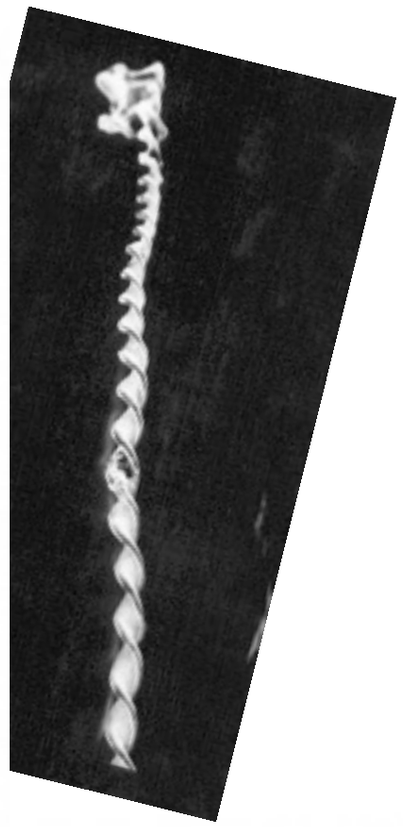

Helicoscamus Australiensis (Bitter Springs)
Schopf J. of Paleontology 42 (1968) 651

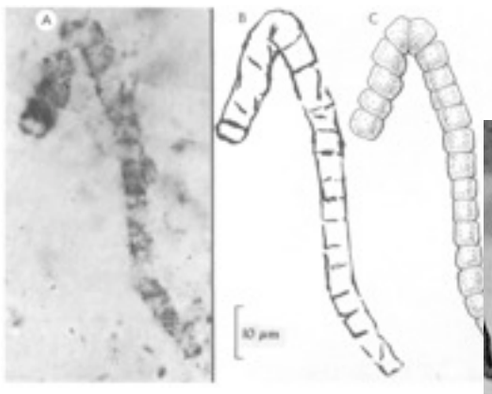

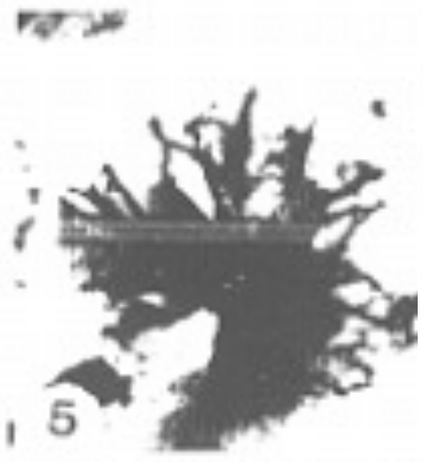

Eoastrion Barghoon (DUCK CREEK)

From: Knoll and Barghoorn Origins of Life 7 (1976) 417

Large amounts of chert precipitated during Archean times

High — Weathering of alkaline rocks / Sorption by clays and organic ➡ Supersaturated brines of silica

Ultramafic rocks plus water yields high pH fluids, reducing environments, H2 and organic volatiles by serpentinization of olivine.

or

All the putative Precambrian microfossils have been found in cherts. Cherts formed from silica gels. In many cases the cherts containing PM are baritic cherts

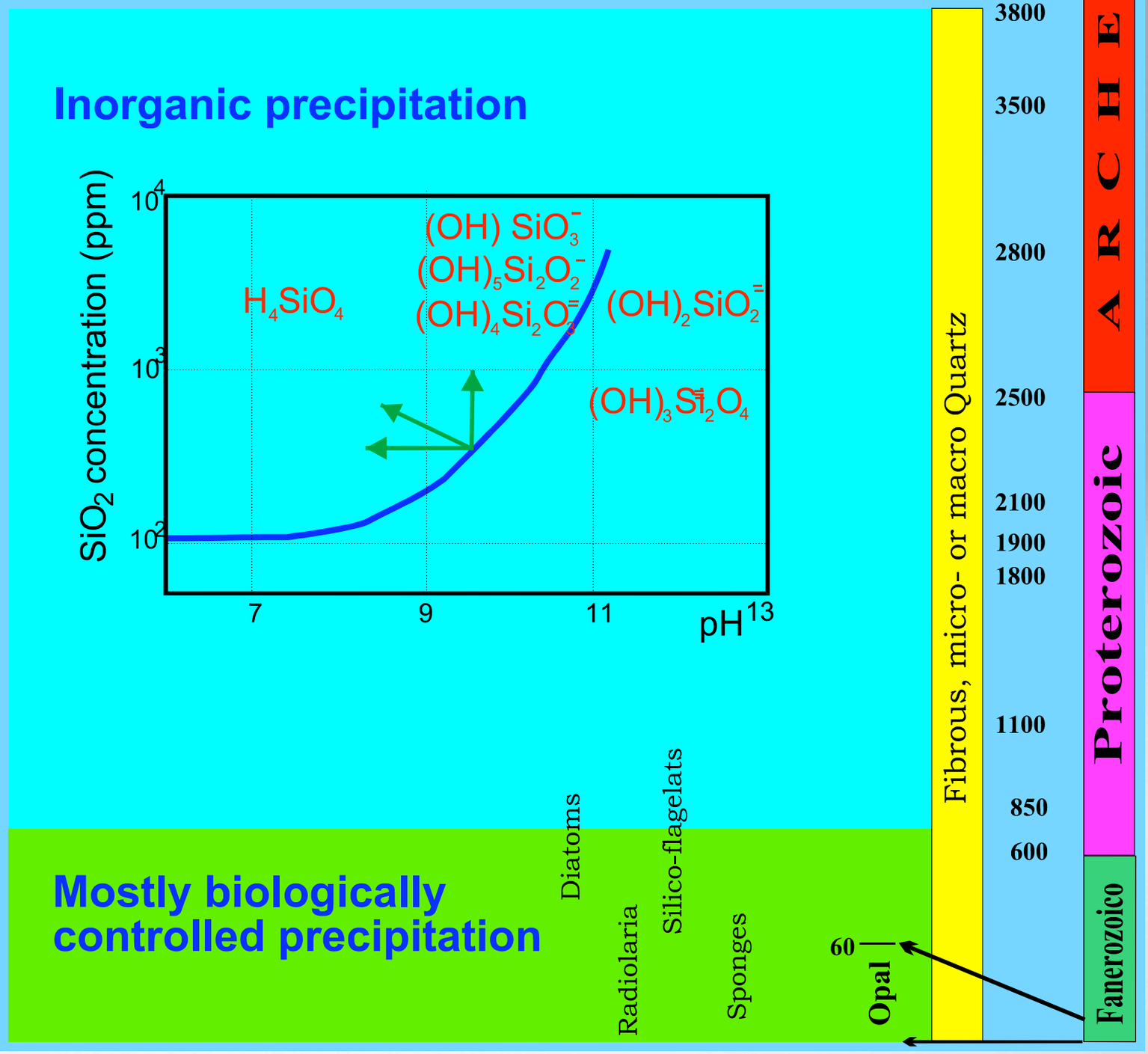

Neither morphology nor chemical composition can be used as unambiguous tools for life detection

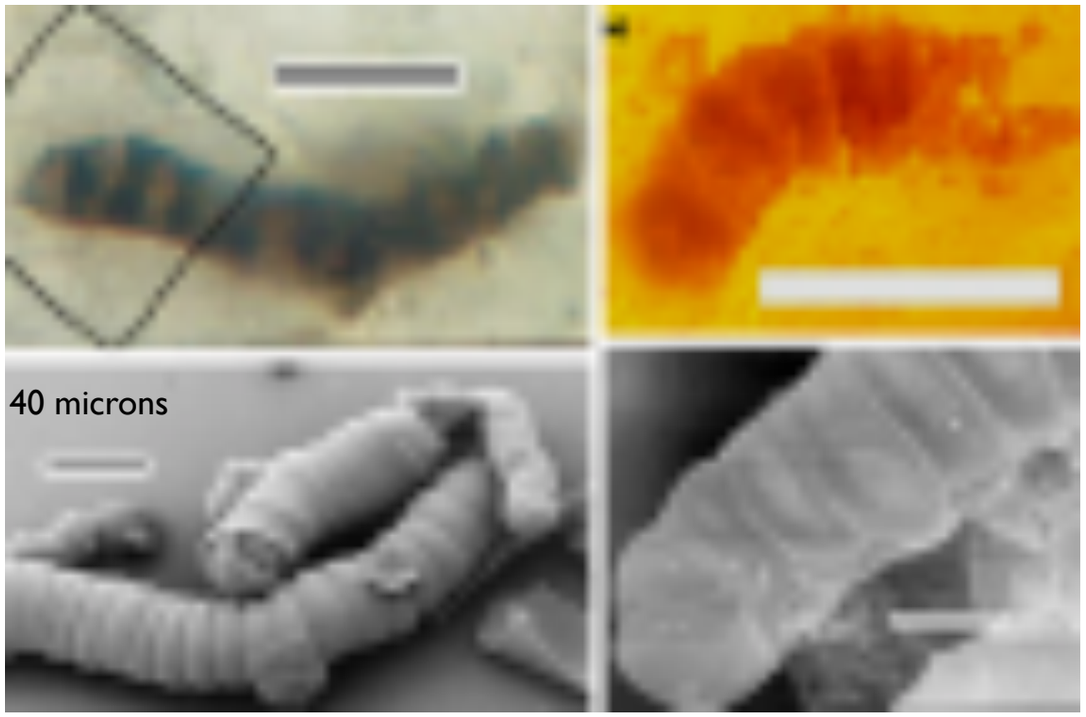

Heating siderite at 300 °C simple aromatic hydrocarbons form (McCollom & Seewald, Geochem & Cosmoch. Acta, 67 (2003) 216)

$$FeCO_3 + H_2O \rightarrow Fe_3O_4 + CO_2 + CO + H_2 + PAH$$

Mixtures of phenol-formaldehyde adsorb in silica biomorphs. After heating at 350 °C kerogen is made. This kerogen has the same Raman spectra that the one obtained from structures considered the oldest microfossils found on Earth

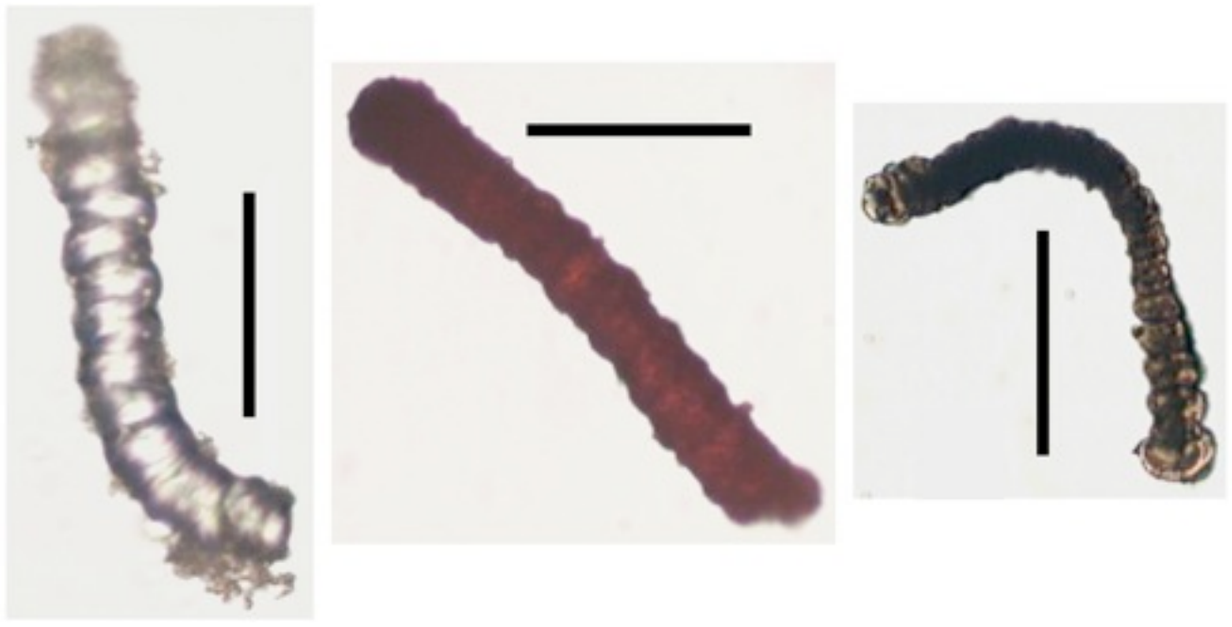

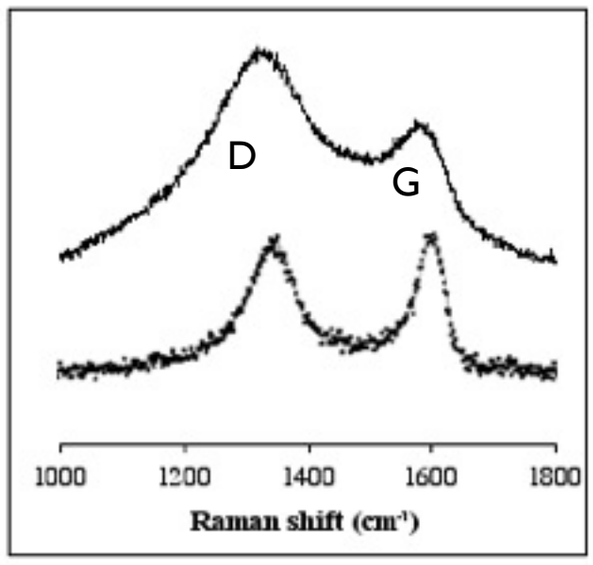

Highly disordered carbonaceous material

J.M. García-Ruiz. Origins of Life and Evolution of the Biosphere, 24 (1994) 451-467

J.M. García-Ruiz, A. Carnerup, A. Christy, N. J. Welham, and S. Hyde, Astrobiology 2 (2002) 335

J.M. García-Ruiz, S.T. Hyde, A. Carnerup, A.G. Christy, M.J. Van Kranendonk, N.J. Welham. Science 302 (2003) 1194.

MICROFOSSIL RECOGNITION IN ARCHEAN ROCKS

After R. Buick, Palaios 5 (1990) 441-459

Proving Antiquity:

- Rock units of proven Archean Age
- ✔ Embedded in the rock matrix
- Singenetic

Proving Biogenicity:

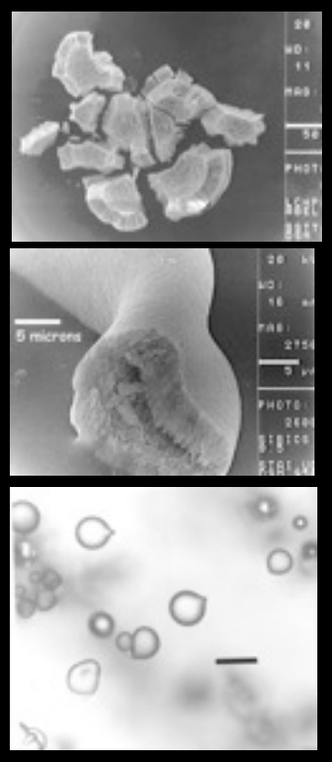

- The PM should occur in a petrographic thin section
- The PM should occur in a sedimentary or low grade metasedimentary rock
- ✔ The PM should be larger than the smallest extant living organisms
- ✓ The PM should be composed of kerogen
- ✔ The PM should display a well-defined SD
- ✔ The PM should occur with others of similar morphology
- ✔ The PM should be hollow
- ✔ The PM should show cellular elaboration

Those Precambrian microstructures which were considered dubio-fossilss or non-fossils should also be revisited.

- Does not apply for biomorphs
- ✔ Fulfilled by biomorphs
- To be published

Morphology does not contain unequivocal genetic information

Primitive and extraterrestrial life detection cannot be only based on morphology

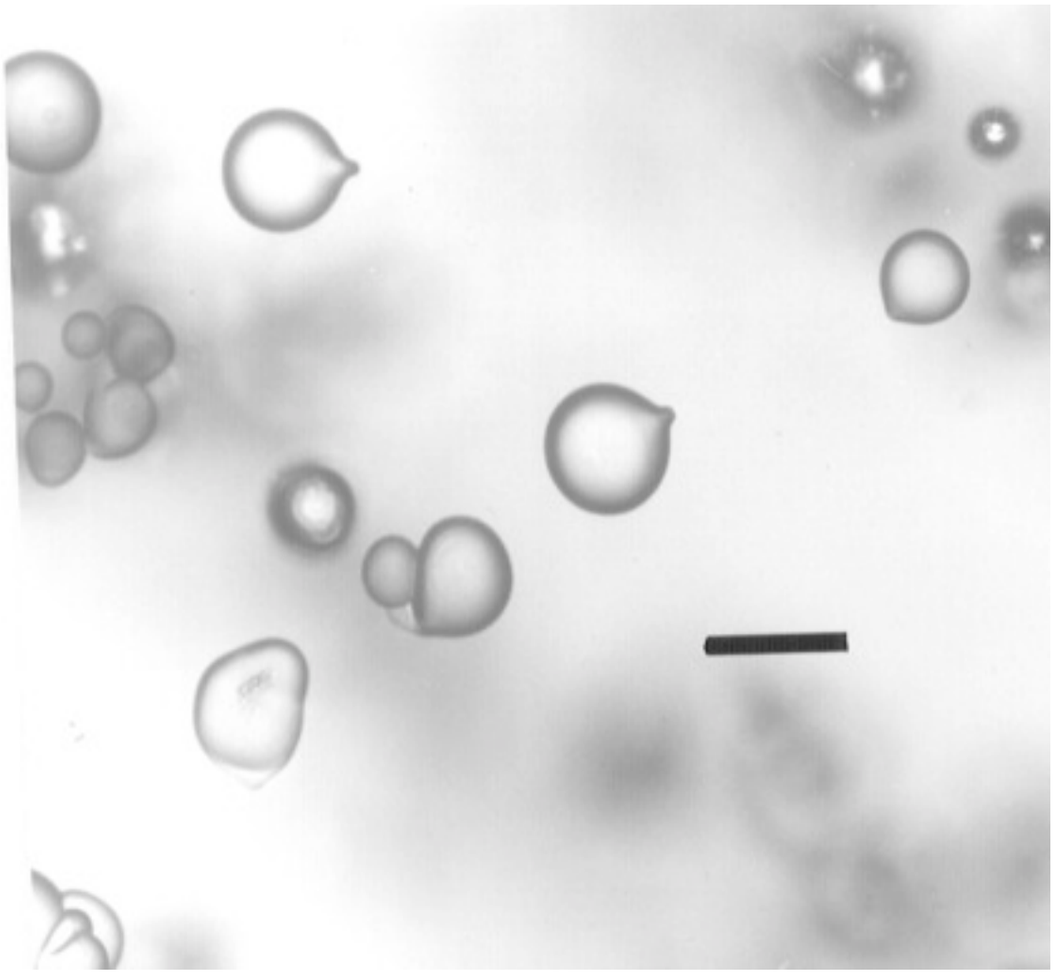

Morphology can be used only as a tool for life detection when it becomes a darwinian character. Before that critical and I guess late step, morphology of living organisms where controlled by the same physical parameters that control the shape of abiotic self-assembled structures, namely surface tension, membrane elasticity and porosity and osmotic forces.

Morphology does not contain genetical information

We know this remnant is biogenic not because its complex morphology but because **comparative anatomy**

Morphology does not contain genetical information

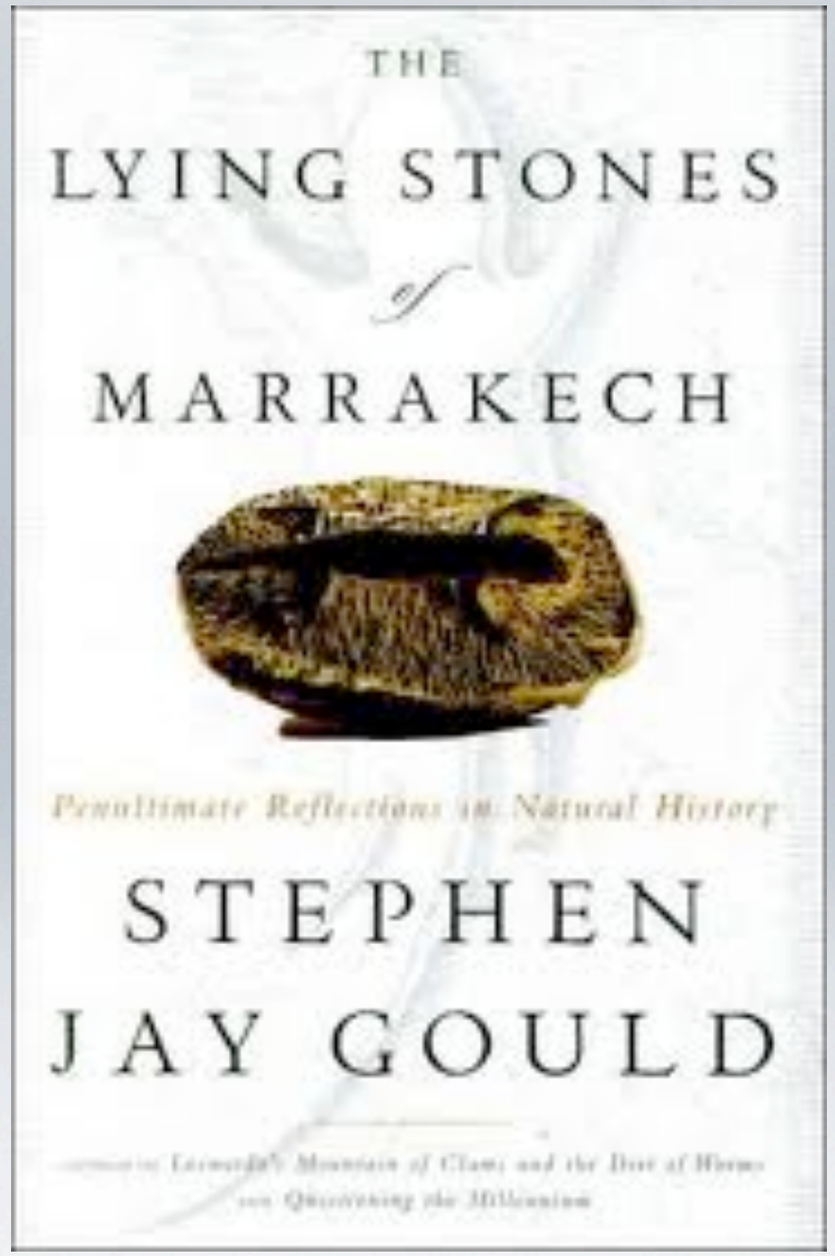

We know they are abiotic not because of the morphology but because comparative anatomy

The problem of primitive life detection is that there is not complexity enough to apply comparative anatomy

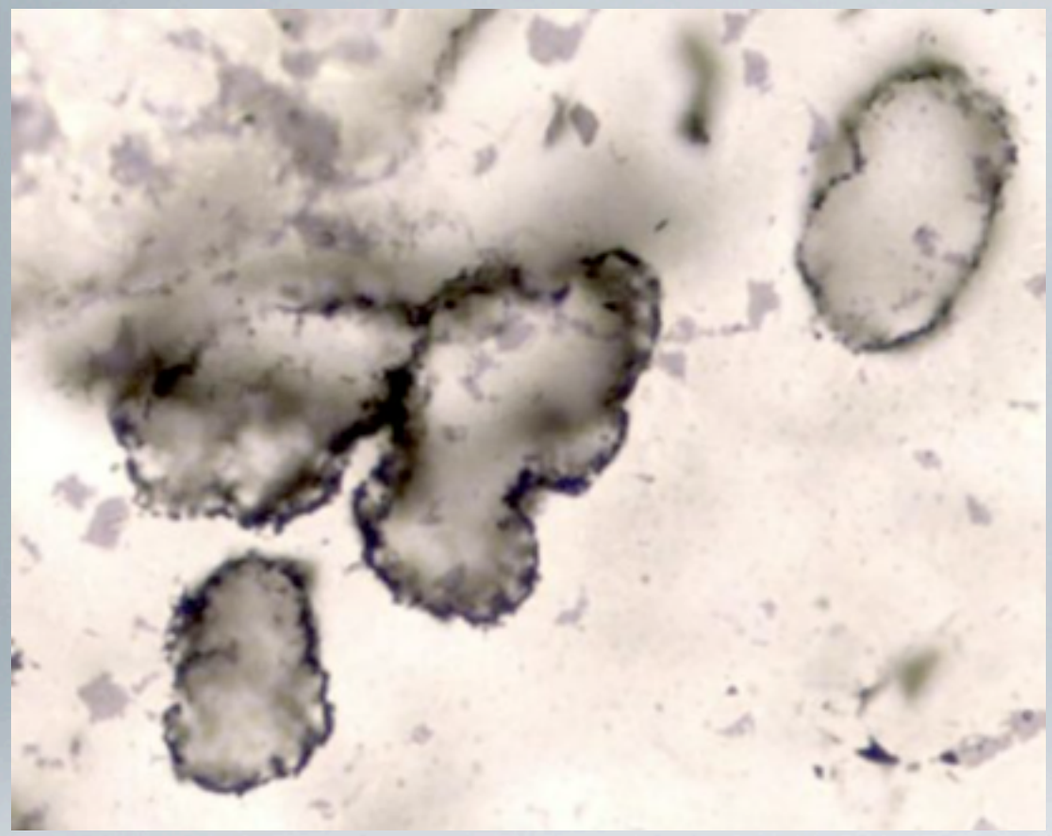

D. Wacey et al., *Nature Geoscience*, 2011
from Shelley Pool (Australia)

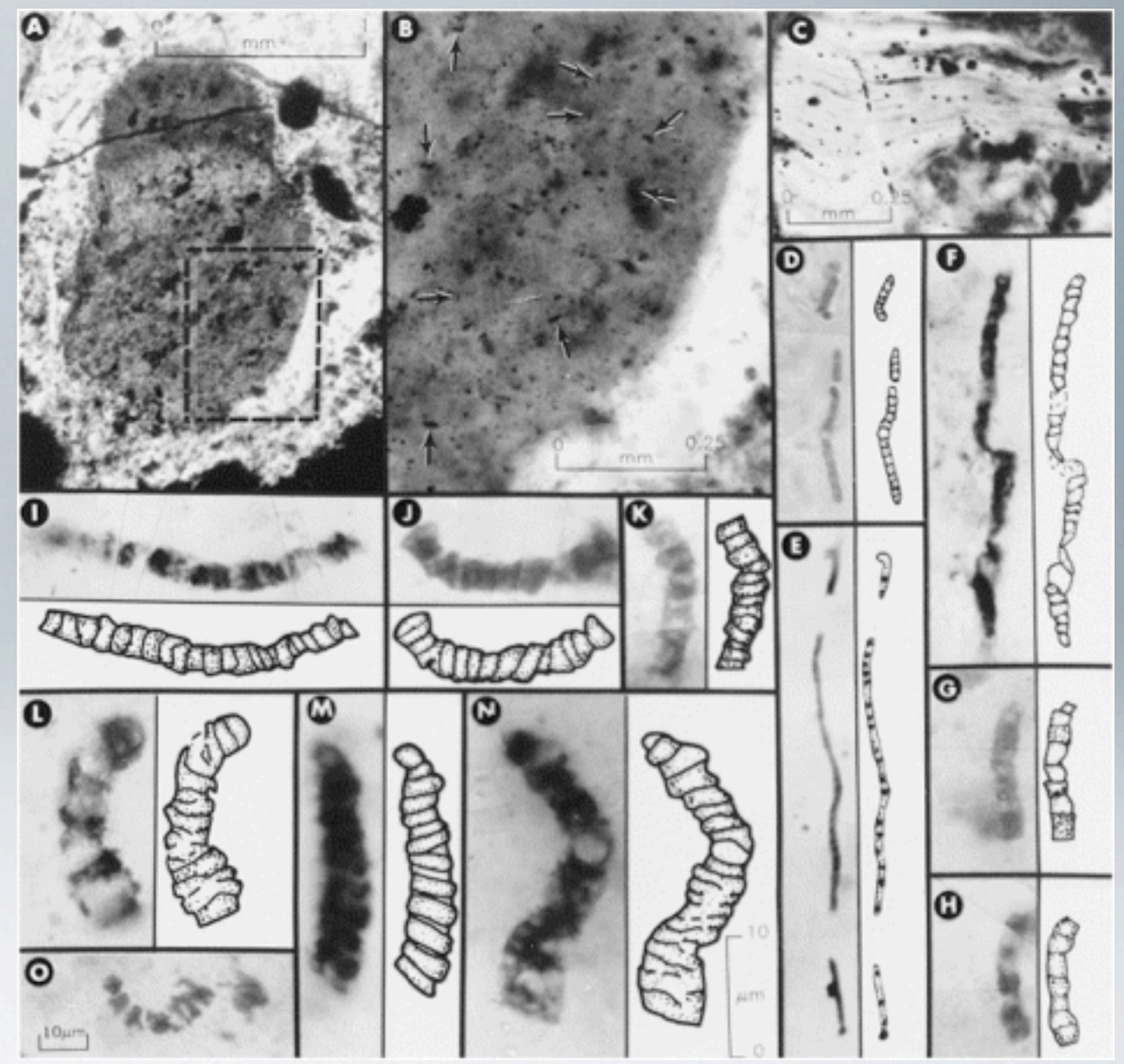

W. Schopf, 1993 Science. From Apex Chert of Australia

Morphology does not contain genetical information

Earth

Orange

Spheres; $V = L^3$

Does Earth planets form from trees?